MODELING AND OPTIMIZATION OF CHEMICAL MECHANICAL POLISHING OF SEMICONDUCTOR MATERIALS

A Thesis

by

Wazir Akbar

Submitted to the
Graduate School of Science and Engineering
In partial fulfillment of the requirement for
the degree of

Doctor of Philosophy

In the
Department of Mechanical Engineering

Özyeğin University
December 2021

MODELING AND OPTIMIZATION OF CHEMICAL MECHANICAL POLISHING OF SEMICONDUCTOR MATERIALS

Approved by:

Dr. Ing. Özgür Ertunç
Assistant Professor
Department of Mechanical Engineering Özyeğin University

Dr. Polat Sendur
Assistant Professor
Department of Mechanical Engineering Özyeğin University

Dr. Eralp Demir
Senior Research Associate
Department of Mechanical Engineering.
University of Bristol, UK

Dr. Altuğ Başol
Assistant Professor
Department of Mechanical Engineering Özyeğin University

Dr. Sedat Nizamoğlu
Associate Professor
Department of Electrical and Electronics Engineering, Koc University, Turkey

Date Approved:

To,

My family, friends and teachers

ABSTRACT

Chemical mechanical polishing (CMP) is a process of planarization of metal and dielectric surfaces typically in microelectronic devices manufacturing. Planarization is achieved by removing material from the wafer surface due to the synergistic effect of chemical and mechanical actions. In a typical CMP machine the upper part is referred to as the head. It holds the wafer, rotates and applies a force on the wafer against the lower part. The lower part is a rotating platen with an attached relatively softer pad. During CMP slurry is externally provided at a desired flow rate. The slurry is composed of chemicals (oxidizer, chelating agents, corrosion inhibitor and surfactants etc.) and nanometer-sized hard abrasive particles. The chemicals react with surface and modify the surface properties while the abrasive particles indent into the wafer surface and remove material from the wafer surface due to relative motion between the wafer and pad.

The combination of chemical and mechanical effects limits our ability to understand the complex material removal mechanism in CMP. Intensive efforts have gone into developing models to explain the complex mechanism of material removal in CMP processes. The material removal rate in chemical mechanical processes have a linear dependency on applied down pressure. However, some experimental studies have reported nonlinear relationship between MRR and applied pressure. The nonlinearity can be attributed to complex interactions among the wafer, pad, abrasive particles, and chemical agents in the slurry. Therefore, in modelling CMP process coupling of both the chemical and mechanical actions is imperative to provide insight into the nonlinear behavior of MRR. Since, treating the chemical effects only as a mere means of softening the wafer surface fails to explain the nonlinear behavior of MRR in silicon dioxide CMP. Here, we present a model that couples micro-contact mechanics with diffusion of slurry

into the wafer and predict MRR in CMP of silicon dioxide. The model is validated with experimental results available in the literature. In case of barrier CMP, different materials are simultaneously polished and CMP is expected to achieve a planar surface. The developed model can be utilized to optimize CMP input conditions to achieve similar material removal during barrier CMP.

The material removal depends on material properties and the process input parameters. Several studies have investigated the role of slurry chemistry to achieve a certain material removal selectivity of different materials on a patterned wafer. Here we propose a methodology of achieving planar patterned surface of Cu/Mn/MnN system using a model-based optimization for mechanical process parameters. The parameters include applied force, slurry solid concentration, and abrasive particle size. The methodology has been developed via optimization using a genetic algorithm. The proposed methodology suggests that a lower downforce is the key parameter to achieve the desired material removal selectivity and planarity. The first part of the study suggests a low material removal rate (MRR) to achieve a lower standard deviation in MRR. The second part investigates the standard deviation in the thickness removed in the average time needed to remove a known thickness of the materials under consideration. It has been found that the application of lower downforce can also minimize the standard deviation in the thickness removed and a planar patterned surface can be achieved.

Another way to achieve uniform material removal of different materials is the formulating of slurry chemistry. During chemical mechanical planarization process for nodes of 10nm and beyond, galvanic corrosion, material removal rate selectivity and defectivity issues need to be addressed. Better understanding of atomic scale chemical and mechanical interactions at the wafer surface to can provide useful insight and guidelines.

This study also experimentally investigates the CMP Cu/Mn/MnN system with different slurry formulating. Ex-situ electrochemical analyses of Cu/Mn/MnN system were conducted to evaluate the passivation in different slurry formulations. The slurry formulations used were 0.1 M, 0.2 M, 0.3 M and 0.5 M oxidizer (H_2O_2) with abrasive solid loading of 2.5 %wt. The results of electrochemical analyses are compared with post CMP surface topography and material removal rate selectivity. It has been found that material removal selectivity of 1:0.8:0.88 can be achieved for Cu/Mn/MnN system, for a slurry composition of 0.3 M H_2O_2, under 30 N down force and 2.5 %wt. solid concentration of the slurry. The effect of mechanical components such as slurry solid concentration and applied force was also investigated. It was found that for an optimized concentration of oxidizer, more control over material removal selectivity can be achieved by optimizing the mechanical input parameters. The application of lower applied force and lower slurry solid concentration are needed to achieved the objective. This finding is in agreement with the material removal selectivity predicted with model based optimization.

The model developed in this work can be used to predict MRR in a typical CMP. Also, the model can be used to optimize the CMP input conditions to achieved a desired MRR. The experimental approach proposed in this work can be beneficial to the barrier layer CMP for advanced interconnect integration schemes for sub-10 nm.

ÖZET

Genel olarak mikroelektronik cihazların imalatında kullanılan Chemical-Mechanical Polishing (CMP), veya Türkçe tabirle kimyasal-mekanik parlatma olarak bilinen işlem metal ve dielektrik yüzeylerin düzlemselleştirmelerinde kullanılır. Kimyasal-Mekanik Parlatma (düzlemselleştirme) işleminden geçen bir malzeme aynı anda hem kimyasal hem de mekanik olarak işlemlere maruz bırakılarak yüzeyinden mikroskobik olarak parçalar çıkartılır. Tipik bir CMP makinesindeki üst kısma "baş" olarak tabir edilir ve tabakayı yerinde tutup belirlenen bir hızda döndürerek altta bulunan bir parçanın üstüne güç uygular. Altta bulunan tablanın üzerine işlemden geçecek malzemeye nispeten yumuşak bir malzemeden yapılan bir levha bağlanır. CMP işleminde içi nanometre-boyutlu parçacıklarla dolu kimyasalı (oksitleyici, şelatlayıcı, korozyon önleyici ve yüzey aktif maddelerden oluşan bir solüsyon), aynı zamanda bulamaç (slurry) olarak adlandırılır, istenilen debide malzemenin yüzeyine pompalanır. CMP süresince kimyasal yüzeyle reaksiyona girip özelliklerini değiştirirken, içinde bulunan nano-parçacıklar dönme hareketi nedeniyle yüzeyi fiziksel olarak değiştirir.

CMP'deki kimyasal ve mekanik etkiler nedeniyle ortaya çıkan kompleks malzeme kaldırma mekanizmasını anlama kabiliyetimizi sınırlamaktadır. Bu mekanizmayı açıklamak ve çeşitli modeller geliştirmek için yoğun çabalar harcanarak malzeme kaldırma hızının levhanın üzerine uygulanan basınçla lineer bir ilişki içinde olduğu ortaya çıkmıştır; fakat yakın zamanlarda yapılan deneylerde bu ilişkinin lineer olmadığını ispatlayan veri ortaya çıkmıştır. Malzeme yüzeyinin altta bulunan yumuşak levha ile teması, nano-parçacıklarla ve kimyasal solüsyonla olan etkileşimi lineer olamayan ilişkiye neden olabilir. Bu nedenle, CMP işlemini modellerken her iki etkileşimin (kimyasal ve mekanik) birbirine olan bağımlılıkları malzeme kaldırma hızının lineer olmayan davranışını açıklığa kavuşturmak için önemlidir. Kimyasal etkilerin

yalnızca silikon devre levhası (wafer) yüzeylerini yumuşatmanın bir yolu olarak ele alınması, silikon dioksitin CMP'deki MRR'sinin doğrusal olmayan davranışını açıklayamamasına neden olabilir. Bu çalışmada, nano-parçacıkların yüzey ile teması ve kimyasalın yüzeye olan difüzyonu arasındaki ilişkiyi göz önünde bulundurarak, silikon dioksitin CMP'deki malzeme kaldırma hızını tahmin edebilen bir model sunuyoruz. Geliştirdiğimiz model, literatürde mevcut olan deneysel sonuçlar ile doğrulanmıştır. Buna ek olarak model artan basınçla silikon dioksitin malzeme kaldırma hızındaki (MRR) doğrusal olmayan artışı açıklamak için kullanılabilir. Bariyer malzemelari için yapılan CMP'de, farklı malzemeler aynı anda parlatılır ve CMP'nin düzlemsel bir yüzey elde etmesi beklenir. Ayrıca, geliştirilen model bariyer CMP işlemi sırasında homojen malzeme kaldırma elde etmek için CMP koşullarını optimize etmek için kullanılabilir.

Malzemenin özelliklerine ve CMP'ye parametrelerine göre malzeme kaldırma işlemi farklılık gösterir. Yapılan çeşitli araştırmalarda, istenilen miktarda malzeme kaldırımını gerçekleştirebilmek için bulamaç (slurry) kimyasının farklı malzemelerle yapılan desenli levhaların üzerindeki etkisi gözlemlenmiştir. Burada, mekanik işlem parametrelerini optimize edebilmek için bahsedilen modeli kullanarak Cu/Mn/MnN sistemlerinin düzlemsel desenli yüzeyini elde etmek için bir metodoloji öneriyoruz. Uygulanan kuvvet, bulamaç katı konsantrasyonu ve aşındırıcı parçacık boyutları istenilen yüzey karakteristiklerini yakalamamızı sağlayacak parametrelerdır. Bu parametreleri kullanarak genetik algoritma yardımı ile model tabablı optimizasyon yapılmıştır. Ortaya çıkan metodoloji, istenilen malzeme kaldırma oranı ve düzlemselliğini elde edebilmek için düşük düzeyde uygulanan kuvvetin önemli bir parametre olduğunu öne sürüyor. Araştırmanın ilk kısmı, malzeme kaldırma oranında (MRR) daha düşük bir standart sapma elde etmek için düşük bir MRR öneriyor. Araştırmanın ikinci kısmı ise, gereken ortalama süre içinde kaldırılan malzeme kalınlığındaki standart sapmayı incelemektedir.

Uygulanan kuvveti azaltmak, çıkartılan malzeme kalınlığındaki standart sapmayı en aza indirebileceği ve düzlemsel desenli yüzey elde edilebileceği bulunmuştur.

Farklı malzemelerin homojen bir şekilde kaldırmasını sağlamanın bir başka yolu, bulamaç kimyasının formüle edilmesidir. 10nm ve daha küçük düğümler (nodes) için kimyasal ve mekanik düzlemselleştirme işlemi sırasında galvanik korozyon, istenilen malzeme kaldırma oranı ve kusurluluk sorunlarının göz önünde bulundurulması gereklidir. Levha üzerindeki atomik boyutlarda olan kimyasal ve mekanik etkileşimlerin daha iyi bir şekilde anlaşılması faydalı bilgiler ve öneriler sağlayabilir.

Bu çalışma aynı zamanda Cu/Mn/MnN sistemlerinin CMP'de çeşitli bulamaç (slurry) formülasyonları deneysel olarak araştırmaktadır. Farklı bulamaç formülasyonlarında pasivasyonu değerlendirmek için Cu/Mn/MnN sistemlerinin ex-situ elektrokimyasal analizleri yapılmıştır. Kullanılan bulamaç formülasyonları sırasıyla 0.1 M, 0.2 M, 0.3 M, 0.4 M, 0.5 M oksitleyici (H_2O_2) ve %2.5 bulamaç katı konsantrasyonu içermektedir. Elektrokimyasal analizlerden gelen veriler, CMP işlemi sonrası yüzey topografisi ve malzeme kaldırma oranı seçiciliği ile karşılaştırılmıştır. Cu/Mn/MnN sistemleri için 1:0.8:0.88'lik malzeme kaldırma seçiciliğine ulaşabilmek için, 0.3 M H_2O_2 bulamaç birleşimi, %2.5'luk katı konsantrasyonu ve 30 N kuvvetin gerekli olduğu bulunmuştur. Bulamaç katı konsantrasyonu ve uygulanan kuvvet gibi mekanik bileşenlerin etkisi de araştırmıştı. Amaca ulaşmak için daha düşük uygulama kuvveti ve bulamaç katı konsantrasyonu kullanılması gerekli olduğu bulunmuştur.

Bu çalışmada geliştirilen model, tipik bir CMP işleminde MRR'yi tahmin etmek için kullanılabilir. Ayrıca geliştirilen model, istenilen MRR'ye ulaşmak için CMP giriş koşullarını optimize etmek için kullanılabilir. Bu çalışmada önerilen deneysel yaklaşım,

10-nm ve altı için geliştirilmiş ara bağlantı entegrasyon şemaları bariyer katmanı CMP için faydalı olabilir.

ACKNOWLEDGMENTS

I would first like to thank my thesis advisor Dr.-Ing. Özgür Ertunç, Assistant Professor in the department of mechanical engineering at Özyeğin University Istanbul Turkey. The door to Dr. Ertunç's office had always been open for me whenever I faced a problem or needed guidance and has consistently steered me in the right direction to accomplish this work.

I am grateful for the useful discussions with Dr. Polat Sendur about the optimization of CMP input parameters for achieving the desired objectives, and Dr. Eralp Demir for expanding this work by incorporating the anisotropy of the wafer into the model.

Finally, I must express my very profound gratitude to my family and friends for their unfailing support and encouragement throughout this study. This work would not have been accomplished without you. Thank you!

Author,

Wazir Akbar

TABLE OF CONTENTS

LIST OF TABLES

LIST OF FIGURES

NOMENCLATURE

Symbol	Parameter/property
A_p	Area of average size particle
A_a^e	Contact area between wafer and asperity in the elastic region
A_a^{ep}	Contact area between wafer and asperity in the elastoplastic region
A_a^p	Contact area between wafer and asperity in the plastic region
$A_{p/a}$	Area covered by effective abrasive particles
C	Concentration of water
D	Diffusion coefficient of water
D_p	Dilution ratio of slurry
E_a	Elastic modulus of asperity
E_p	Elastic modulus of particle
E_w	Elastic modulus of wafer
F_{ap}	Total force applied by an abrasive particle on asperity
F_{app}	Applied downforce
F_{wp}	Total force applied by an abrasive particle on wafer
F_a^e	Force applied by wafer on asperity in the elastic limit
F_a^{ep}	Force applied by wafer on asperity in the elastoplastic limit
F_a^p	Force applied by wafer on asperity in the plastic limit
H_a	Hardness of asperity
H_w	Hardness of wafer
k_e	Constant for elastic deformation
k_p	Constant for plastic deformation

l_o	Initial thickness of the wafer
N_{eff}	Number of effective particles per unit area
MRR	Material removal rate
R_a	Radius of asperity
R_p	Radius of particle
s	Distance between mean asperity height plan and wafer surface
u	Velocity of moving boundary
W_s	Slurry concentration before dilution (solid to liquid ratio)
V_p	Volume of average size particle
V_{rel}	Relative velocity
ε_a	Elastic modulus of asperity
ε_p	Elastic modulus of particle
ε_w	Elastic modulus of the wafer
ζ_t	Time dependent dimensionless coordinate
η	Number of asperities per unit area
μ	Distance between the two mean planes
υ_a	Poison's ratio of asperity
υ_p	Poison's ratio of particle
υ_w	Poison's ratio of the wafer
ρ_p	Density of particle
ρ_s	Density of slurry
σ	Average surface roughness (asperity height)
ω_{ap}	Indentation depth of particle into asperity
ω_{wp}	Indentation depth of particle into wafer

ω_{mrr}	Indentation depth responsible for material removal
ω_{ap}^{e}	Critical interference at elastic limit between asperity and particle
ω_{aw}^{e}	Critical interference at elastic limit between asperity and wafer
ω_{wp}^{e}	Critical interference at elastic limit between wafer and particle
ω_{ap}^{p}	Critical interference at plastic limit between asperity and particle
ω_{aw}^{p}	Critical interference at plastic limit between asperity and wafer
ω_{wp}^{p}	Critical interference at plastic limit between wafer and particle

CHAPTER I

INTRODUCTION

1.1 Background

Chemical mechanical planarization (CMP) is a process of planarization of metal and dielectric surfaces typically in microelectronic devices manufacturing. Planarization is achieved by removing material from the wafer surface due to the synergistic effect of chemical and mechanical actions [1]. A typical CMP machine as shown in Figure 1.1, is composed of the following parts

i. Head:

The upper part is referred to as the head. It holds the wafer, rotates, and applies a force on the wafer against the lower part.

ii. Platen:

The lower part is referred to as platen and also rotates with a certain velocity. A relatively softer pad is mounted on the platen.

iii. Slurry supply system:

A CMP tool also has an external source of slurry, that provides the slurry at the desired flow rate. The slurry is composed of chemicals (oxidizer, chelating agents, corrosion inhibitor and surfactants, etc.) and nanometer-sized hard abrasive particles.

iv. Conditioner

It is used for pad conditioning. It has diamond grit on it which helps in removing polishing debris and maintaining pad surface roughness during CMP.

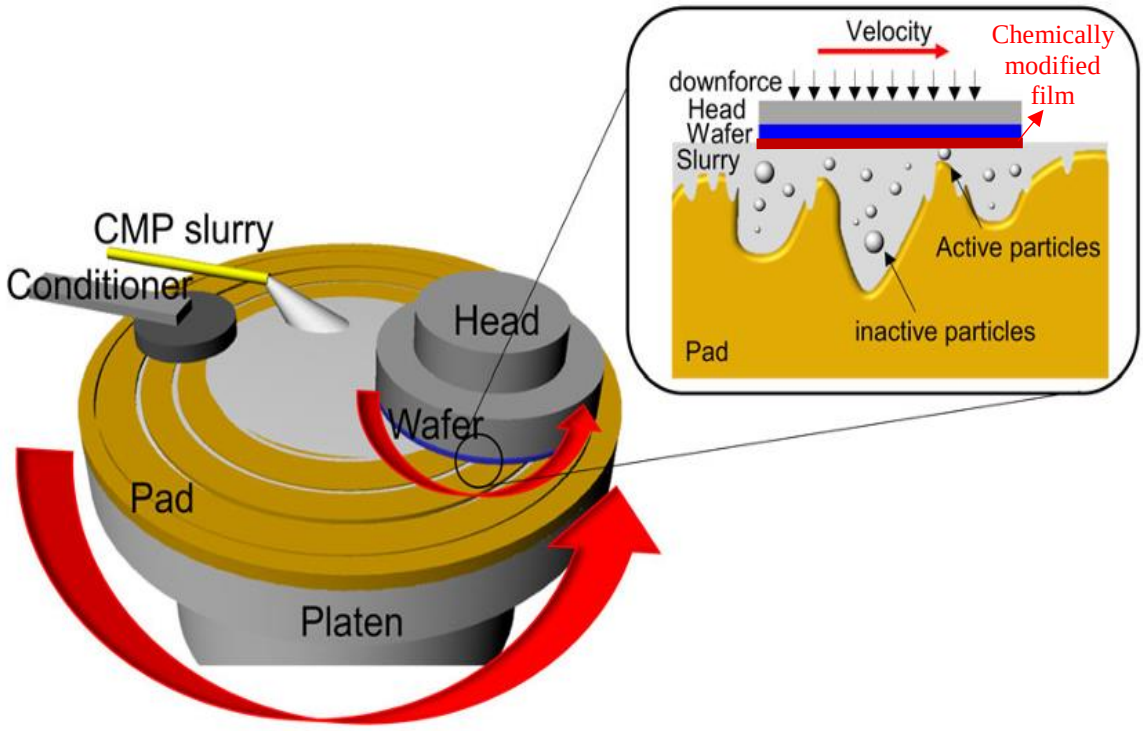

Figure 1.1 Schematic of chemical mechanical polishing tool [1].

Traditional polishing processes have been used for centuries for smoothening of optical glasses and ceramics [1]. The idea of CMP was first introduced by Klaus D. Beyer in 1983 at IBM Base Technology Lab in the USA. The objective was to achieve a highly planar surface to minimize the distortion in subsequent lithographic imaging. In 1986 IBM launched a project for oxide CMP development and a pilot line. Outside of IBM, Sematech adopted CMP in its manufacturing processes in 1988. In 1995, the IC manufacturing industry embraces the technology, and CMP was included in the Semiconductor Industry Association (SIA) roadmap for the first time. Today CMP is a "mainstream" process in the IC manufacturing industry and is used in all three areas of semiconductor devices manufacturing, as shown in Figure 1.2.

i. The front end of the line (FEOL): The transistor device part

ii. The middle of the line (MOL): The contact metal part

iii. The back end of the line (BEOL): The interconnect part

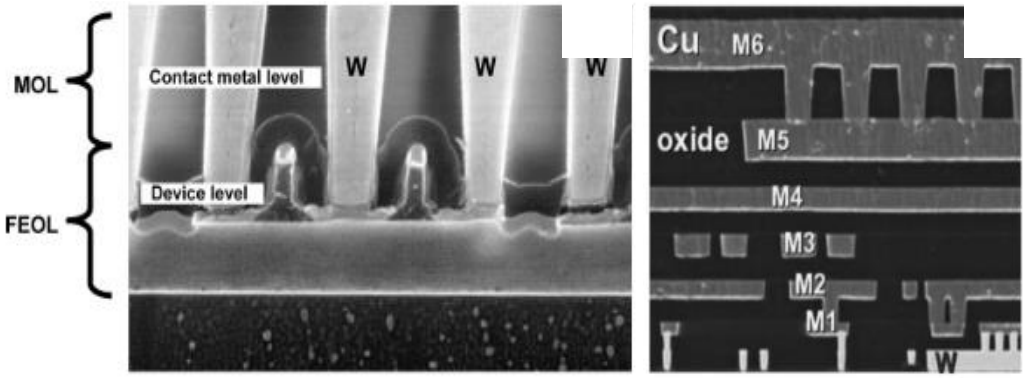

Figure 1.2 Cross-sectional SEM Image showıng (a) device (FEOL) and contact metal levels (MOL) and (b) of six-level Cu interconnect structure (BEOL) [2].

1.2 Why CMP?

In the early semiconductor manufacturing processes, a single level of interconnect wiring was used to connect multiple devices in the complementary metal oxide semiconductor (CMOS) device. In a single-level metallization scheme, a significant area of the chip was occupied by the wiring. CMOS had a high interconnect delay. The interconnect delay is generally calculated as RC delay. RC delay is defined as the time taken by the voltage at one end of the metal line to reach 63% of the applied step input at the other end [3-5].

To decrease the RC delay multilevel metallization was introduced. Multilevel metallization is the process of connecting many devices by several layers of metal interconnects which are separated by a dielectric material and connected by vertical vias [3].

Multilevel metallization needs the planarization of the surface before deposition of another layer. Figure 1.3a shows multilevel metallization without planarization of the surface between several deposition steps. The irregular deposition hinders the efficiency

of lithography, can cause variations in the thickness of lines, and possibly result in short-circuiting. Figure 1.3*b* shows an IC where CMP was used to planarize the surface before each deposition step.

In CMP, the materials in higher regions are removed faster than those in lower regions which leads to planarization. The following objectives/purposes make CMP a crucial process in semiconductor manufacturing.

i. Control over topography
ii. Lithography is better with planar surfaces. Small depth of focus problems can be avoided
iii. CMP enabled multiple levels of metal
iv. Shallow trench isolation in CMOS processes
v. Helps in patterning hard to etch materials

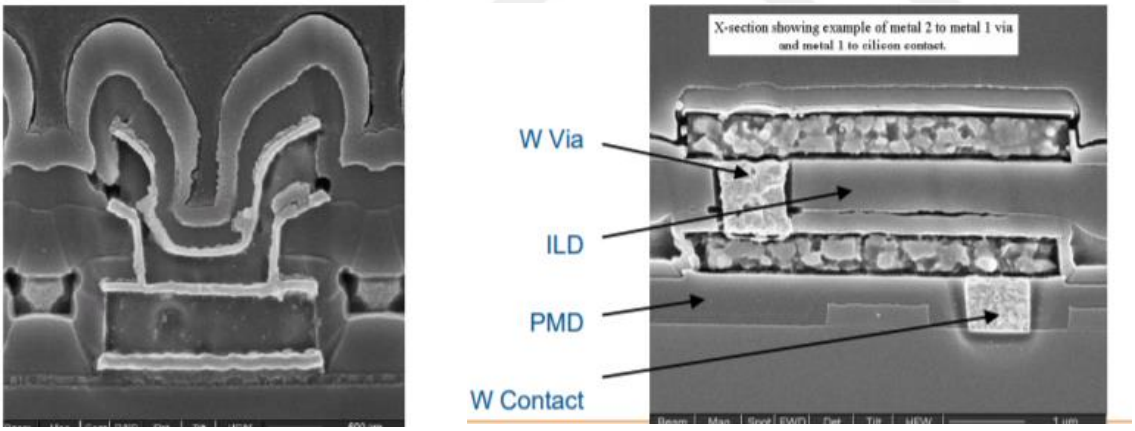

(a) (b)

Figure 1.3 Integrated circuit (a) without performing CMP: traditional device (a) after performing CMP[3].

1.3 Consumables/Components of CMP

Slurry: Slurry is the most important component of CMP process. It contains submicron-sized abrasive particles and chemicals. Slurry flows between the sample surface i.e. wafer and the pad for material removal by mechanical and chemical action. Different materials have different properties and CMP of any material requires different abrasives and different slurry chemistry. Most commonly used abrasive particles for metal CMP are SiO_2 [4,5], Al_2O_3 [6] and while CeO_2 [7] is mostly used for oxide and glass CMP. Different chemical agents used in a metal slurry are listed below.

- Oxidizer: Most commonly used oxidizer is H_2O_2
- Chelatıng agent: forms a metal complex
- Corrosion inhibitor: protects metal against corrosion
- Surfactant: helps in changing wafer surface properties
- pH adjuster: controls the acidic or basic nature of the slurry

Pad: Different pads used for different materials to be polished. They vary in material type, porosity, pad thickness, grooving type, density and hardness.

Speed:

- Rotational speed of the head carrying the sample
- Rotational speed the platen having the pad mounted on it.

Force: Force is applied on the wafer which presses the wafer against rotating pad.

The combination of all the above consumables enable the removal of material from the wafer surface and result a wafer with highly planar surface can manufactured.

1.4 CMP process modeling: Literature Review

The combination of chemical and mechanical effects limits our ability to understand the complex material removal mechanism in CMP. There have been several attempts to model MRR in CMP. The models have been divided into particle scale, feature scale and wafer scale [8]. Figure 1.4 shows the possible contact mechanism of the wafer and pad in a typical CMP process. Here we divide the models into three different categories; i) Empirical models ii) Hydrodynamics and lubrication theory based models and iii) contact mechanics based models. Different models in the literature are briefly explained here.

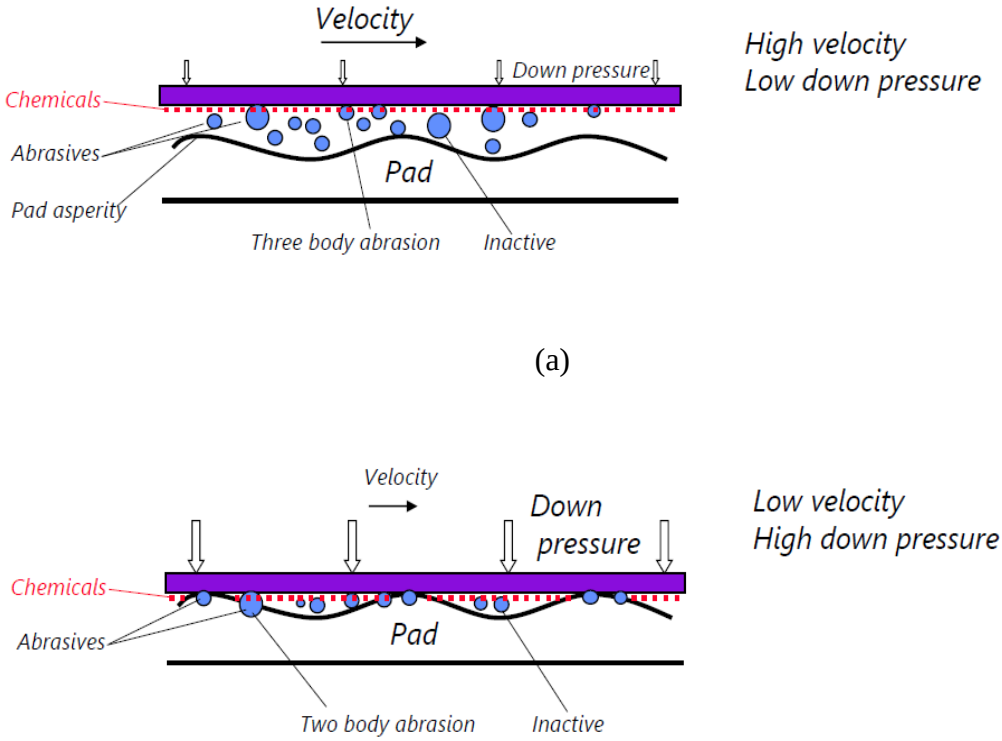

Figure 1.4 Possible contact modes in CMP (a) Hydrodynamic contact mode (b) solid-solid contact mode [8]

1.4.1 Analytical Models

Intensive efforts have gone into developing models to explain the complex mechanism of material removal in CMP processes. First and the most famous material removal model was proposed by Preston [9]. The model is based on experimental results for glass polishing. The model relates MRR to the pressure (P) and relative velocity (V) between the pad and the wafer, as follows

$$MRR = K\,PV \qquad (1.1)$$

where K is known as Preston's constant which accounts for the combined effect of all the remaining parameters. Preston's equation shows a linear dependence of MRR on the product of relative velocity (V) between the pad and the wafer, and the pressure (P). A similar model, in the area of wear, was developed by Archard [10]

$$MRR = K\,\frac{PV}{H} \qquad (1.2)$$

where H is the hardness of the material's surface from which material gets removed. Both Preston and Archard's equations show a linear dependence of MRR on the applied pressure times velocity. However, experimental data in many cases have shown nonlinear relationship with pressure times velocity. Moreover, Preston's model is unable to explain the effect of polishing pad and slurry properties.

Over the time several modified forms of Preston's equation were proposed. Maury et al. [11] added a fitting parameter (MRR_o) to Preston's equation, since the MRR cannot be extrapolated to zero. Their developed model is given as

$$MRR = K\,PV + MRR_o \qquad (1.3)$$

Luo et al. [12] investigated the dependence of copper material removal rate on the applied load, relative velocity between the wafer and pad, and abrasive concentration in the slurry. Based on their experimental results they proposed a model as

$$MRR = (KP + B)V + R_c \qquad (1.4)$$

where K is Preston constant, while parameters B and R_c are calculated from experimental results.

Later Wrschtk et. al [13] proposed a nonlinear model with two fitting parameters α and β, to obtain a better fit of the experimental data. Wrschk et. al equation is given as

$$MRR = K\,P^{\alpha}V^{\beta} \qquad (1.5)$$

Tseng and Wang [14] and re-examined the material removal rate dependence on pressure and relative velocity and proposed models as

$$MRR = K\,P^{5/6}V^{1/2} \qquad (1.6)$$

Shi and Zhao [15] proposed a model with MRR's nonlinear dependence on the applied pressure with a linear dependence on the relative velocity between the pad and the wafer.

$$MRR = K\,P^{2/3}V \qquad (1.7)$$

The models developed by Wrschk, Tseng, Shi and Zhao, and Wang suggest nonlinear dependence of MRR on downforce (P) times velocity (V). A major problem with the Preston model and its modified versions is their inability to consider the effects of the pad properties and CMP consumables such as the abrasive particle properties, effect of effect of particle size and concentration.

1.4.2 Hydrodynamics based models

Some studies have analyzed CMP process using fluid mechanics. These studies assume that the pad and wafer are completely separated by a thin film of slurry. These studies have investigated the slurry hydrodynamics to find expressions for relevant parameters of CMP process. The parameters include the distribution of slurry film thickness, pressure field, shear stress and shear rate. Some of these models are briefly discussed here.

Runnel and Eyeman [16] solved steady state 3D Navier–Stokes equation and continuity equation to investigate the slurry flow in the gap between the wafer and pad during CMP process.

$$u \cdot \nabla u = -\frac{1}{\rho}\nabla P + \mu \nabla^2 u \qquad (1.8)$$

$$\nabla \cdot u = 0 \qquad (1.9)$$

where u is the velocity vector at any point in the flow, P is the pressure, ρ and μ are the density and dynamic viscosity of the slurry, respectively. The slurry was modelled as incompressible Newtonian fluid. To determine the slurry (fluid) layer the assumed the slurry film is stable and fully supports the wafer carrier and applied load.

They reported the effect of viscosity of the slurry, the dome height and rotation speed on the slurry film thickness. They provide compelling trends in the slurry film thickness. However, the existence of this film may be the reason behind the complex nature of the CMP and determines whether mode of non-contact, partial or full contact between the wafer and pad.

Sundararajan et al. [17] developed a 2D model based on lubrication and mass transport theory. Initially they assumed that the wafer had a curvature and solved 1D steady state Reynolds equation for a convex slurry film. The film is called convex when the wafer is bent downwards i.e. towards the wafer. If the wafer is bent upwards i.e. away from the wafer in the middle, the film is referred to as concave. They solved the equation for calculating the pressure and slurry film thickness. Then, they utilized the equation for Couette/Poiseulle flow to determine slurry velocity distribution $u(x, y)$.

$$u(x,y) = U\left(1 - \frac{y}{h}\right) - \frac{dp}{dx}\frac{h^2}{2\mu}\frac{y}{h}\left(1 - \frac{y}{h}\right) \qquad (1.\ 10)$$

where U is the relative velocity, p is the dynamic pressure and h is the slurry film thickness. In this work the material removal due to mechanical abrasion by particles embedded in the pad was ignored and slurry erosion was considered as the main wear mechanism. Finally, to predict the MRR over the wafer's surface, they combined their lubrication study results with mass transport theorem.

Cho et al. [18] developed a model for predicting pressure distribution and slurry film thickness during a typical CMP process. They assumed flat surface of the wafer as well as the pad. They solved polar form of Reynolds equation for a slurry formulated as

a Newtonian fluid, free from abrasive and incompressible. The authors were able to predict the pressure distribution and slurry film thickness by coupling the forces and moments on the wafer with the tilt on the wafer.

Nishioka et al. [19] developed an analytical model. The wafer was modeled as flat surface while the pad was modeled as 3D sinusoidal surface. They investigated the slurry film thickness and the friction coefficient between pad and wafer, during a typical CMP process. They derived expressions for the mean shear stress developed on the wafer, and the mean hydrodynamic pressure as function of the slurry film thickness. They provided a comparison between the experimentally measured coefficient of friction and the coefficient of friction of predicted by the model.

Shan et al. [20] and Chen and Fang [21] calculated the hydrodynamic pressure distribution over the wafer using 1D Reynolds equation and validated it with experiments. They assumed the wafer to be stationary and solved Reynolds equation over a line of constant pad velocity. They assumed they a contact stress distribution over the wafer to estimate the slurry film thickness. They found the largest film thickness in the middle wafer and smallest at the edges. Moreover, their simulations and experiments have shown areas of subambient pressure. The model developed by Chen and Fang [21] predicted pressures during CMP greater than atmospheric.

Higgs III et al. [22] expanded the work of Shan et al. [20] and performed 2D analysis over the entire surface of the wafer. In this study polar form of Reynold's equation was used, as given below

$$\frac{\partial}{\partial r}\left(rh^3\frac{dp}{dr}\right)+\frac{1}{r}\frac{\partial}{\partial \boldsymbol{\theta}}\left(h^3\frac{\partial p}{\partial \boldsymbol{\theta}}\right)=6\mu(r\omega)\frac{\partial h}{\partial \boldsymbol{\theta}} \qquad (1.\ 11)$$

where ω is the rotational speed of the pad, μ is the dynamic viscosity of the slurry. The slurry film thickness was found from contact stress distribution. Here as well, the authors found regoins of subambient pressure. Moreover, they validated their predicted results with experiments.

Thakurta et al. [23] presented a model that takes into account pad porosity and its deflection, to predict the slurry velocity and film thickness. In their model both the wafer and pad are moving. They modeled the wafer surface as a parabolic shape and utilized lubrication calculations to simplify Navier-Stokes equation for an abrasive-free Newtonian fluid. The developed the governing equation as given as follows

$$-12\mu\nabla[(h_w-s)^3\nabla p]+\frac{(h_w-s)}{2}\nabla\cdot\left(\vec{U}_w+\vec{U}_p\right)+\frac{(\nabla h_w+\nabla s)}{2}\cdot\left(\vec{U}_p-\vec{U}_w\right)+V_w-V_p=0 \qquad (1.\ 12)$$

The authors were able to determine the slurry flow field, pressure field and the slurry film thickness distribution. It has been shown that the slurry flow near the pad surface follows the motion of the pad while as the vertical distance increases i.e. going towards the wafer the flow of slurry follows the motion of the wafer.

Tichy et al. [24] developed a 1D deterministic model using hydrodynamic lubrication theory and solid contact mechanics. Their model was able to predict the magnitude and the trends of the experimentally measured sub-ambient pressures in the CMP process.

Nagayama et al. [25] studied the slurry flow between the wafer and pad using FLUENT; a CFD code. The governing equation used were continuity, Navier-Stokes and diffusion equations. The analyzed the effect of pad grooves on the slurry distribution. The pads investigate had radial grooves, circular groove and flat wafer i.e. pad without any grooves. It has been reported that in case of flat pad the slurry remains close the pad center for longer time. This is undesirable in CMP; fresh slurry needs to be provided. In case of circular grooves, the slurry does not move in the radial direction. However, the fresh slurry flows in the gap between the wafer and pad when the pad has radial grooves, since the pad grooves pass through the entire surface of the wafer. Figure 1.5 shows the tangential velocity magnitude at the center of gap between the wafer and pad.

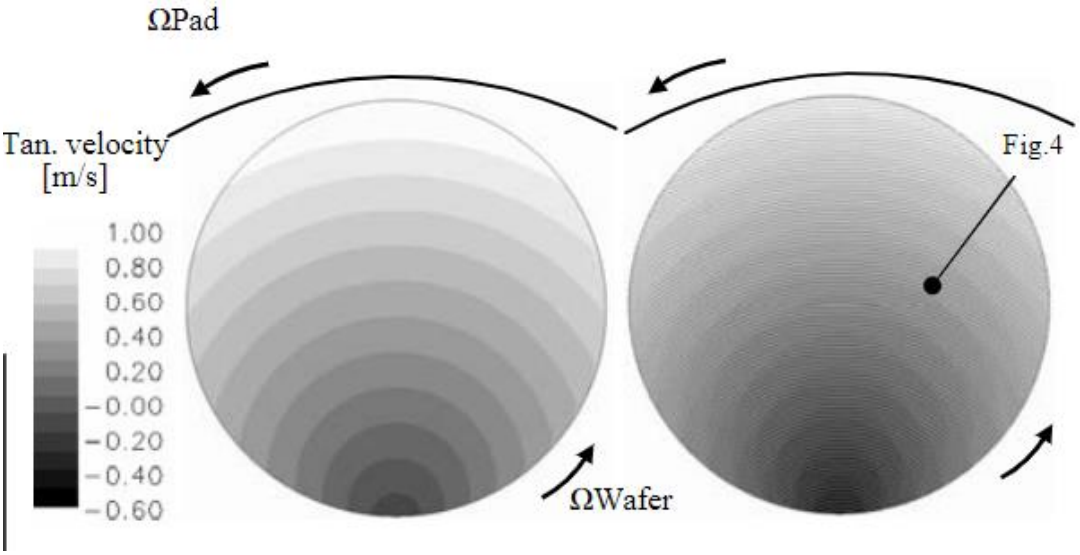

Figure 1.5 Tangential velocity distribution in nongrooved (left) and radially grooved (right) pad

Bae et al. [26] numerically solved Navier-Stokes equation and diffusion equation to investigate the effect of chemical reactions on MRR and surface planarity in a CMP process. The authors first performed simulation for a pore; numerical domain as shown in Figure 1.6a and then integrated the results over the entire wafer. Several parameters

including concentration of chemical agent, aspect ratio of the pore, slurry film thickness, relative velocity of the wafer were investigated. The chemical agents (ferrycyanide and ammonium hydroxide) used in their study facilitate copper dissolution and they have reported an increase in copper MRR with increase in concentration of chemical agent as can be seen in Figure 1.6b. The authors propose a pore aspect ratio of 1.6 for optimum MRR and surface planarity as shown in Figure 1.6c. The MRR increases as the relative velocity of the wafer increases, however, it saturates above a critical value. Moreover, higher velocity results in thicker slurry film and uniform surface planarity can be achieved.

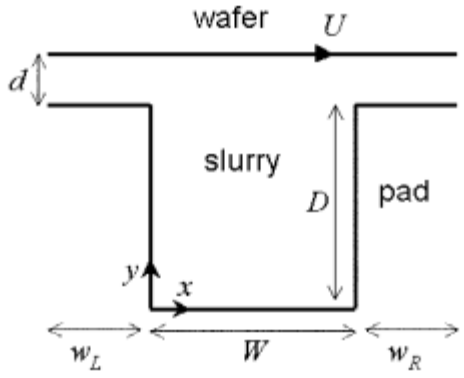

(a)

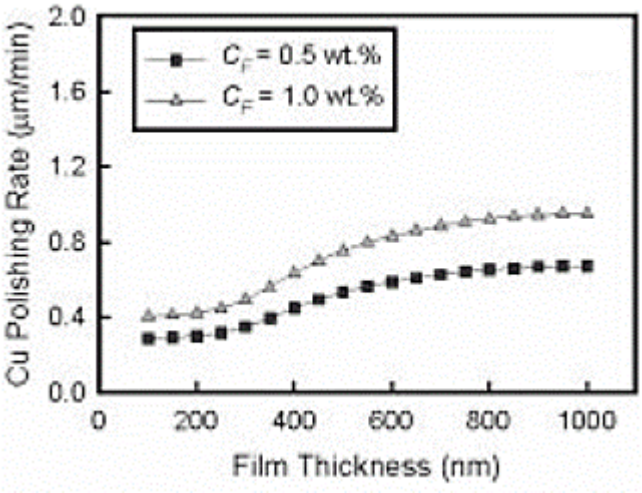

(b)

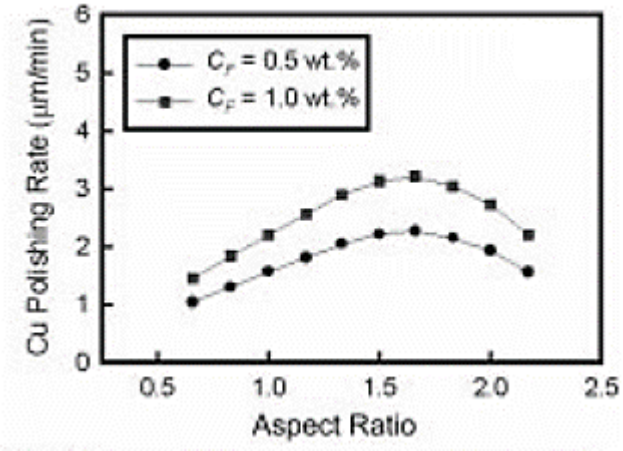

(c)

Figure 1.6 Gap between pad and the wafer, and results of Ref [26], (a) numerical domain for the assumed pore for calculations (b) Effect of chemical agent concentration on MRR (c) effect of pore aspect ratio on MRR

Tian et al. [27] presented a CFD model to simulate the flow of slurry in gap between the pad and wafer for a multi-wafer configuration of CMP. The authors found a gradual increase in the flow velocity along the radius of the polishing pad. For each wafer the highest slurry flow velocity was observed at wafer periphery (farthest from the pad center as shown in Figure 1.7). Their study can be expanded by incorporating the abrasive particles into the model, to understand the behavior of slurry flow field in the presence of abrasive particles during CMP.

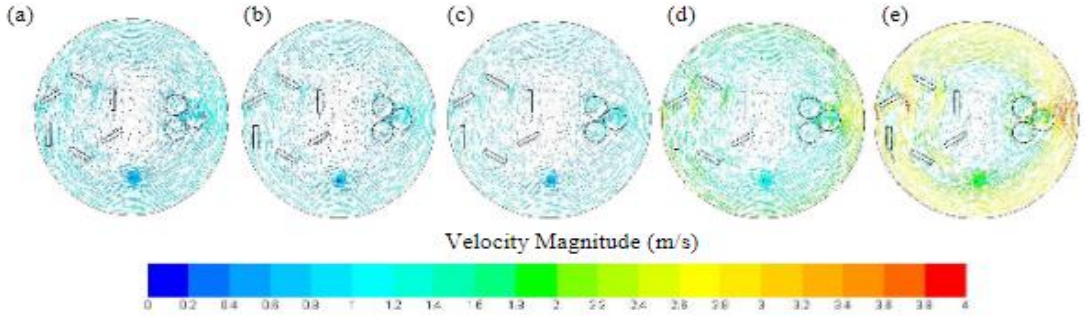

Figure 1.7 Velocity vector field for three wafers configuration simulated under following process variables: conditioner 35 rpm (a) pad 60 rpm, wafer 60 rpm, (b) pad 60 rpm, wafer 120 rpm, (c) pad 60 rpm, wafer 180 rpm, (d) pad 120 rpm, wafer 60 rpm and (e) pad 180 rpm, wafer 60 rpm [27]

The models described till this point did not take into account the effect of abrasive particles. Abrasive particles is one of the key parameters in CMP process. The model developed by Jeng and Tsai [28] couples the granular flow analysis with lubrication theory to account for the effect of abrasive particles. Upon simplification, the combination of the two approaches resulted in the governing equations which describe particle-fluid motion. They found that the MRR increases with increase in particle size. The main focus of their studies was the effect of abrasive particles and they assumed that the slurry was solely composed of the abrasive particles. However, in reality the slurry has very low concentration of abrasive particles usually ranging from 3-5 wt%.

The hydrodynamic and lubrication based modeling of CMP can be of great interest, if the wear rate of the wafer can be related to the behaviour of slurry. Runnel and Eyeman [16] and Runnel [29] solved Navier–Stokes equation to study wear rate and lubrication in CMP processes. They related MRR to the shear and normal stresses developed on the wafer surface during CMP process. They assumed that, in the hydrodynamic lubrication region, the wear rate of the wafer surface is directly proportional the shear rate of the slurry. They proposed the following equation

$$MRR = K\,\sigma\tau \qquad (1.\,13)$$

where σ is normal stress, τ is shear stress of slurry during CMP and K is all purpose constant i.e. Preston coefficient. However, the equation is valid only in the hydrodynamic region i.e. the slurry film thickness is greater than the average surface roughness. When film thickness is smaller than the average surface roughness there will be areas of solid-solid contact and contact mechanics based models need to be developed/used.

Hydrodynamics and lubrication-based models assume slurry film between the wafer and pad. This means that the abrasive particles are unable to indent into the wafer due to the absence of solid-solid contact between the wafer and pad. Then, the models fail to explain the actual purpose of abrasive particles since they are modeled as mere means of changing the viscosity of the slurry.

Another thing is let's say there is a slurry film between the wafer and pad, in that case, the momentum of the particles is not enough to cause wear of the wafer as the relative velocity in most CMP processes is around 1 m/s. Therefore, contact mechanics models are needed to provide insight into the material removal mechanism and predict MRR in a CMP process.

1.4.3 Contact mechanics based models

The empirical models discussed above can be thought of as starting point for contact mechanics based models since they derive equations for MRR as function of the pressure and the wafer-pad interface. However, they do not provide insight into the effect of concentration of solid particle in the slurry, abrasive particle size and properties. They are also unable to the explain the effect of the pad surface topography and mechanical properties. The hydrodynamics and lubrication theory based models assume a slurry film between the wafer and the pad. However, depending upon the applied load, mechanical and surface properties of wafer and pad this layer may or may not exit. Wafer and the pad or wafer, particle and the pad are in contact when the slurry film thickness is smaller than the average surface roughness of either pad or the wafer. Therefore, several contact mechanics based models have been proposed to predict MRR in CMP processes. Some of models from the recent literature are briefly explained here.

Larsen-Basse and Liang [30] investigated possible wear mechanism in CMP. They utilized different sets of data and logical reasoning with simple calculations. They were able to show that the major material removal mechanism in CMP is wear by abrasion of slurry particles. They proposed the following equation for MRR

$$MRR = C_p s_n t v \qquad (1.\ 14)$$

where C_p is Preston coefficient, $s_n$is pressure or normal stress, t is the shear stress in the slurry liquid and v is the sliding velocity.

Cook [7] developed a physical model and incorporated the elastic modulus (E) of the wafer into Preston equation, as follows

$$MRR = K\,\frac{PV}{2E} \qquad (1.\ 15)$$

Cook proposed a Hertzian elastic contact between the abrasive particle and wafer. Based on this model the relation between down pressure P, abrasive particle diameter x, solid concentration of the slurry k and the surface roughness R_s of the wafer was obtained as follows

$$R_s = \frac{3}{4x}\left(\frac{P}{2kE}\right)^{2/3} \qquad (1.\ 16)$$

Liu et al. [31] developed an MRR model based on Hertzian elastic contact and a statistical method. Their model also involves the pad surface hardness and Young's modulus along with wafer surface hardness and Young's modulus:

$$MRR = C\left(\frac{H_w}{H_w + H_p}\right)\left(\frac{E_s + E_s}{E_s E_w}\right)PV \qquad (1.\ 17)$$

Where C an all-purpose constant accounting the effect of slurry chemistry and other input parameters. The models presented by Cook and Liu suggests a linear

dependence of MRR on the down pressure and the relative velocity; similar to Preston equation. However, these two models provide insight into effect other input parameters as well.

Cook and Liu assumed Hertzian elastic contact for particles indentation into the wafer. However, Zhang and Busnaina [32] found that the contact pressure at the particle wafer interface is more than the yielding strength of the wafer. Therefore, to remove material from surface being polished the indentation of particle is more likely to be in the plastic deformation regime.

Most of the model assumed spherical shape abrasive particles. Mazaheri and Ahmadi [33] treated the abrasive particles as bumpy spheres, and their indentation is approximated as the indentation of the bumps into the wafer. The models till this point assume that the slurry particles are embedded into a flat pad surface and indent into wafer under some applied down pressure.

The pads used in CMP process are not flat, they have certain topographical features. Moreover, the material properties of the pad play key role in material removal process in CMP. Yu et al. [34] developed a model that incorporates the pad properties. They assumed the pad to have a certain number of asperities. The pad asperities height follows a Gaussian distribution about a mean plane and the asperities are hemispherical near the peaks. The model shows the real contact area is smaller than the nominal contact area and is proportional to the applied down pressure. Zhao and Shi [15] also proposed a similar model except with the difference that the asperities did not have a Gaussian distribution. Based on Hertzian elastic contact they a relationship between the area of contact and applied pressure as $A \propto P^{2/3}$ and approximated material removal rate as $MRR = K(V)P^{2/3}$, where $K(V)$ is a function of relative velocity between the wafer and

pad, and other input parameters. The authors further argued that the friction between the wafer surface and abrasive particle determine the rolling kinematics of the particles, and the rolling particles have negligible effect of MRR. To avoid the particles rolling the applied down pressure P_{app} must be greater than a threshold down pressure P_{th}. They formulated MRR as follows

$$MRR = K(V)\left({P_{app}}^{2/3} - {P_{th}}^{2/3}\right) \qquad \text{When } P_{app} > P_{th}$$
$$MRR = 0 \qquad \text{When } P_{app} < P_{th} \tag{1. 18}$$

The MRR dependency on down pressure in Yu et al. and Zhao and Shi's model is due to the dependency of contact area between the wafer and pad on the down pressure. Therefore, a complete model incorporating the particle indentation as function of applied down pressure is needed, since MRR is equal to material removed by a single abrasive particle times the number of abrasive particles.

Cook [7] assumed that the wafer and pad are not in direct contact and separated by abrasive particles. He introduced the particles indentation into model to predict MRR. He assumed the particle to be spherical and closely packed on the pad surface. Based on these assumptions the force experienced by a single abrasive can be calculated as follows

$$f_p = \frac{2\sqrt{3}\,P\,R^2}{K} \tag{1. 19}$$

Where K is the fill fraction of the abrasive particles on the pad, P is the down pressure and R is the radius of the abrasive. Cook's model was expanded by Ahmadi and Zia[35] and Zhao and Shi for hard and soft pads, respectively. Zhao and Shi suggested the load from the wafer is supported by the pad asperities as well as the particles

embedded in the pad. This idea was utilized by Luo and Dornfeld [32–34] and were able to show that this force is proportional to abrasive particle size and the contact pressure. Furthermore, the number of particles embedded in the pad is dependent on the pad properties as well as the distribution of abrasive particle size. The authors also presented a more complex scenario i.e. not all particles take place in material removal process. The particles embedded in the pad the indenting into the wafer contributes to material removal and are called as effective particles. The number of effective particles is function of material properties of the pad, size and concentration of the abrasive particles in the slurry. Since MRR is determined by the effective particles therefore, calculating the number of effective particles is crucial.

Zhao and Chang [39] assumed uniform distribution of abrasive particles in the bulk slurry as well as in the contact area. This results in higher number of effective particles and eventually overestimating MRR. Their calculations of the number of effectives is based on the following assumption. i) The particles are spherical in shape and have an average diameter D. ii) The abrasive particles are uniformly distributed in the bulk slurry. iii) The distribution of particles embedded in pad is the same as in the bulk slurry. Based on the above assumption they proposed the number of effective particles as follow

$$N_{eff} = A_c \left(\frac{6\, C_v}{\pi D^3}\right)^{2/3} \qquad (1.\ 20)$$

Where A_c the area contact between the wafer and pad, C_v is the volume concentration of abrasive particles in the slurry and D is the average diameter of abrasive particles. They assumed plastic contact between the wafer and the particle while elastic contact between the pad and the particle, for determining the depth of indentation of the

particle into the wafer. Furthermore, they used Gaussian distribution of pad asperity heights. To calculate the area of contact they used force balance on the wafer-asperity interface. Their force balance did not incorporate the effective particle. First the area of contact between the wafer and pad was calculated and then number of effective particles was calculated using equation. Yongwu Zhao [40] developed a model based on micro-contact mechanics to explain the transition from elastic to plastic deformation of asperities.

Moon[41] experimentally studied the synergistic effect of chemical and mechanical effects in CMP. He used three slurries i. chemical-less slurry ii. abrasive-less slurry and iii. slurry that had both chemicals and the abrasive particles. He found that MRR is significantly lower (0.4-0.8 times) when chemical-less or abrasive-less slurries were used as compared to when slurry containing both the chemicals and the abrasive particles was used. This means that the increase in MRR in CMP is only when both chemical and mechanical components of the slurry act simultaneously.

1.4.4 Coupled Models

There have been several attempts to combine the chemical and mechanical actions, during a CMP process, to develop a coupled material removal model. It is important to note that these models treat the chemical effects as a mere means of changing surface properties of wafer and/or multiply MRR by correction factor to account for the chemical effects. Most of the earlier models have focused one effect i.e. chemical effect or mechanical effect. Or relying on only one type of interaction i.e. the interaction between particle and wafer or only the interaction between chemicals and the wafer. These models can be misleading. For example, in contact mechanics based modeling if only the interaction between the particle and the wafer is considered then MRR increases with increase in particle size. However, during particle-pad-asperity interaction the

number of effective particles decrease with increase in particle size and eventually MRR decreases.

In CMP process material removal occurs due to the synergistic effect of chemical and mechanical actions. Therefore, developing a comprehensive model of CMP process is needed, that takes into all the possible interactions.

Luo and Dornfeld [36-38] have developed a material removal model by integrating i) the interaction between the abrasive and the wafer, ii) the interaction between the abrasive and the pad, iii) the interaction between the wafer and the pad iv) the interaction between the chemicals in the slurry and the wafer surface. These different types of interactions can be seen in Figure 1.8.

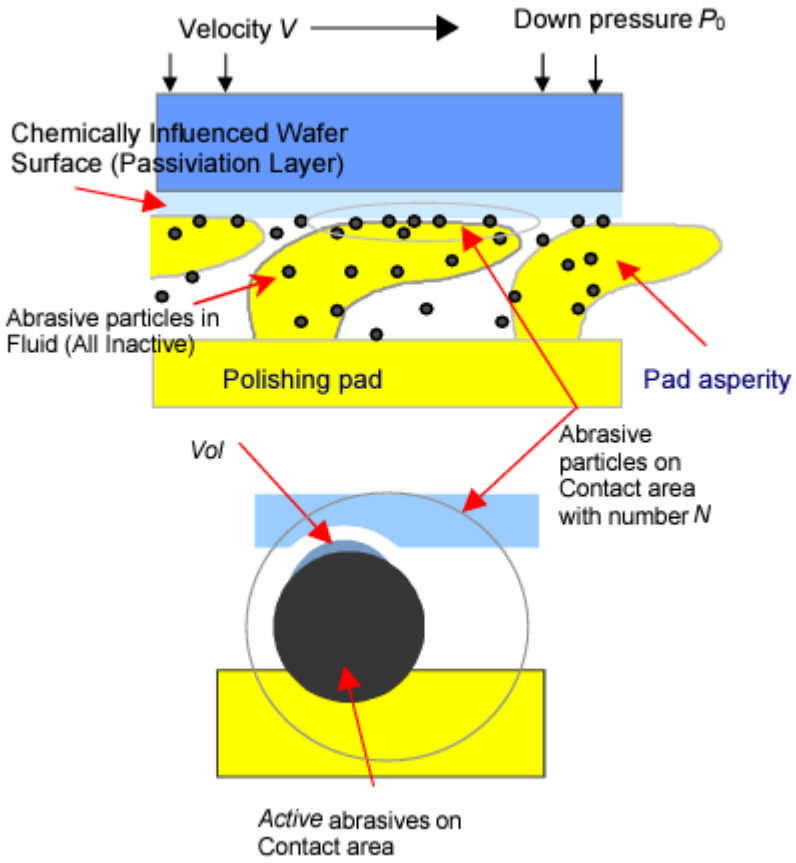

Figure 1.8 Interaction among wafer, slurry abrasives particle and polishing pad [36]

The chemicals in the slurry react with the wafer surface and change the mechanical properties of the surface layer i.e. modified layer forms on the wafer surface. The pad is rough and has certain number of asperities with uniform height distribution. Under applied down force the asperities contact the wafer. Upon this contact some abrasive particles are captured in the contact area. These particles are known as effective particles. The effective particles indent into the chemically modified film and remove material from the surface by sliding along the surface with relative velocity. In the integrated model developed the contact between the abrasive and wafer is modeled as plastic while the interaction between the abrasive and pad asperity is modeled as elastic; the interaction between the wafer and pad asperity is modeled as elastic Hertzian contact and finally the interaction between the chemicals in the slurry and the wafer surface is modeled as passivation.

Zhao et al. [42] developed a mathematical model that describes the mechanism of material removal in CMP process, based on the synergistic effects of chemical and mechanical actions. They modelled the chemical reaction on the wafer surface as the conversion of strongly bonded atoms/molecules to weakly bonded molecular species. While the mechanical actions were modelled as the source of necessary energy to remove these weakly bonded surface molecular species.

The Zhao and Maietta [40] and Zhao and Chang [39,40] models were combined and extended by Oh and Seok [43] by incorporating the effective particle in the pressure balance, and using diffusion of water into the wafer to account for chemical action of slurry in CMP. Seok modeled the number of effective particles as a function of slurry

bulk concentration, particle radius and the surface topography of the pad. The contact between the abrasive and wafer as well as the contact between the abrasive and pad was modeled as elastoplastic. The pad asperity height was considered as Gaussian and the contact area was measured by applying a force balance on the wafer-particle-asperity interface. In first step of their model the abrasion removes material from the wafer surface and then the diffusion equation is solved for characteristic time which is defined as the time needed for abrasive particles to remove thickness equal to characteristic length (1Å). However, in modelling chemical effects of slurry as the diffusion of water into the wafer the initial condition for diffusion is set to zero for every step of solving diffusion equation and the MRR reported is independent of time. Moreover, the contact models described above assume plastic contact between particle and the wafer which results in predicting higher MRR as compared to experimental results. Therefore, further investigation of the type of contact between particle and the wafer is crucial to predicting MRR in CMP processes.

1.5 Research gap/questions

Despite a plethora of literature available on modeling of CMP process, there is an ample gap in developing a model that integrates different interactions occurring in CMP. Following are the questions that need to be answered to develop a model that predicts MRR in a CMP process.

i) Does the material removal happen due to a thin layer of slurry i.e. is the material removal due to 3-body interaction? Why or why not?

ii) Does the material removal happen due to contact between wafer, abrasive particle and pad i.e. is the material removal due to 2-body interaction? Why or why not?

iii) What is the actual material removal mechanism during CMP?

iv) How can the contact between the wafer, abrasive particle and pad be modeled? Which deformation regime do the contacts belong to?

v) How can the chemical interactions between the chemicals in the slurry and the wafer surface be modeled?

vi) How can the chemical and mechanical effects be integrated together to predict MRR in a typical CMP process?

vii) What are input process parameters that effect the performance of CMP process?

viii) Develop a methodology to realize a specific material removal selectivity of various materials during CMP. What are the key parameters in achieving minimum standard deviation in thickness removed, in case of simultaneous polishing of different materials?

ix) What is the importance of ex-situ electrochemical analyses of the wafer and how it can help in achieving specific material removal selectivity of various materials during CMP?

1.6 Hypotheses

The material removal mechanism is wear due to contact between the wafer, abrasive particle, and pad.

The contact between the wafer and the pad asperities depends upon the material properties of the wafer and the pad, and the applied down pressure.

A force balance has to be applied on the wafer-particle-asperity interface to calculate the average contact area between the wafer and pad.

The chemical effect of slurry can be modeled as a diffusion process and here it is limited to the diffusion of water into the wafer.

1.7 Assumptions

The wafer is considered smooth.

The pad is assumed to be rough and has 10^8 asperities per square meter.

The asperities round near the peaks and have a radius of $40\mu m$.

The asperity heights have a Gaussian distribution.

The abrasive particles are uniformly distributed in the bulk slurry.

The abrasive particles have an average radius R_p in the order of tens of nanometers.

Only effective particles are responsible for material removal.

The contact between the abrasive particle and the wafer is assumed to elastoplastic. The contact between the abrasive particle and the pad is assumed to be elastoplastic.

The chemical effects can be modelled as diffusion of water into the wafer. The diffused sites have different hardness and an average hardness can be taken to calculate MRR.

1.8 Objectives of the study

1.8.1 Main objectives

i. The main objective of this work is to develop a model that couples chemical effects with mechanical effects to predict MRR in a typical CMP process.
ii. Model-based optimization of CMP input parameters for uniform material removal of for different materials

iii. Electrochemical analysis based investigation for 1:1:1 material removal selectivity of Cu, Mn and MnN

1.8.2 Specific objectives

To model different types of interactions happening in a CMP process

- Mechanical interactions
  - **i.** The interaction between the wafer and the pad
  - **ii.** The interaction between the abrasive particle and the wafer
  - **iii.** The interaction between the abrasive particle and the pad
- Chemical interactions
  - **i.** The interaction between the chemicals in the slurry and the wafer surface

1.9 Methodology

In this work we developed an integrated model to predict MRR during CMP. The model couples the chemical effects with mechanical effects.

The methodology for developing a model for mechanical actions during CMP process is briefly discussed here.

The wafer is considered smooth while the pad is rough with a certain number of asperities per unit area. The asperity heights have a Gaussian distribution.

The number of effective particles is determined using the bulk slurry solid concentration, particle size and the wafer surface topography.

A force balance applied on the wafer-particle-asperity interface to calculate the average contact area between the wafer and pad.

A force balance on the particle is applied to determine the depth of indentation of the particle into the wafer. The indentation depth is used to determine the area of the cut.

MRR is calculated as the number of effective particles time the volume removed by a single particle.

The chemical effect of slurry is modeled as the diffusion of water into the wafer. 1D diffusion equation is solved to determine the number of water diffused sites along the wafer thickness. The number of diffused sites of water along the wafer thickness is used to find the average surface hardness of the modified wafer surface.

The newly calculated value of the surface hardness is then fed to the mechanical contact model and MRR is calculated and the diffusion is solved again to get the number of diffused sites.

This cycles repeats for a desired number of steps and finally the average MRR for a certain amount of time is calculated.

The model is then used for Optimization of input parameters for uniform material removal of for different materials.

1.10 Organization of thesis

This dissertation is divided into five chapters: Chapter one introduces the process of chemical mechanical polishing in details. It also provides literature review on models developed to predict MRR in CMP process.

Chapter two describes the integrated model developed. First, the contact mechanics based model is developed. A force balance, incorporating the abrasive particles, on wafer-particle-asperity contact is used to calculate area of contact, the number of effective particles and MRR. In the second part 1D diffusion equation is solved

for water diffusing into the wafer. As a result of water diffusion the hardness of wafer changes. In the final part, the diffusion and contact models are coupled to predict MRR in typical CMP process.

Chapter three utilizes the model developed in chapter two and optimizes input process parameters to achiever a desired material removal selectivity.

Chapter four provides electrochemical evaluation of Cu and barrier materials. The barrier materials used in this study are Mn and MnN. The effect of the concentration of H2O2 is investigated on the electrochemical behavior of the materials under consideration. The chapter provides insight into the relationship between the concentration of H2O2 and material removal selectivity during CMP of Cu, Mn and MnN system, and the surface planarity after CMP. Chapter five provides the concluding remarks and future directions/studies.

CHAPTER II

DEVELOPING COUPLED MATERIAL REMOVAL MODEL FOR CMP PROCESS

2.1 Introduction

Chemical mechanical polishing (CMP) is a process of planarization of metal and dielectric surfaces typically in microelectronic devices manufacturing. Planarization is achieved by removing material from the wafer surface due to the synergistic effect of chemical and mechanical actions. In a typical CMP machine, shown in Figure 2.1. the upper part is referred to as the head. It holds the wafer, rotates and applies a force on the wafer against the lower part. The lower part is a rotating platen with an attached relatively softer pad. During CMP slurry is externally provided at a desired flow rate. The slurry is composed of chemicals (oxidizer, chelating agents, corrosion inhibitor and surfactants etc.) and nanometer-sized hard abrasive particles. The chemicals react with surface and modify the surface properties while the abrasive particles indent into the wafer surface and remove material from the wafer surface due to relative motion between the wafer and pad.

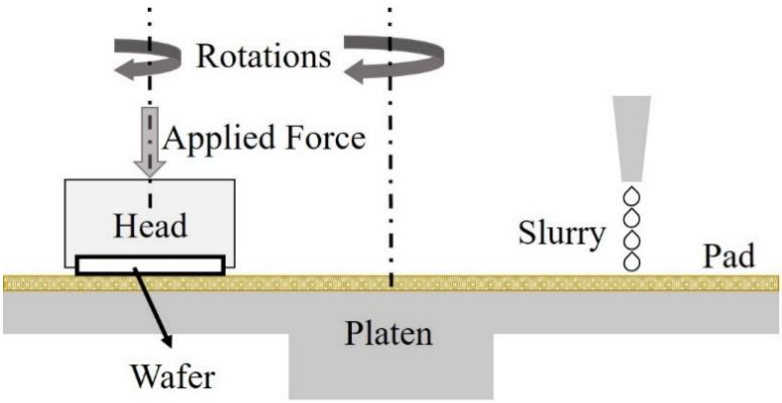

Figure 2.1 Schematic of a typical CMP setup

The combination of chemical and mechanical effects limits our ability to understand the complex material removal mechanism in CMP. Intensive efforts have gone into developing models to explain the complex mechanism of material removal in CMP processes. Initially Preston proposed a model i.e. MRR $= K\,PV$, known as Preston's equation, to predict MRR in CMP of glass.[9] Preston's equation shows a linear dependence of MRR on the product of relative velocity (V) between the wafer and pad, and the downforce (P), and K is known as Preston's constant which accounts for the combined effect of all the remaining parameters. Over the time several modified forms of Preston's equation were proposed. Tseng and Wang[14] and Shi and Zhao[15] re-examined the material removal rate dependence on pressure and relative velocity and proposed models as MRR=$K\,P^{5/6}(\mathrm{V})^{1/2}$ and MRR=$K\,P^{2/3}V$, respectively. Their models suggest nonlinear dependence of MRR on downforce (P). Luo et al[12] investigated the dependence of copper material removal rate on the applied load, relative velocity between the wafer and pad, and abrasive concentration in the slurry. Based on their experimental results they proposed a model as MRR = $(K\cdot P + B)*V + R_c$, where K is Preston constant, while parameters B and R_c are calculated from experimental results.

Runnel and Eyeman[29], [44] numerically solved Navier-Stokes equation to study wear rate and lubrication in CMP processes. They considered slurry as an incompressible Newtonian fluid and provided insight into the flow behavior of slurry between the wafer and pad. They related MRR to shear and normal stresses developed on the wafer during CMP process. In an another study Reynolds equation was solved to determine the hydrodynamic pressure and the slurry film thickness in CMP.[45] In this work the material removal due to mechanical abrasion by particles embedded in the pad was ignored and slurry erosion was considered as the main wear mechanism. Tichy et al[24]

developed a 1D deterministic model using hydrodynamic lubrication theory and solid contact mechanics. Their model was able to predict the magnitude and the trends of the experimentally measured sub-ambient pressures in the CMP process. Larsen-Basse and Liang[30] investigated possible wear mechanism in CMP. They utilized different sets of data and logical reasoning with simple calculations. They were able to show that the major material removal mechanism in CMP is wear by abrasion of slurry particles. Yu et al[46] studied the wear mechanism in CMP based on the distribution of pad surface asperity heights. They developed a model that explains the combined effect of the slurry hydrodynamics and pad roughness on MRR.[47] Liu et al[31] studied the wear mechanism in CMP processes based on the rolling kinematics of slurry particles between the wafer and pad. Moon[48] experimentally studied the synergistic effect of chemical and mechanical effects in CMP. He used three slurries i.e. chemical-less, abrasive-less and slurry that had both chemicals and the abrasive particles. He found that MRR is significantly lower (0.4-0.8 times) when chemical-less or abrasive-less slurries were used as compared to when slurry containing both the chemicals and the abrasive particles was used. This means that the increase in MRR in CMP is only when both chemical and mechanical components of the slurry act simultaneously. Yongwu Zhao[40] developed a model incorporating slurry particles in micro-contact. Their model is based on micro-contact mechanics and abrasive wear theory. The model was extended by Seok[43] by incorporating diffusion of water into the wafer to account for chemical action of slurry in CMP. In first step of their model the abrasion removes material from the wafer surface and then the diffusion equation is solved for characteristic time which is defined as the time needed for abrasive particles to remove thickness equal to characteristic length (1Å). However, in modelling chemical effects of slurry as the diffusion of water into the wafer the initial condition for diffusion is set to zero for every step of solving diffusion equation

and the MRR reported is independent of time. Moreover, the contact models described above assume plastic contact between particle and the wafer which results in predicting higher MRR as compared to experimental results. Therefore, further investigation of the type of contact between particle and the wafer is crucial to predicting MRR in CMP processes. Other important factors, while modelling CMP, are the initial condition for solving the diffusion equation and how the micro-contact mechanics model and the diffusion model may be coupled. Since, modelling chemical effects as diffusion of water into the wafer may result in diffused site beyond characteristic length. Therefore, for the successive diffusion step the initial condition needs to be updated to measure the wafer surface hardness as a function of time and eventually MRR in the following mechanical abrasion step.

In this work, we propose a model for predicting MRR in a typical CMP process. The model is based on elastoplastic contact theory along with diffusion of water into the wafer. The contact mechanics and diffusion models are coupled in two-step cycle. In the first step MRR due to abrasion is calculated. In the next step, 1D diffusion equation is solved for a moving boundary. The boundary is moving with a velocity equal to MRR. Based on the number of water diffused sites along the wafer thickness new value of surface hardness is calculated and is fed to contact mechanics model to obtain MRR for the next step and the cycle continues for the desired time. The MRR obtained is averaged over the desired time. The MRR predicted is in good agreement with MRR reported in the literature.

2.2 Model Description

The wafer is assumed to be smooth while the pad is considered rough and has $2*10^8$ asperities per unit area[49]. The asperities are round near the peaks and have a

diameter of 50μm[49]. The asperity height distribution function, relative to the mean plane of asperity peaks is known for uncompressed pads and is assumed to be Gaussian. The coordinate system employed for contact modeling is rigidly attached to the mean volume plane. Mean volume plane is defined such that the volume of asperities above is equal to the volume of the valleys below the plane. Each asperity deforms in vertical direction (z-axis) and its deformation is treated independent of the other asperities. The wafer is subjected to a normal load and undergoes a certain displacement into the pad. The local contact forces applied on the wafer are transmitted through the asperities as well as the abrasive particles and are treated in an average sense. The total area of contact, the number of effective particles and the indentation depth of abrasive particle into the wafer are calculated to determine MRR.

The chemical effect of slurry is modelled as, and limited to, the diffusion of water into the wafer. Diffusion changes the surface hardness and this change in hardness is taken as a key role of the chemical action of the water in the slurry. The two models are then coupled in two-step cycle i.e. in the first step the material is removed due to abrasion and in the next step the diffusion equation is solved to obtain the number of diffused sites along the wafer thickness and a new hardness value is calculated. The steps are repeated until the desired time i.e. the time for which the CMP experiments are carried out. Figure 2.2 shows the overall algorithm of the developed model. Different parts of the model are explained in the following sections.

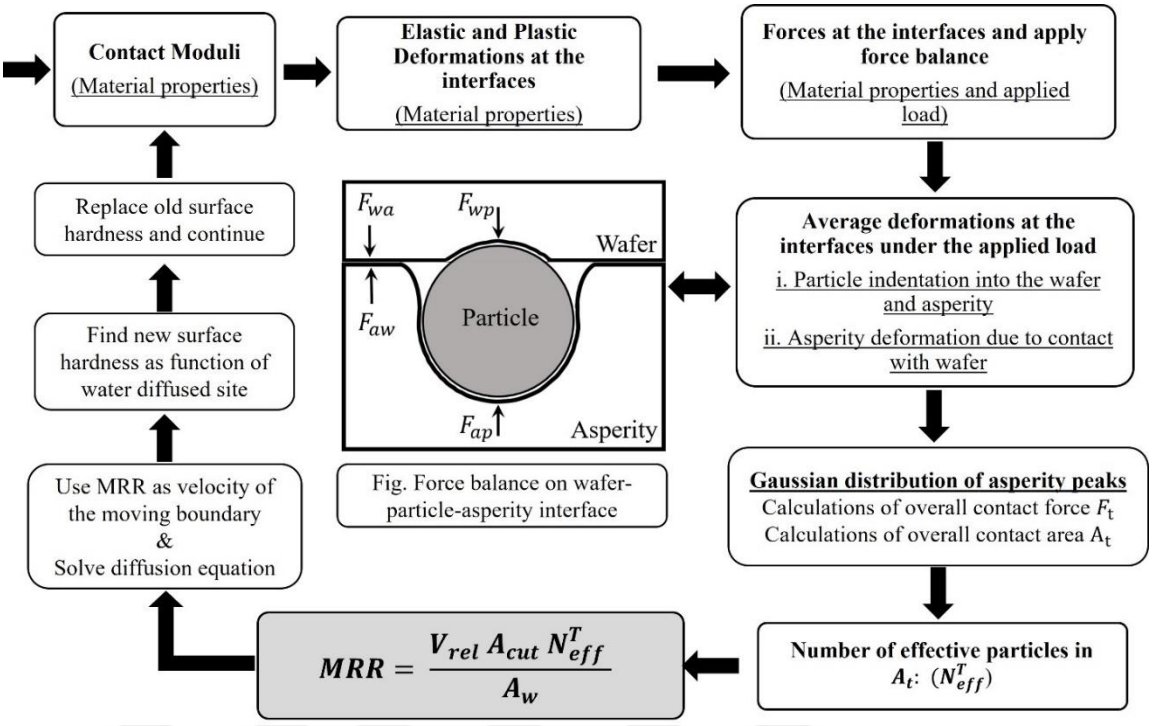

Figure 2.2 Algorithm for material removal rate calculation considering both chemical and mechanical actions

2.3 Modeling the number of effective particles

In a typical CMP process a known amount (%weight or %volume) of abrasive particles is well distributed in the slurry. These abrasive particles are a few tens of nm in diameter. Under some external downforce some of these particles act mechanically (indent) on the wafer and remove material from the wafer by sliding along its surface with relative velocity between pad and the wafer. The particles indenting into the wafer (or in other words the particles trapped in the contact area between pad asperities and the wafer) are known as effective particles. The remaining particles are assumed to flow freely in the gap between the wafer and pad and hence have no wear effect.[50] Determination of the number of effective particles is crucial to predict MRR in CMP processes. Intuitively, the number of effective particles is dependent on the solid concentration in the slurry, average particle size and the contact area between the wafer and pad asperities. The

contact area between the wafer and pad asperities is dependent on the material properties of the wafer and pad, geometric properties of the pad and the applied downforce. Jeng and Huang[51] estimated the number of effective particles, trapped in average total contact area between the wafer and pad. They considered the number of abrasive particles in a unit volume and geometric factors such as pad asperity heights and deformation of asperity. Here, we use the same approach and propose equation (2.1) for calculating the number of effective particles per unit area (N_{eff}).

Figure 2.3 shows the geometric factors influencing the number of effective particles. Average asperity height about mean asperity height plane is σ. The distance between mean asperity height plane and the mean volume plane is μ.[49] The number of effective particles can be written as

$$N_{eff} = \left(\frac{\rho_s W_s D_s}{\rho_p V_p}\right)(\mu + 3\sigma - s) \qquad (2.1)$$

Where ρ_s is density of the slurry, W_s is the ratio of abrasive weight to fluid weight in the slurry, D_s is slurry dilution ratio, ρ_p is density of the abrasive particle, V_p is the average abrasive volume, and s is the separation distance between mean asperity height plane and wafer's surface. In equation (2.1) only the separation distance "s" is unknown and is found later using force balance at the wafer-particle-asperity interface. Upon fully developed contact the area covered by effective abrasive particles can ($Ap_{/a}$) be written as

$$Ap_{/a}(s) = N_{eff}(s) * A_p \qquad (2.2)$$

where A_p is area of an average size single abrasive particle.

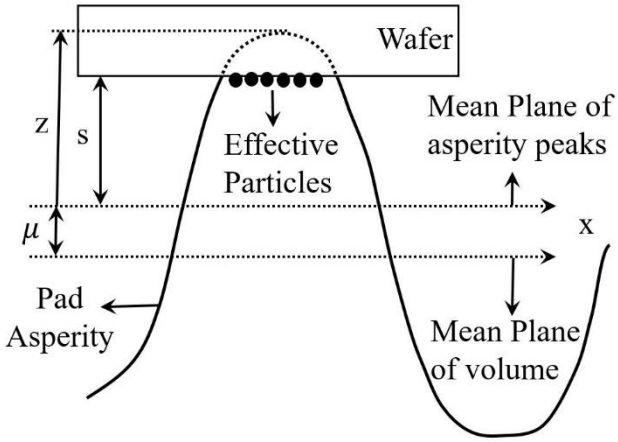

Figure 2.3 Illustration of asperity contact with wafer showing the mean planes for determination of the number of effective particles

2.4 Contact Mechanics: Modelling mechanical effects

Appropriate modelling of contact mechanism at the interface of the wafer, slurry particle and pad asperities is imperative to predict the performance of CMP processes. Figure 2.4 shows the assumed contact between the wafer, abrasive particle and the asperity. Tseng and Wang [14] in an attempt to modify Preston's equation, attributed the normal stress at the particle-wafer contact to elastic indentation of the particle into the wafer surface. Zhang et al [32] found that the Hertzian contact stress at the wafer-particle interface is much larger than the yield strength of the wafer. Therefore, the deformation of wafer due to contact with abrasive particle is not solely elastic.

Zhao and Chang [39] developed a contact mechanics based model which treats deformation of pad asperity due to contact with abrasive particle as fully elastic. While the contact between the wafer and abrasive particle is assumed to be fully plastic. They

have modelled the number of effective particles, the total area of contact between the wafer and pad asperities, and the depth of indentation of abrasive particle into the plastically deformed wafer. This indentation however, results in over-predicting MRR. Jeng and Huang[51] modified Zhao and Chang's model.[40] They treated the deformation of pad asperities due to contact with abrasive particle as elastoplastic, which can be attributed to material properties of the pad asperity and the abrasive particle and the applied load. These studies assume the contact between the wafer and particle as fully plastic.

Here we present a systematic approach to micro-contact analysis of CMP process. In CMP the abrasive particle simultaneously penetrates the wafer and asperity.

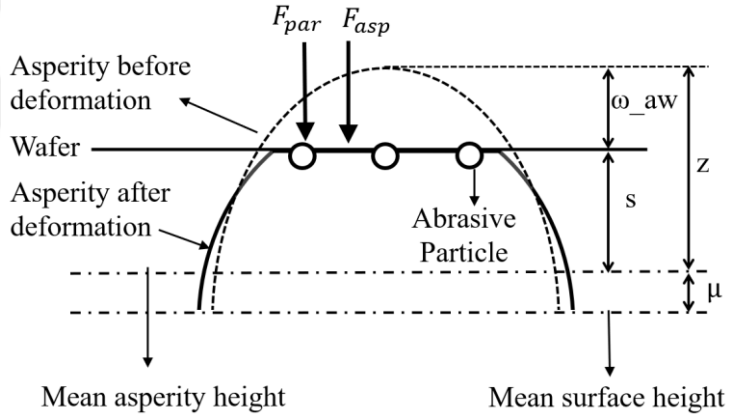

Figure 2.4 Wafer-particle-asperity contact in CMP processes (Fapplied = Fpar + Fasp)

Let E_{ap}, E_{aw} and E_{wp} be the effective Young's moduli at the asperity-particle, asperity-wafer and wafer-particle interface respectively and can be calculated as follows

$$E_{ap} = \left(\frac{1-\upsilon_a^2}{E_a} + \frac{1-\upsilon_p^2}{E_p}\right)^{-1} \tag{2.3}$$

$$E_{aw} = \left(\frac{1-\upsilon_a^2}{E_a} + \frac{1-\upsilon_w^2}{E_w}\right)^{-1} \quad (2.4)$$

$$E_{wp} = \left(\frac{1-\upsilon_w^2}{E_w} + \frac{1-\upsilon_p^2}{E_p}\right)^{-1} \quad (2.5)$$

Where υ is the Poisson's ratio, E is the Young's modulus of the material and subscripts *a*, *w* and *p* refer to asperity, wafer and the abrasive particle, respectively. The framework of the elastoplastic model proposed by Zhao et al[40] and Seok [43] is employed in this work. From intuition one can say that a small, applied load will cause less deformation i.e. elastic deformation and a large force may result in plastic deformation. The actual deformation (ω_{xy}) of material x due to contact with material y is a function of material properties and applied load. We assume that the elastic and plastic deformations that occur due to contact forces are two extremes determined by the amount of the applied load. The critical interference values that determine the elastic limit (ω_{xy}^e) and fully plastic limit (ω_{xy}^p) are given in equations (2.6)-(2.8)[40]. Here subscripts x and y refer to wafer (w), particle (p) and asperity (a), while superscripts 'e' and 'p' refer to elastic and plastic limits, respectively.

$$\omega_{ap}^e = \left(\frac{3*\pi*k_e*H_a*\sqrt{R_a}}{4*{E_{ap}}^2}\right)^2 \quad \text{and} \quad \omega_{ap}^p = k_p * \omega_{ap}^e \quad (2.6)$$

$$\omega_{aw}^e = \left(\frac{3*\pi*k_e*H_a*\sqrt{R_a}}{4*{E_{aw}}^2}\right)^2 \quad \text{and} \quad \omega_{aw}^p = k_p * \omega_{aw}^e \quad (2.7)$$

$$\omega_{wp}^e = \left(\frac{3*\pi*k_e*H_a*\sqrt{R_a}}{4*{E_{aw}}^2}\right)^2 \quad \text{and} \quad \omega_{wp}^p = k_p * \omega_{wp}^e \quad (2.8)$$

Zhao and Change [40] found that for deformation of materials in contact to be fully plastic, the condition $\omega_{xy} \geq 54 * \omega_{xy}^{e}$, needs to be satisfied. Therefore, $k_e = 0.4$ $k_p = 54$ is used in this work[40]. The contact is elastic if $\omega_{xy} < \omega_{xy}^{e}$ and if $\omega_{xy} > \omega_{xy}^{p}$ the contact is fully plastic. However, if $\omega_{xy}^{e} < \omega_{xy} < \omega_{xy}^{p}$ the contact is elastoplastic.

2.4.1 Particle indentation into the wafer

For wide range of contact forces the deformations of wafer and asperity due to contact with the abrasive particles belong to the elastoplastic deformation regime[43]. So, the total force applied by an abrasive particle on asperity (F_{ap}) and the wafer (F_{wp}) can be written as[40]

$$F_{ap} = H_a \left[(1 - (1 - k_e) \left(\frac{ln(\omega_{ap}^{p}) - ln(\omega_{ap})}{ln(\omega_{ap}^{p}) - ln(\omega_{ap}^{e})} \right) \right] * \left[1 - 2 \left(\frac{\omega_{\mathrm{ap}} - \omega_{ap}^{e}}{ln(\omega_{ap}^{p}) - ln(\omega_{ap}^{e})} \right)^3 + 3 \left(\frac{\omega_{\mathrm{ap}} - \omega_{ap}^{e}}{ln(\omega_{ap}^{p}) - ln(\omega_{ap}^{e})} \right)^2 \right] 2\pi R_p \omega_{\mathrm{ap}} \tag{2.9}$$

$$F_{wp} = H_w \left[(1 - (1 - k_e) \left(\frac{ln(\omega_{wp}^{p}) - ln(\omega_{wp})}{ln(\omega_{wp}^{p}) - ln(\omega_{wp}^{e})} \right) \right] * \left[1 - 2 \left(\frac{\omega_{\mathrm{wp}} - \omega_{wp}^{e}}{ln(\omega_{wp}^{p}) - ln(\omega_{wp}^{e})} \right)^3 + 3 \left(\frac{\omega_{\mathrm{wp}} - \omega_{wp}^{e}}{ln(\omega_{wp}^{p}) - ln(\omega_{wp}^{e})} \right)^2 \right] 2\pi R_p \omega_{\mathrm{wp}} \tag{2.10}$$

Figure 2.5shows the wafer-particle-asperity contact. We assume that upon fully established contact the particle is fully embedded into asperity and the wafer. Applying

force balance on a single particle ($F_{wp} = F_{ap}$) and using the geometry ($\omega_{ap} = 2R_p - \omega_{wp}$) in Figure 2.5(b) provides a system of two equations with two unknowns i.e. the indentation of abrasive particle into asperity (ω_{ap}) and the wafer (ω_{aw}). Hence, the indentation of the abrasive particle into the wafer can be found.

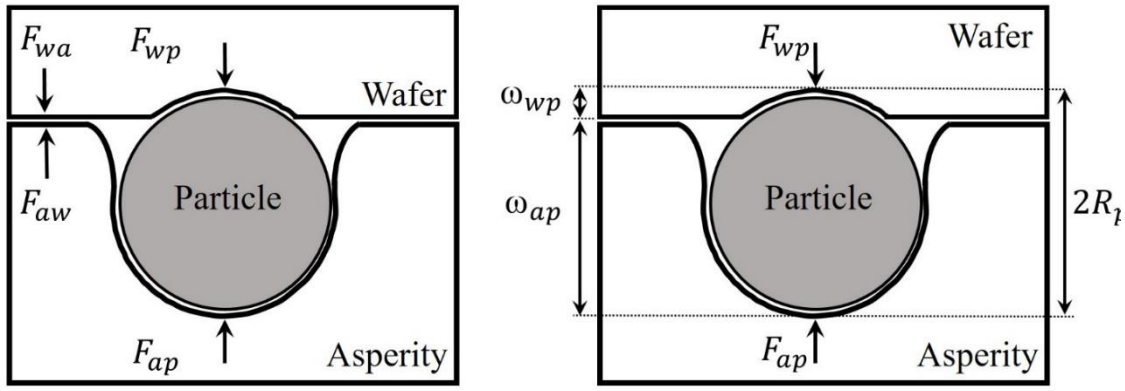

(a) (b)

Figure 2.5 Force balance on (a) wafer-particle-asperity interface (b) single abrasive particle

2.4.2 Overall contact and MRR

The slurry particles are generally embedded in the polishing pad. In CMP a smooth and harder wafer is compressed against a rough and relatively softer pad and moves along its surface with a relative velocity (V_{rel}). Therefore, CMP can be described as a two-body abrasion problem. The pad has a certain number of asperities per unit area. Figure 2.4 shows the contact of single asperity with wafer under applied force (to find the deformation of asperity, the particles are introduced into the force balance later in equations (2.17) and (2.18)). Depending upon the applied load, materials properties, number of asperities per unit area and height of asperities, the asperities may deform

differently. They may deform elastically, plastically or even elastoplastically. The contact forces experienced by the asperities in different deformation regimes can be written as[40]

$$F_a^e = \frac{4}{3} E_{aw} \sqrt{R_a} \, (\omega_{\mathrm{aw}})^{3/2} \tag{2.11}$$

$$F_a^{ep} = H_a \left[(1 - (1 - k_e) \left(\frac{ln(\omega_{aw}^p) - ln(\omega_{aw})}{ln(\omega_{aw}^p) - ln(\omega_{aw}^e)} \right) \right] * \left[1 - 2 \left(\frac{\omega_{\mathrm{aw}} - \omega_{aw}^e}{ln(\omega_{aw}^p) - ln(\omega_{aw}^e)} \right)^3 + 3 \left(\frac{\omega_{\mathrm{aw}} - \omega_{aw}^e}{ln(\omega_{aw}^p) - ln(\omega_{aw}^e)} \right)^2 \right] 2\pi R_a \omega_{\mathrm{aw}} \tag{2.12}$$

$$F_a^p = 2 \, \pi \, H_a \, R_a \, \omega_{\mathrm{aw}} \tag{2.13}$$

Similarly, the contact area of asperities with the wafer for different deformation regimes can be written as

$$A_a^e = \pi \, R_a \, \omega_{\mathrm{aw}} \tag{2.14}$$

$$A_a^{ep} = \left[1 - 2 \left(\frac{\omega_{\mathrm{aw}} - \omega_{aw}^e}{ln(\omega_{aw}^p) - ln(\omega_{aw}^e)} \right)^3 + 3 \left(\frac{\omega_{\mathrm{aw}} - \omega_{aw}^e}{ln(\omega_{aw}^p) - ln(\omega_{aw}^e)} \right)^2 \right] \pi R_a \omega_{\mathrm{aw}} \tag{2.15}$$

$$A_a^p = 2 \, \pi \, R_a \, \omega_{\mathrm{aw}} \tag{2.16}$$

In Equations (2.11)-(2.16) the subscript *a* refers to asperity, *aw* refers to asperity-wafer interface while the superscripts *e, ep* and *p* refer to plastic, elastoplastic and fully plastic deformation regimes, respectively. For other parameters refer to **Error! R eference source not found.**. To understand the effect of abrasive particles on the contact mechanism in CMP it is necessary to apply a force balance at the wafer-particle-asperity

interface. The total contact force transmitted to the asperity is equal to the force transmitted by the wafer due to direct contact with asperities (F_{asp}^{T}) plus the force transmitted through the abrasive particles (F_{par}^{T}).

$$\mathrm{F_{applied}} = F_{asp}^{T} + F_{par}^{T} \tag{2.17}$$

$$\mathrm{F_{applied}} = \mathrm{F_{asperity}}(1 - A_{wp}/A_{contact}) + N_{eff}\, A_{wp}\mathrm{F_{wp}} \tag{2.18}$$

Where $A_{contact}$ is given in Equation 20. A_{wp} is the contact area between the abrasive particle and the wafer and can be obtained using an equation similar to equation (2.15). Using the G-W model[52] the averaged total contact force ($F_{asperity}$) exerted by the wafer on asperities in the absence of abrasive particles can be obtained by summing the contact forces for the all the three deformation regimes and can be written as follows

$$F_{asperity} = \eta * \mathrm{A_w} * \left[\int_{s}^{s+\omega_{aw}^{e}} F_a^e * \phi(\mathrm{z})\,\mathrm{dz} + \int_{s+\omega_{aw}^{e}}^{s+\omega_{aw}^{ep}} F_a^{ep} * \phi(\mathrm{z})\,\mathrm{dz} + \int_{s+\omega_{aw}^{p}}^{s+3\sigma} F_a^{p} * \phi(\mathrm{z})\,\mathrm{dz}\right] \tag{2.19}$$

where η is the number of asperities per unit area, $\phi(z)$ is the probability density function of the asperity heights, and z is the coordinate value representing the asperity height measured from the mean plane of the asperity heights. The integrals in equations (2.19) and (2.20) are evaluated using five points Legendre-Gauss quadrature. Inserting equations (2.19) and (2.20) into equation (2.17) and (2.18) the separation distance 's' i.e. the distance between the mean plane of asperity height and the wafer surface can be calculated. Once "s" is known the total contact area can be calculated as

$$A_{contact} = \eta * \mathrm{A_w} * \left[\int_{s}^{s+\omega_{aw}^{e}} A_a^e * \phi(z)\,dz + \int_{s+\omega_{aw}^{e}}^{s+\omega_{aw}^{ep}} A_a^{ep} * \phi(z)\,dz + \int_{s+\omega_{aw}^{p}}^{s+3\sigma} A_a^p * \phi(z)\,dz\right] \quad (2.20)$$

After calculating the total area of contact the number of total effective particles (N_{eff}^{T}) can be determined using equation (2.1) and multiplying by $A_{contact}$.

Since the indentation of the particle into the wafer (ω_{wp}) belongs to the elastoplastic deformation regime, only the plastic portion of the indentation (ω_{mrr}= $\omega_{wp} - \omega_{wp}^{e}$) is used in calculating MRR i.e. the portion of elastic recovery is assumed to not contribute to MRR. Area of cut (A_{cut}) due to ω_{mrr} is approximated as a triangular area of the indentation ($A_{cut} = \sqrt{2R_p} * (\omega_{mrr})^{3/2}$), since ω_{mrr} is in the order of 1Å. Finally, MRR can be calculated as

$$MRR = \frac{V_{rel}\, A_{cut}\, N_{eff}^{T}}{A_w} \quad (2.21)$$

where V_{rel} is the relative velocity between the wafer and pad, $N_{eff}^{T} = N_{eff} * A_{contact}$ is the number of total effective particles and A_w is area of the wafer.

2.5 Diffusion of water into wafer: Modelling chemical effects

Diffusion of mass is defined as the net movement of mass from higher to a lower concentration region. The diffusion of water into silica is known to reduce its surface hardness[7],[53]. Here we model the chemical effect of slurry in CMP as the diffusion of water into the wafer. Silica layer was chosen as the target material surface to be polished. The chemical effect of slurry is limited to only the diffusion of water into the wafer. Chemical etching is ignored. The diffusivity or diffusion rate is assumed to be independent of the pressure i.e. diffusion coefficient is constant. Water hydrates the

wafer's surface by reacting with it and partly changing surface sites of Si-O-Si to Si-OH. Therefore, the reacted and unreacted sites coexist and have different hardness values.[54] 1D diffusion equation i.e. Fick's second law[55] for a moving boundary (originally proposed by Stefan for solid-liquid phase changes [56]) was solved to calculate the concentration of water-diffused sites as a function of time along wafer's thickness. Since, the boundary is moving because of material removal from the wafer surface this problem requires special treatment of the boundary. Therefore, a new time dependent dimensionless coordinate ζ(t) is introduced as

$$\zeta_t = \frac{x}{l_t} = \frac{l_t - l_r}{l_t} \tag{2.22}$$

where l_r is the equal to characteristic length and l_t is the time dependent thickness of wafer at time t, such that $l_{t-1} < l_t$. Therefore, we can write

$$l_t = l_{t-1} - \int_{t_o}^{t} u\, dt \tag{2.23}$$

where u is the rate of change of thickness of the wafer i.e. MRR and is given by

$$u = \frac{\partial l_t}{\partial t} = MRR \tag{2.24}$$

The substitution of equations (2.22)-(2.24) in 1D diffusion equation and its corresponding initial and boundary conditions result in a diffusion equation of the form

$$\frac{\partial C}{\partial t} = \frac{D}{l_t^2}\frac{\partial^2 C}{\partial \zeta^2} + \frac{u_t}{l_t}\zeta_t \frac{\partial C}{\partial \zeta} \tag{2.25}$$

with initial and boundary conditions as C (ζ_t, 0) = 0, C (0, t) = C_o and $\frac{1}{\zeta_t}\frac{\partial C}{\partial \zeta}(l, t) = 0$. It is important to keep in mind that C (ζ_t, 0) = 0 applies only to the first timestep of solving diffusion equation and increases for every successive step (updating the initial condition). The characteristic time for each step is taken as the time required for the abrasive particles to remove characteristic length. Figure 2.6 shows material removal due to abrasive particles indentation into the wafer (on the right) and diffusion of water into the wafer (on the left). Equation (2.25) and corresponding initial and boundary conditions are simultaneously solved (using MATLAB's built-in function *pdepe* to determine the concentration of water diffused sites along wafer thickness. *pdepe* is used to solve initial-boundary value problems for parabolic-elliptic PDEs in one space variable and time.

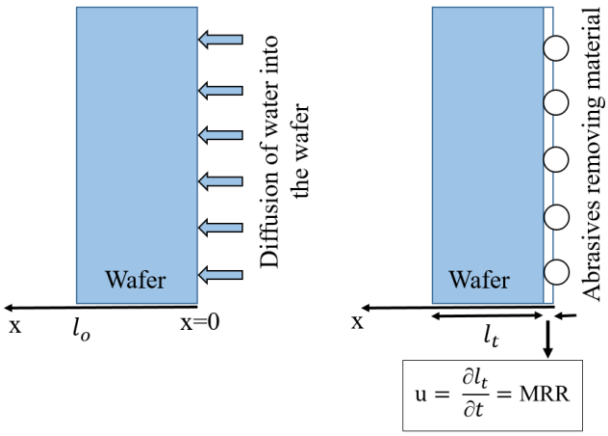

Figure 2.6 Illustration of diffusion into the wafer with moving boundary

2.6 Coupling

The algorithm employed to couple the mechanical and chemical effects can be seen in Figure 2.7. The model first removes material from the wafer's surface by mechanical effects i.e. abrasion and the characteristic time is calculated. Next, the diffusion equation is solved for the characteristic time to determine water diffused sites along thickness of the wafer. Based on the concentration of diffused sites along wafer thickness till particles indentation depth, average hardness of the modified layer is calculated. Finally, the mechanical model recalled with newly determined hardness value of the wafer, and the cycle repeats. After each step of mechanically removing l_r, the concentration of diffused sites along $l_t - l_r$ is used as initial condition for the following diffusion step.

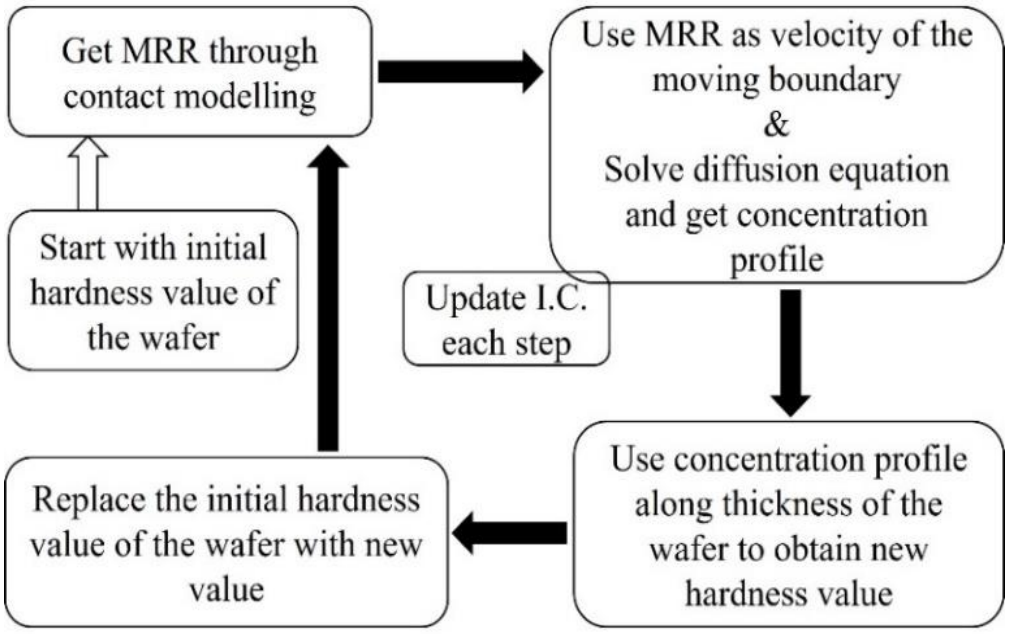

Figure 2.7 Algorithm for coupling the mechanical and chemical effects to accurately predict material removal rate

2.7 Results and Discussion

2.7.1 Contact mechanics model validation with experimental results

The elastoplastic contact between wafer-particle and asperity-particle is used to determine the depth of indentation of slurry particle into the wafer. The contact area between wafer and asperity is calculated using force balance incorporating slurry particles. The model developed is evaluated against the experimental results of tungsten and silicon dioxide CMP. Beilman et al. [57] investigated MRR of tungsten using Al_2O_3 slurry having average particle diameters of 0.29μm, 0.38μm, 0.6μm, 0.88μm and 2μm. The slurry concentration used was 4.5% while the downforce was 6.5psi (44.82kPa). Figure 2.8a shows comparison between the experimental MRR and the MRR predicted by our contact mechanics model. The MRR predicted shows decrease with increase in particle size. Similar trends have been reported by several researchers [50],[33],[58]. Figure 2.8b shows a comparison of experimental MRR of silicon dioxide with the MRR predicted by the model as a function of increasing downforce for an average particle size of 80nm. The MRR is observed to increase linearly with increasing down force. These results suggest that the contact mechanics model alone can predict the trends but underestimates MRR. Therefore, the effect of chemical action of the slurry needs to be modelled and coupled with contact model to predict MRR in CMP processes.

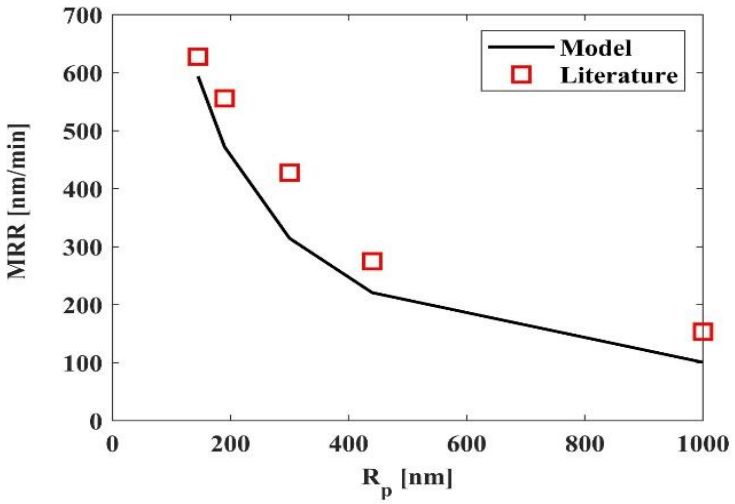

(a)

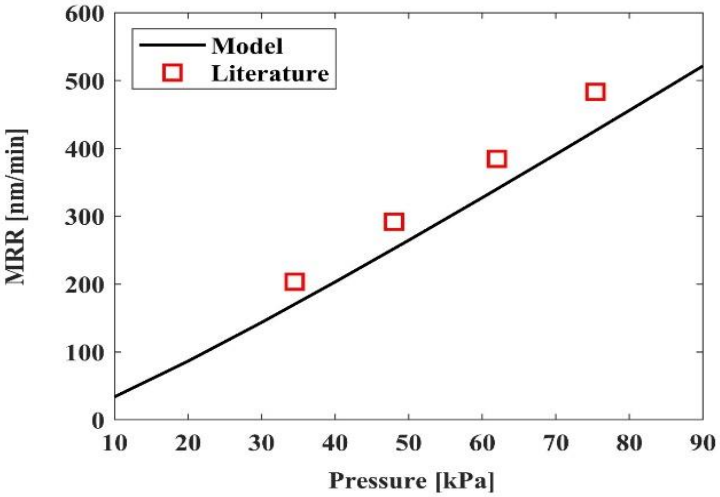

(b)

Figure 2.8 Model validation: comparison with experimental results for (a) tungsten (Hw = 5GPa Ew=411GPa, υw=0.26, Ep=310GPa, υp=0.26) Ref[57] and (b) silicon dioxide (Hw=10.5GPa Ew=74GPa υw=0.17, Ep=74GPa υp=0.17) Ref [59]. Other parameters are given in Table 2.1.

2.7.2 Parametric study with contact mechanics model

Figure 2.8 validates the developed contact mechanics model to a modest accuracy. In this section the model is utilized for a parametric study of CMP process. Here, we investigate the effect of downforce, slurry particle size, slurry solid concentration and wafer surface hardness. All the relevant parameters can be seen in **Error! Reference s ource not found.**.

In a CMP process the wafer is pressed against a relatively softer pad. The separation distance between the wafer's surface and mean asperity heights plane is dependent on material properties as well as downforce. The separation distance determines the contact area and the number of effective particles. The separation distance is found using force balance at the wafer-particle-asperity interface. If we neglect the force transferred to asperity through particles in force balance the separation remains the same for any size of abrasive particles. However, for the same downforce an increase in particle size results in a decrease in separation, as can be seen in Figure 2.9a. Conversely, the opposite has been observed for overall contact area (Figure 2.9b), number of effective particles (Figure 2.9c) and MRR (Figure 2.9d). The reason behind these observations is presented in Figure 2.9e. As the particle size decreases the number of particles per unit volume of the slurry increases and hence the number of effective particles increases. The smaller the particle size the higher the fraction of contact area covered by the total effective particles. Therefore, less force is directly transferred to the asperity from the wafer and more through the effective particles which results in smaller separation distance as shown in Figure 2.9b. Hence, for smaller particles the area of contact between the wafer and asperity is more which results in higher number of effective particles. Since, MRR is directly proportional to the number of effective particles therefore MRR decreases as the particle size increases. The above discussion can be summarized as: smaller particles result in lesser separation distance which leads to higher contact area and higher number of effective particles ($N_{eff} \propto A_{contact}$) and as a result we have higher MRR. For the same particle size with increase in downforce the separation distance decreases, while area of contact, the number of effective particles and MRR increase as shown in Figure 2.9**Error! Reference source not found.**a, b, c and d respectively.

Table 2.1 Parameters used in CMP process analysis

Parameter/property	Symbol	Value [Ref]
Wafer		
Elastic modulus of the wafer	E_w	74GPa[43]
Poison's ratio of the wafer	υ_w	0.17[43]
Hardness of wafer	H_w	10.5 GPa[43]
Pad Asperity		
Elastic modulus	E_a	357.1 MPa[60]
Poison's ratio	υ_a	0.4[49]
Hardness	H_a	90 MPa[39]z
Radius	R_a	50 µm[49]
Average surface roughness (asperity height)	σ	6.7 µm[49]
Distance between the two mean planes	μ	2 µm[49]
Number of asperities per unit area	η	2e8 /m^2 [49]
Slurry Particle		
Elastic modulus	E_p	73GPa[43]
Poison's ratio	υ_p	0.17[43]
Radius	R_p	10,20,30,40,50 nm
Density	ρ_p	2650 kg/m3
Others		
Dilution ratio of slurry	D_s	0.1
Density of slurry	ρ_s	1000 kg/m^3
Slurry concentration before dilution	m_s	4.5 %[57]
Constant for elastic deformation	k_e	0.4[40]
Constant for plastic deformation	k_p	54[40]
Relative Velocity	V_{rel}	0.144[57]
Downforce (Pressure)	P_{app}	10,20,30,40,50,60 kPa

Figure 2.9f shows the model ability to reproduce the applied downforce. Since the indentation was calculated assuming fully developed contact using elastoplastic contact

of particle with the wafer and asperity. The model reproduces the applied downforce with an error in the order of 10^{-8}.

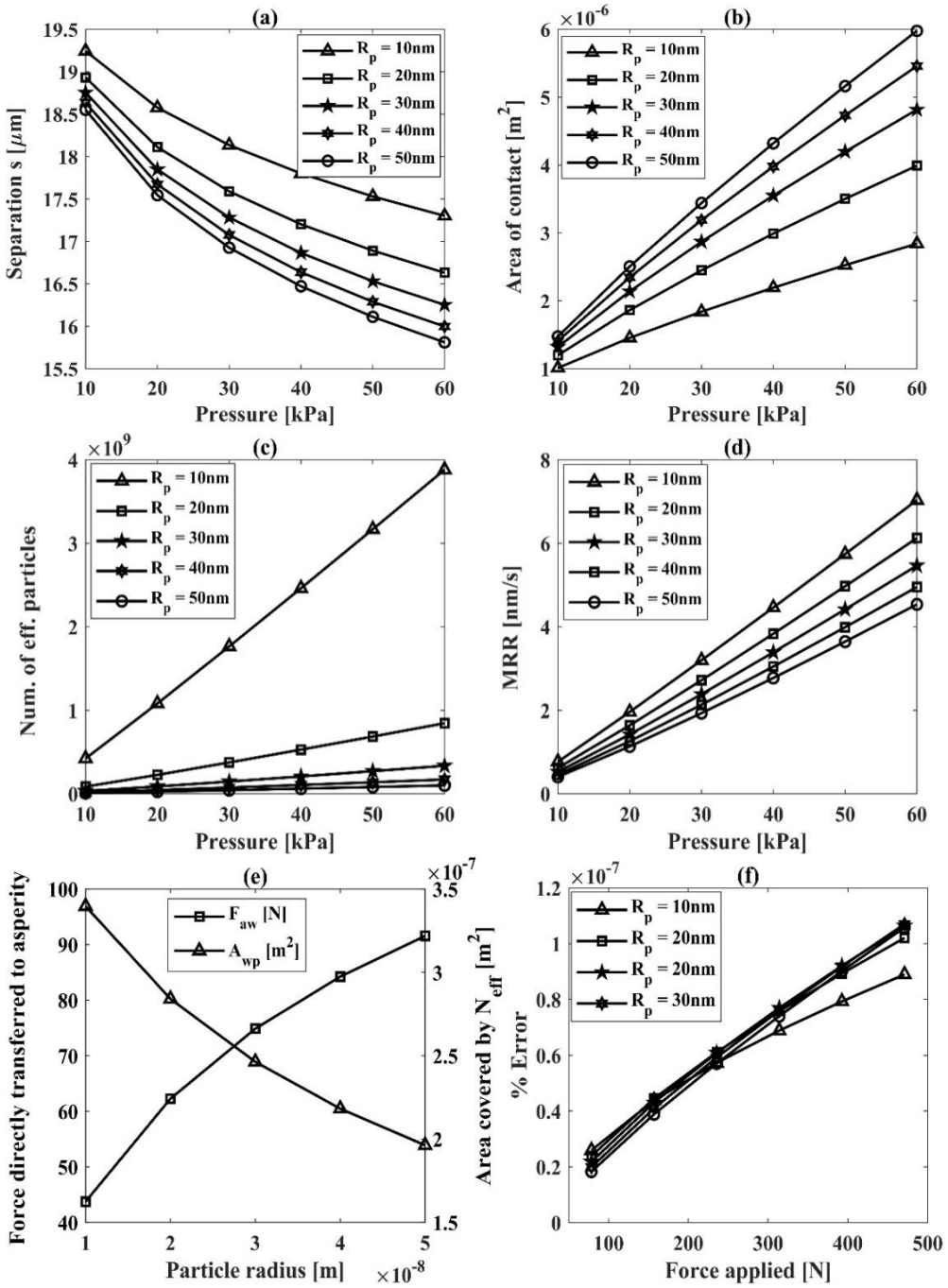

Figure 2.9 Effect of downforce and particle size on (a) separation distance between mean asperity heights plane and wafer's surface (b) Area of contact (c) Number of effective particles and (d) material removal rate. (e) shows the effect of particle size on the force directly transferred to asperity by the wafer and the area covered by the effective particles and (f) % Error in reproducing the force applied using indentation obtained from elastoplastic contact assumption.

Material removal rate is not only a function of downforce and particle size, but it is also strongly dependent on the concentration of abrasive particles in the slurry. Forsberg [61] reported a rapid decrease in MRR with decreasing abrasive concentration for low concentration regime while a gradual decrease for high concentration regime was observed. Figure 2.10a shows that under low pressure regimes increase in slurry dilution ratio results in a linear increase in MRR. However, for higher dilution ratios MRR increases nonlinearly as the pressure increases. Similar behavior has been reported for MRR in copper CMP[62]. This can be attributed to the fact that the separation distance decreases nonlinearly with increasing pressure which results in nonlinear increase in contact area and the number of effective particles.

Figure 2.10b shows MRR dependence on wafer surface hardness as a function of increasing downforce. In generating the results shown in Figure 2.10b all the parameters in Table 2.1 are kept the same except wafer surface hardness. MRR increases with increasing downforce. Also, as the hardness of the wafer decreases MRR increases. Although the contact area and the number of effective particles does not significantly increase with decrease in wafer surface hardness since the asperity deformation is mainly determined by material properties of the asperity and downforce. Therefore, higher MRR for lower wafer surface hardness can be attributed to the higher indentation depths of the slurry particle into the softer wafer as compared to harder wafer for the same pad and slurry particle.

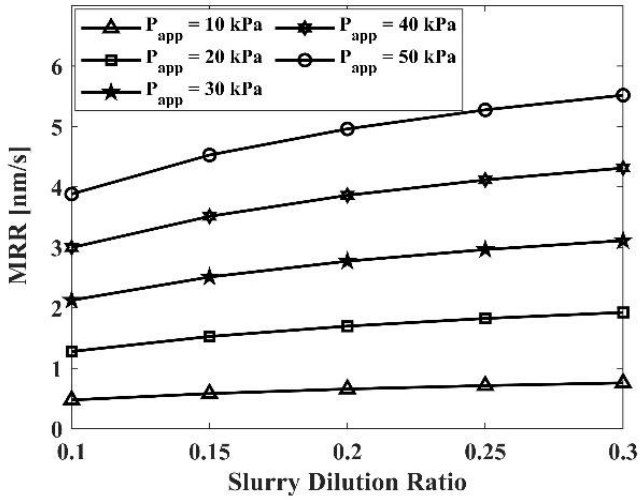

(a)

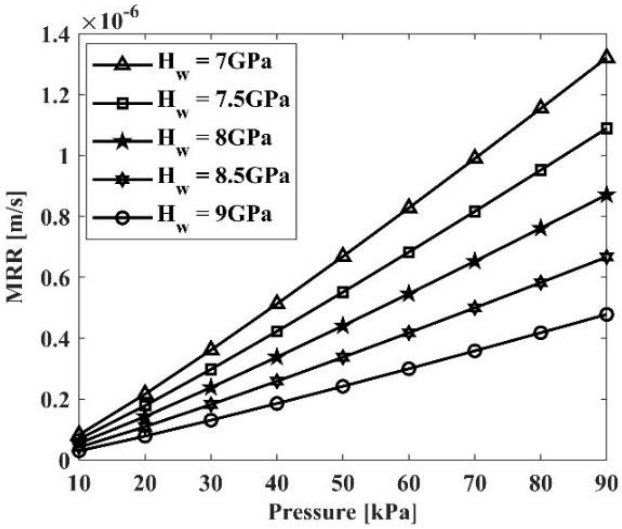

(b)

Figure 2.10 (a) MRR as a function of slurry dilution ratio and pressure. Concentration of slurry before dilution was 4.5% and (b) MRR as a function of wafer surface hardness and pressure.

2.7.3 Validation of coupled model

The contact mechanics model (mechanical action) and diffusion model (chemical action) are coupled in commercial software package MATLAB. Figure 2.8a and b shows that MRR calculated using parameters given in Table 2.1 is good in agreement with experimental results of ref [57] [59]. Figure 2.10b suggests that MRR is inversely proportional to hardness of the wafer. In CMP process the slurry chemical reacts with the

wafer surface resulting in a modified (relatively softer) layer on the surface. Therefore, chemical action leads to increase in MRR. Here we present the results of modelling the chemical effects of slurry as the diffusion of water into the wafer and simultaneously removing material from wafer surface due to abrasion. A characteristic length of 1Å and a characteristic time equal to $1Å/MRR$ are used in this study. Average number of diffused sites over a thickness equal to ω_{wp} was used to calculate average surface hardness of the wafer. After the removal of characteristic length due to abrasion the diffusion equation was solved to obtain the number of diffused sites along wafer thickness. Figure 2.11a shows the %concentration of water diffused sites along nondimensional thickness of the wafer as well as the updated initial condition for diffusion in successive cycles. The diffusion coefficient plays a key role in determining how far the water diffuses. For higher diffusion coefficient (1e-19 m^2/s) the water diffuses deeper into silicon dioxide wafer as compared to lower diffusion coefficient (1e-22 m^2/s) and results in a thicker, softer layer (hydrated silica). It can be seen that %concentration increases after each step of diffusion. This is due to the updated initial condition i.e. water diffuses into the wafer beyond the characteristic length. Thus, the diffused sites exist along wafer's thickness after mechanically removing characteristic length. Therefore, concentration of diffused sites along the remaining thickness of the wafer increases each step. Figure 2.11b shows the change in MRR with downforce and different values of diffusion coefficient for a total simulation time of 60 seconds. At lower downforce MRR is lower which results in higher characteristic time which allows diffusion of water into the wafer for longer time and results in the formation of a thicker modified (softened) layer. Therefore, under low pressure MRR is mainly due to chemical action of the slurry. On the other hand, for higher downforce the MRR due to abrasion is high which results in lower characteristic time. Hence, the diffusion is allowed to happen for a shorter period and a thinner modified layer

forms and the new average hardness value calculated is higher as compared to hardness values in case of lower down force. Hence, under higher down force MRR is dominated by mechanical abrasion.

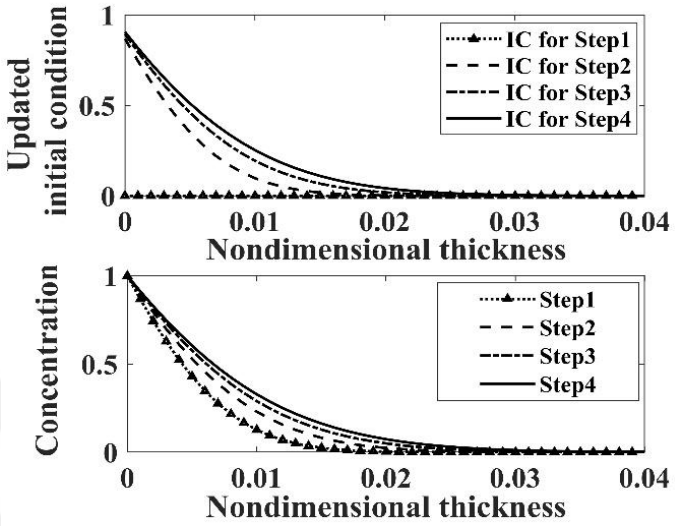

(a)

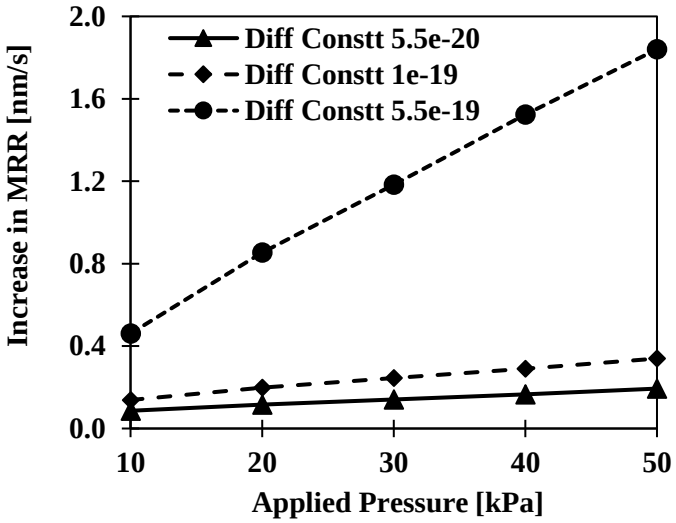

(b)

Figure 2.11 (a) Concentration of water diffused sites as function of time along wafer thickness and initial condition successive diffusion step (b) Increase in MRR obtained using coupled model (simulation time 60s). For diffusion constant higher than 1e-19 nonlinear increase in MRR can be observed

Figure 2.10b shows linear increase in MRR for different values of wafer's hardness as the down force increases. However, using diffusion coefficient higher than

1e-19 results in nonlinear increase in MRR with increasing down force as shown in Figure 2.11b. In the developed coupled model obtaining the steady state values of MRR take longer than the actual time required for a typical process CMP. Therefore, the MRR reported here is the average MRR for a total simulation time of 60 seconds. The reason behind the nonlinear dependence of MRR on down force can be explained as follows. Under higher down force the MRR is higher due to abrasion which results in shorter characteristic time. With each step of simulation, the concentration of diffused sites along wafer thickness increases. Therefore, the concentration profile gradually grows as the number of steps increase as can be seen in Figure 2.11a. However, under low down force the MRR due to abrasion is lesser which results in higher characteristic time. A thicker, softer layer formation under low pressure results in rapid increase in MRR. Figure 2.12a**Error! Reference source not found.** shows decrease in wafer hardness which results in increase in MRR as a function of time. For lower downforce, the hardness and MRR quickly reach steady state values as can be inferred from the slopes of hardness and MRR in Figure 2.12a This explains the dominance of either chemical or mechanical effects on MRR. At lower downforce the chemical effects i.e. diffusion dominates while at higher downforce the MRR is mainly due to mechanical effects i.e. abrasion. We observed that at higher pressure the increase in MRR is slower as compared to increase in MRR at lower pressure and thus we have a nonlinear increase in MRR with increase in down force for higher diffusion coefficient (5.5e-19) as shown in Figure 2.11b. Moreover, if the slurry has chemical agents such as an oxidizer or an inhibitor the diffusion coefficient can be tuned accordingly i.e. increased for oxidizer or decreased for inhibitor (this investigation is beyond the scope of this work). This approach is expected to enable the developed coupled model to capture the actual effect of chemical agents in the slurry in CMP processes. Finally, the developed coupled model is validated against

experimental data of Shih [59] and MRR data obtained using a similar model available in the literature [43], and can be seen in Figure 2.12b.

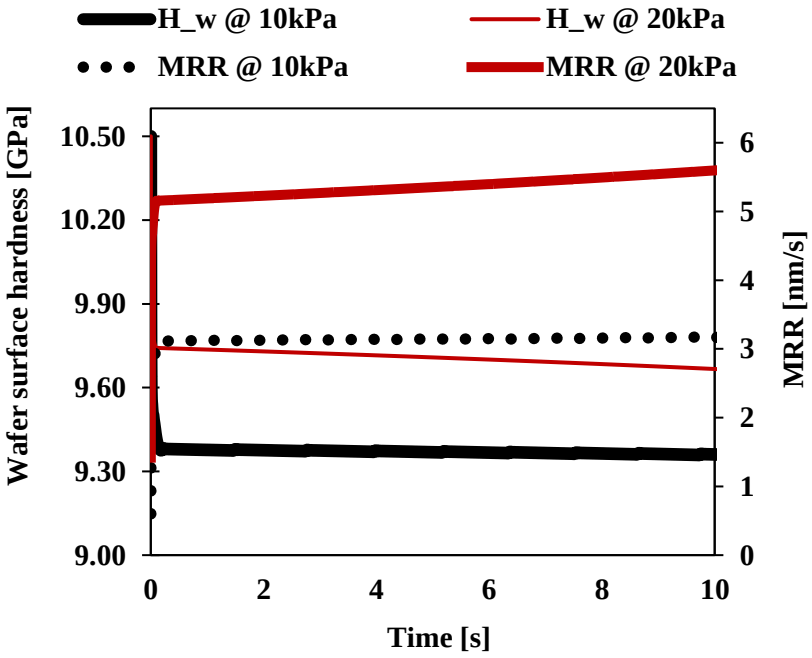

(a)

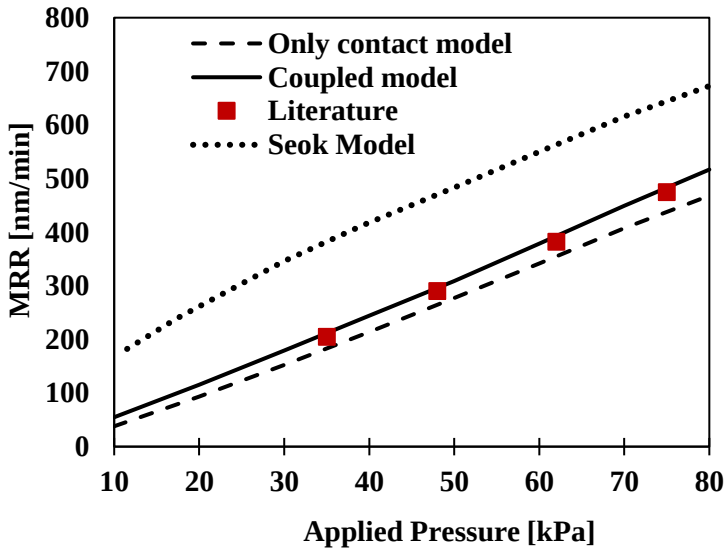

(b)

Figure 2.12 MRR and Hw as a function of time for particle size 40 nm and diffusion coefficient 1e-19 (b) Coupled model validation: comparison with experimental results in the literature[59] and results obtained using a similar model[43]. Literature in the above figure refers to the experimental results of Ref [59].

2.8 Limitations of the model

In modelling the contact between the wafer and abrasive particle hardness of the wafer is used (equation (2.10)). Similarly, in modelling the contact between the abrasive particle and pad asperity hardness of asperity is used (equation (2.9)).

Chemical effect of slurry is limited to diffusion of water into the wafer only. Chemical etching of the wafer is ignored. Chemical effect of slurry on abrasive particle and pad asperity is ignored.

For calculating the indentation depth of particle into the wafer, the contact between the wafer and abrasive particle is assumed to be elastoplastic. And in the formulation ((2.10)) the hardness of the wafer is used. Therefore, the hardness of the abrasive particle is considered greater than the hardness of the wafer. As generally accepted; a particle softer than wafer deforms instead of indenting into the wafer and hence for a slurry particle with hardness less than that wafer's hardness, the model will result in negative MRR (negative indentation).

2.9 Conclusion

In CMP processes both the chemical and mechanical effects work simultaneously. For a model to correctly predict MRR in CMP processes both effects need to be consistently modelled and coupled. The model presented in the work utilizes elastoplastic contact between the wafer and particle, and particle and the asperity while the chemical effects are modelled as diffusion of water into the wafer. The elastoplastic contact model shows a linear dependence of MRR on the applied pressure but under-predicts MRR. Coupling of chemical effects with contact model provides in depth understanding of material removal mechanism and nonlinear i.e. non-Prestonian behavior of MRR in CMP. It is the formation of thicker modified layer at low pressures that results in increased

MRR. Therefore, at low down pressure the MRR is determined by chemical effects while at higher pressure it is dominated by mechanical effects. Moreover, the updated initial condition for diffusion results in near linear decrease in wafer surface hardness which in turn results in increase in MRR as function of time. Higher diffusion coefficient results in nonlinear increase in MRR. The model can be further improved by adjusting the diffusion coefficient value to correctly account for chemical agents in the slurry in CMP processes.

CHAPTER III

OPTIMIZATION OF CMP PROCESS PARAMETER FOR MATERIAL REMOVAL SELECTIVITY

3.1 Introduction

In 1997 IBM replaced Al with Cu as interconnect material.[63] Cu's lower electrical resistivity and high melting point enables it to have a smaller gate delay [63]. Therefore, advanced integrated circuits utilize copper wires for interconnections between transistors. Using copper as an interconnect material has some challenges. The Cu wires are isolated by low-dielectric constant materials(ULK) known as barrier materials. The barrier material is needed to have good adhesion to Cu and at the same time is supposed to prevent the diffusion of Cu into the neighboring region.[64] Another serious challenge is the corrosion of Cu during chip manufacturing. Different transition metals have been used as barrier layers such as tantalum (Ta)[65], tungsten (W)[66], titanium (Ti)[67] and their composites with nitrogen (N), carbon (C), or Si, such as Ta/TaN[68], W2N[69], TiN[70], TiC[71], TaSiN[72], Si3N4[73]. These barrier metals pose other challenges in the CMP process during chip manufacturing. These barrier materials may cause galvanic corrosion, dishing, or erosion of Cu, and have low MRR as compared to Cu [74]. Copper has relatively high MRR, as compared to barrier materials, due to its lower hardness [75]. Moreover, a copper seed layer is required for these materials which limit the deposition of a uniform copper layer [75]. Therefore, CMP slurry and input process parameters need to be optimized to resolve these issues.

To obtain global planarity CMP is required to remove Cu and barrier material simultaneously and equally from the wafer surface. The chemical component of CMP i.e.

slurry chemistry has been extensively investigated. Different slurry chemistries result in different MRR of Cu and barrier materials [74, 76–83]. Xu investigated the effect of H_2O_2 on MRR and found that the MRR of Cu increases till 10 ml of H_2O_2 per liter of the slurry while it decreases if the concentration of H_2O_2 is increased beyond 10 ml [84]. Cao studied the MRR of TiN, NDC, and Cu and found an optimized slurry formulation that can meet the requirements of the new integration scheme [78]. The formulated slurry results in high MRR of TiN, very low MRR of NDC, and a tunable MRR of Cu.

In a patterned wafer, the contact between Cu and barrier materials may lead to galvanic corrosion of Cu which may adversely affect the device performance due to increased defectivity across the Cu/barrier interface [83]. The key is to control the removal rate of different materials in obtaining reasonable thickness and topography. Yao found the optimized H_2O_2 concentration as well as the optimized speeds of head and platen and was able to obtain near 1:1 MRR selectivity of Cu and ULK [77]. Maryama compared the CMP performance of Ru and Ta and formulated a slurry resulting in dishing of copper less than 30nm when Ru is used as barrier liner [75]. The dishing of Cu reported is less with Ru as compared to dishing of Cu when Ta is used as a barrier liner. This can be attributed to the electrochemical noble nature of Ru as compared to copper. Despite lower dishing in this case a more serious concern is the generation of toxic RuO_4 moreover, barrier materials require a two-step CMP [75]. Therefore, a Mn-based barrier liner stack has been proposed to address these problems [74, 85]. However, the main focus has been the chemical component of CMP to achieve similar material removal selectivity. Since the materials are simultaneously removed from the surface, process inputs such as relative velocity, downforce, and particle size, etc. can also be optimized to obtain the desired removal selectivity of different materials. To the best of the authors' knowledge the mechanical parameters of CMP such as downforce, particle size, and slurry solid

concentration have not been investigated for material removal selectivity. Nor is a model-based optimization of the process parameters conducted.

In this study, we use a material removal model, developed in our previous work,[86] to optimize the CMP process parameters such as downforce (F), slurry solid concentration (D_s), and abrasive particle radius(R_p) to obtain the desired material removal selectivity of different materials. The model couples the contact mechanics with the diffusion of water into the wafer to calculate MRR. The chemical effects are limited to the diffusion of water into the wafer. The model along with its limitations is briefly discussed in the following section. The materials used here are Cu, Mn, and MnN. The optimization is done in two parts. In the first part of the study, the objectives were to maximize the average MRR and minimize the standard deviation in MRR of different materials. It was found that a gentle or low material removal results in achieving a lower standard deviation in MRR of different materials. The second part investigates the standard deviation in the thickness removed in the average time needed to remove a known thickness of the materials under consideration.

3.2 Model Review

The developed and validated model couples contact mechanics (mechanical actions) with the diffusion of water into the wafer as chemical effects to calculate MRR in a typical CMP process[86]. Though a detailed explanation of our model is given in our previous work [86], we provide a brief description here. The model considers only the diffusion of water into the wafer as the sole chemical effect of the slurry and chemical etching of the wafer is negligible. Mechanical properties of the slurry particles and pad are assumed to be independent of water diffusion. The algorithm employed to couple the mechanical and chemical effects can be seen in Figure 3.1.

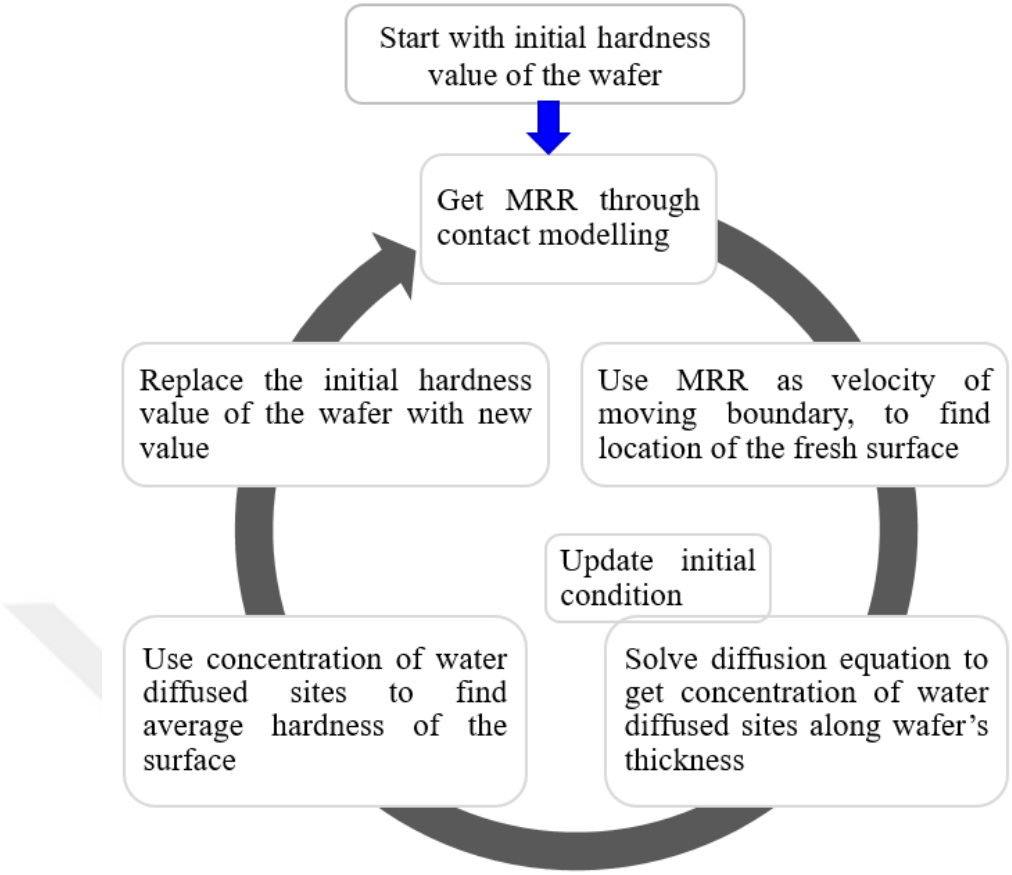

Figure 3.1 Algorithm for coupling the mechanical and chemical effects to predict material removal rate. For details, the reader is advised to refer to ref[86].

The model first removes material from the wafer's surface by mechanical effects i.e. abrasion and the characteristic time is calculated. Characteristic time is defined as the time required for the mechanical actions to remove thickness equal to characteristic length (1Å). Next, 1D diffusion equation is solved for the characteristic time to determine the concentration of water diffused sites along the wafer thickness. Based on the concentration of diffused sites along the wafer thickness, from the surface to the particle's indentation depth, the average hardness of the modified layer is calculated. Finally, the mechanical model is recalled with the newly determined hardness value of the wafer, and the cycle repeats until the desired/required time.

3.3 Problem formulation for optimization of CMP input parameters

CMP process is expected to achieve a planar surface by removing material from a patterned wafer surface. The wafer surface may have different materials and hence different mechanical properties in different locations. Therefore, a methodology, to remove the same thickness of different materials on the surface, is needed to achieve global planarity, reduce the amount of CMP consumables, and accelerate the semiconductor manufacturing process.

We conducted a model-based optimization to achieve the objective using a genetic algorithm. We used MATLAB's built-in function gamultiobj (Multi-Objective Genetic Algorithm). In multi-objective optimization, the concept of Pareto front is widely used and is defined as the set of all Pareto efficient solutions [87, 88]. To find the optimum set of process parameters, we used a multi-objective genetic algorithm along with Pareto front decision making process [87].

The optimization is done in two steps. In the first step, the objectives of optimizing the CMP process parameters were, i) maximize average MRR for all materials and ii) minimize standard deviation in MRR for all materials. Standard deviation in material removal rate during simultaneous polishing of different materials is crucial to achieving the desired planarity on a patterned surface. Therefore, the main objective of this work is to minimize the standard deviation in MRR. In the second step, the objectives were i) minimize standard deviation in a known thickness removed and ii) minimize the standard deviation in the time required to remove a known thickness. The area of the wafer used in this study is 15*15mm^2. Parameters other than F, D_s and R_p are defined inside the objective function.

In the first step, the model runs for 1 second i.e., the values of objectives reported are obtained after 1sec of simulation time. We initially conducted the optimization for Cu and SiO_2, since the diffusion coefficients of water in both materials are known. The objectives, in this case, were i) maximize average MRR and minimize the difference in MRR of Cu and SiO_2. Then we conducted optimization for Cu, Mn, and MnN and propose that the desired material removal selectivity can be achieved provided the diffusion coefficient of water in materials under consideration is known. The diffusion coefficients of water in Mn and MnN are not known. Therefore, we approximated the diffusion coefficient of water in Mn, based on their close atomic number, size, etc to that of copper as 1e-13 m^2/s while for MnN as 1e-15 m^2/s. Table 3.1 provides the mechanical properties of the materials investigated in this study. Table 3.2 provides the process parameters along with the applied bounds.

Table 3.1 Mechanical properties of materials considered in this study

Material	**Hardness (GPa)**	**Young's Modulus (GPa)**	**Poisson's Ratio**
SiO2[86]	10.5	74	0.17
Copper[89]	1.6	110	0.34
Mn[90]	5	160	0.33
MnN[91]	8	175	0.3

Table 3.2 Bounds of the input process parameters

Process parameter	**Lower bound**	**Upper bound**
Applied force F [N]	10	50
Slurry concentration D_s [%wt]	2.5	20
Abrasive particle radius R_p [nm]	10	100

A genetic algorithm finds the minima of a function. Therefore, to maximize the average MRR it needs to be multiplied by -1. It is important to keep in mind that the thickness of the barrier layer which is in the order of a few nanometers and therefore, the average MRR has been restricted to less than 2nm/s. Since CMP cannot be conducted for a second or a fraction of a second. When the average MRR is greater than 2nm/s, the algorithm achieves an undefined positive value and the set of parameters is disregarded. The model calculates MRR for each material. Later, average MRR and standard deviation in MRR are calculated as follows

$$\text{Average MRR} = \frac{1}{N}\sum_{i=1}^{N}(MRR_i) \tag{3.1}$$

$$\text{St. Dev. MRR} = \sqrt{\frac{\sum_{i=1}^{N}(MRR_i - Average\ MRR)^2}{N-1}} \tag{3.2}$$

where N = 3 and i = 1 for Cu, i = 2 for Mn and i = 3 for MnN. The objective functions were set as

$$Objective\ f1 = \begin{cases} -\text{Average MRR}, & \text{if Average MRR} \leq 2\ \text{nm/s} \\ \text{Average MRR} + \infty, & \text{if Average MRR} > 2\ \text{nm/s} \end{cases} \tag{3.3}$$

$$Objective\ f2 = \text{St. Dev. MRR} \tag{3.4}$$

The negative sign in Objective f1 means the maximization of the Average MRR. Finally, the optimization problem is formulated as follows

$$\min Objective\ f1$$

$$\min Objective\ f2$$

3.4 Results and discussion

3.4.1 Cu-SiO2

Figure 3.2shows the Pareto front for the objectives; average MRR and the absolute value of the difference in MRR of Cu and SiO_2 obtained for different sets of CMP input parameters. The input parameters for the points marked in Figure 3.2 can be seen in

Table 3.3. We can see that as the average MRR increases the absolute value of the difference in the MRR of Cu and SiO2 also increases. This can be attributed to the different mechanical properties as well as the different diffusion coefficients of water into Cu (1e-13 m^2/s) and SiO_2 (1e-19 m^2/s).

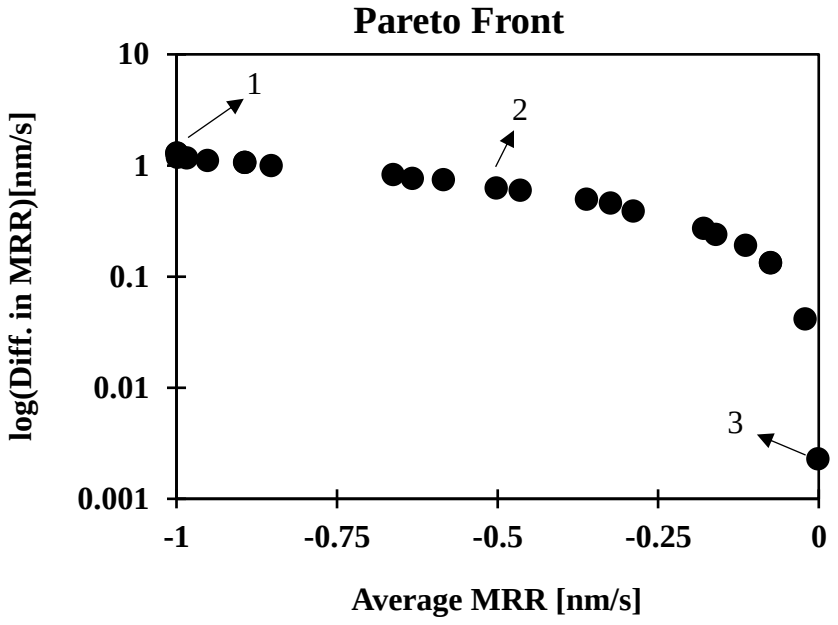

Figure 3.2 Pareto front for Cu and SiO2 optimization. The value of average MRR cannot be negative, the negative sign here is due to the optimization algorithm, gamultiobj finds the minima therefore, we used the negative sign to maximize MRR.

Table 3.3 Values of parameters for marked/numbered points in Figure 3.2 for Cu, SiO2 CMP

S. No.	F	D_s	R_p	Average MRR	Difference in MRR
1	38.61	13.63	46.50	-0.98	1.17
2	31.82	14.23	54.75	-0.50	0.63
3	10.29	5.80	36.87	-1.3e-3	2.3e-3

3.4.2 Cu-Mn-MnN system

Figure 3.3**Error! Reference source not found.** shows the Pareto front for objectives i.e. average MRR, and the standard deviation in MRR of Cu, Mn, and MnN obtained for a total number of generations, as well as population size, of 75. The input parameters for the points marked in Figure 3.3 can be seen in Table 3.4.

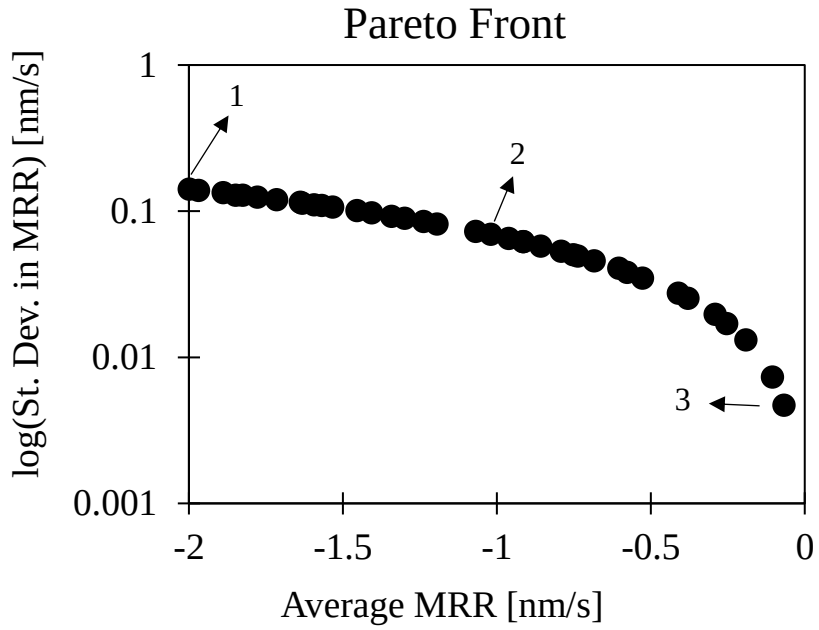

Figure 3.3 Pareto front for Cu, Mn, and MnN CMP parameters optimization. The value of average MRR cannot be negative, the negative sign here is due to the optimization algorithm, gamultiobj finds the minima therefore, we used the negative sign to maximize MRR

Table 3.4 Values of parameters for marked/numbered points in Figure 3.3 Cu, Mn, and MnN system CMP

S. No.	F	D_s	R_p	Average MRR	St. Dev. in MRR
1	28.109	13.203	74.057	-2.000	0.141
2	18.993	13.076	73.409	-1.020	0.069
3	10.968	3.493	56.379	-0.069	0.005

From Figure 3.3 we can see that as the average MRR increases the standard deviation in MRR also increases. Therefore, any set of input parameters that may result in a higher average MRR will result in, undesired, higher standard deviation in MRR. The Pareto front obtained from optimization can be used to understand the relationship between MRR and process input parameters. It is well established that in a CMP process the MRR is directly proportional to the downforce applied and the slurry solid loading and inversely proportional to the size of abrasive particles [86]. The coupled model takes into account only the number of effective particles [86]. Effective particles are defined as the particles trapped in the contact area between the wafer and pad asperities. These particles remove material from the wafer by indenting into the wafer and sliding along its surface. The number of effective particles is inversely proportional to the volume of the average abrasive particle and directly proportional to the slurry solid concentration.[86] The particle size effect MRR in two ways; i) an increase in particle size results in a decrease in MRR, since the number of effective particles decreases, ii) an increase in particle size can also increase MRR, since the depth of indentation of the particle into the wafer increases. The overall effect of the number of effective particles dominates the

effect of the depth of indentation of the particle into the wafer. Therefore, as the particle size increases, we see an overall decrease in MRR.

Figure 3.4 shows the effect of each input parameter on average MRR. The results reported show the effect of a single input parameter without eliminating the effect of the remaining input parameters. The data suggest a strong correlation between applied downforce and average MRR as shown in Figure 3.4a. However, in Figure 3.4b and c we see that the effects of slurry concentration (D_s) and particle radius (R_p) are not significant, as compared to the effect of downforce, as the average MRR can obtain significantly different values for the same values of D_s and/or R_p. A similar trend has been observed for standard deviation in MRR. To understand the combined effect of all the input parameters on average MRR and the standard deviation in MRR we visualize the Pareto front data using 4D plot in Figure 3.5. The color bar shows the values of the dependent parameters; average MRR and standard deviation in MRR of Cu, Mn, and MnN. While the three axes show the values of the independent parameters; force applied (on a wafer with 15*15m^2 area), slurry solid concentration (%wt.), and the particle radius (nm). Standard deviation in MRR depends on average MRR i.e. as average MRR increases standard deviation in MRR also increases and vice versa as shown in Figure 3.5.

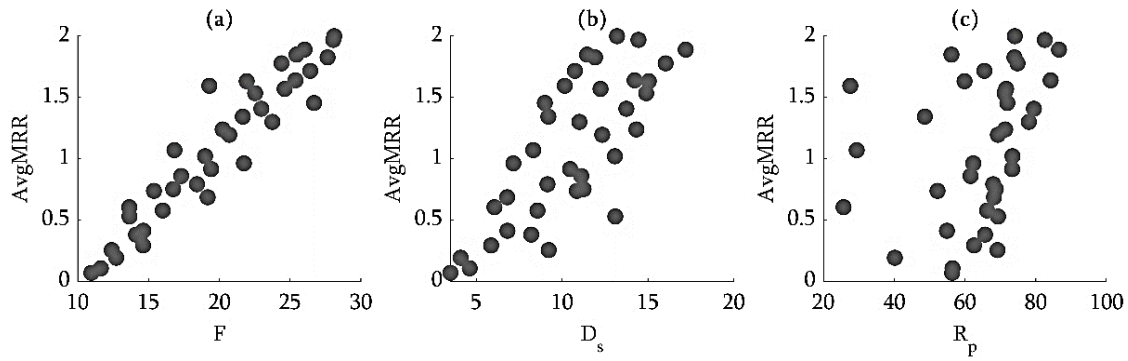

Figure 3.4 Effect of each input parameter on the output parameter (average MRR), without controlling the remaining two input parameters. (a) effect of applied downforce ($\boldsymbol{F}$)on average MRR without controlling slurry solid concentration ($\boldsymbol{D_s}$) and abrasive

particle radius ($\boldsymbol{R_p}$), (b) effect of $\boldsymbol{D_s}$ on average MRR without controlling $\boldsymbol{F}$, and $\boldsymbol{R_p}$, (c) effect of Rp on average MRR without controlling F and Ds.

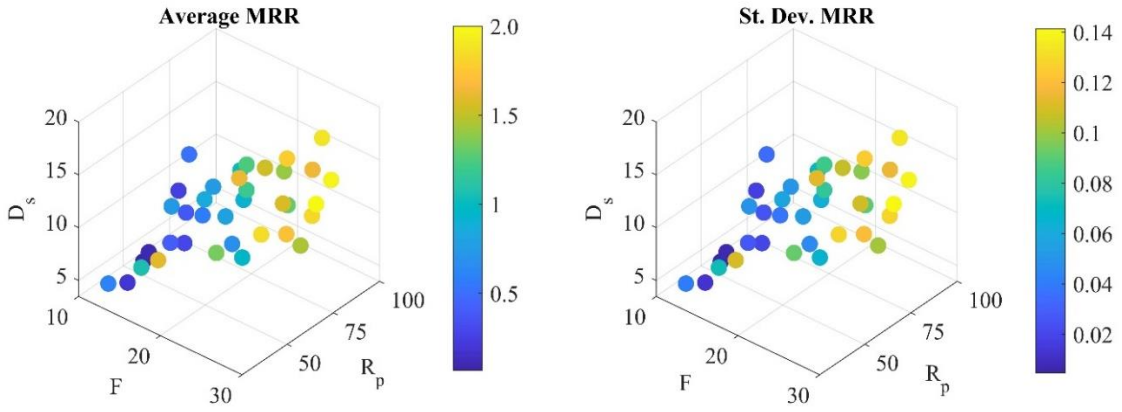

Figure 3.5 The combined effect of varying the input parameters on both the output parameters i.e. average MRR and Standard deviation in MRR of Cu, Mn, and MnN

To understand the relationship between the input parameters i.e. F, D_s and R_p, and the output parameters i.e. average MRR and the standard deviation in MRR, we determined the partial correlation factors (PCRF) and p-values for the parameters. PCRFs were determined to understand the effect of one input parameter while controlling/eliminating the others.

Table 3.5 lists the values of PCRFs and p-values calculated utilizing the sets of parameters obtained from the Pareto front. The largest value of PCRF and the smallest p-values for applied downforce suggest the strongest correlation between the force and the output parameters. However, the weakest correlation between the particle radius and the output parameters is found based on its lowest value of PCRF and highest p-value. The table suggests that the force applied is the key input parameter i.e. by controlling the applied downforce the desired material removal selectivity (~1:1:1 in this case) can be achieved.

Table 3.5 Partial correlation factors (PCRF) and p-values for the parameters: relationship with MRR. The values of PCRF are the same for average MRR and Standard deviation in MRR, this is because the standard deviation in MRR is directly proportional to average MRR

		Force	Slurry Concentration	Particle radius
Partial correlation coefficient	Average MRR	0.949	0.743	-0.674
	St. Dev. MRR	0.949	0.743	-0.674
p-values	Average MRR	1.13E-18	2.10E-7	6.59E-6
	St. Dev. MRR	1.13E-18	2.10E-7	6.59E-6

3.5 Optimization for removing a known thickness of materials

The barrier material is needed to have good adhesion to Cu and at the same time is supposed to prevent the diffusion of Cu into the neighboring region. Therefore, a certain thickness of the barrier layer is deposited on the substrate to serve the purpose. In CMP process Cu and the barrier layer are simultaneously polished. CMP is required to remove equal thickness of different materials i.e. Cu, Mn and MnN in this case, to achieve the required planarity. Here, we optimize the process input parameters to minimize the standard deviation in the thickness removed during CMP.

The model [86] removes 1Å in each time step. In this part of optimization, the model runs for 25 timesteps. Therefore, the time reported here is the time needed to remove 2.5 nm thickness of material from the wafer surface. The objective functions for this case were modified as follows i.e. the first objective was to minimize the standard deviation in the time needed to remove 2.5nm material from Cu, Mn, and MnN surface

while the second objective was to minimize the standard deviation in the thickness removed in average time.

Figure 3.6 a shows the Pareto front obtained from optimization. Figure 3.6b shows that as the average time required to remove 2.5 nm thickness of all three materials. It can be seen that as the average time increases the standard deviation in time also increases. However, when we remove 2.5 nm thickness from the wafer in a shorter time the standard deviation in the thickness removed increases. Figure 3.6c and d show that removing 2.5 nm of thickness from the wafer in a shorter time of CMP process means a higher standard deviation in MRR due to higher average MRR. A higher standard deviation in MRR results in a higher standard deviation in the thickness removed. This results in a rougher surface and limits our ability to achieve ~1:1:1 material removal selectivity i.e. removal of the same thickness from different materials on patterned surface. This can be explained better with an example from Figure 3.6. For an average time of, let's say, 20 seconds of simultaneous CMP to remove 2.5nm of Cu, Mn and MnN can result in a standard deviation of only ± 2 Å in the thickness removed as shown in Figure 3.6a and b. This corresponds to a very low average MRR i.e. 7.5nm/min as can be seen in Figure 3.6d. This suggests that slower material removal can also result in lower standard deviation in the thickness removed and a relatively smoother patterned surface can be obtained.

Figure 3.7 shows the relationship between the average time needed to remove 2.5nm thickness and the individual input parameters. The results in Figure 3.7 complement the PCRF and p-values given in Figure 3.7. The role of slurry solid concentration and the particle radius is important but not as crucial as the effect of applied force. The particle radius and the slurry solid concentration reach stable values while the applied force decreases as the average time increases which result in decreasing average MRR. Therefore, to meet the objective of achieving near similar thickness removal the

process needs to be conducted gently i.e. apply lower force. In other words, the average MRR needs to be minimized. Hence, we propose the application of lower applied force, lower slurry solid concentration, and higher average particle size to achieve ~1:1:1 material removal for different materials on a patterned surface; Cu/Mn/MnN system in this case.

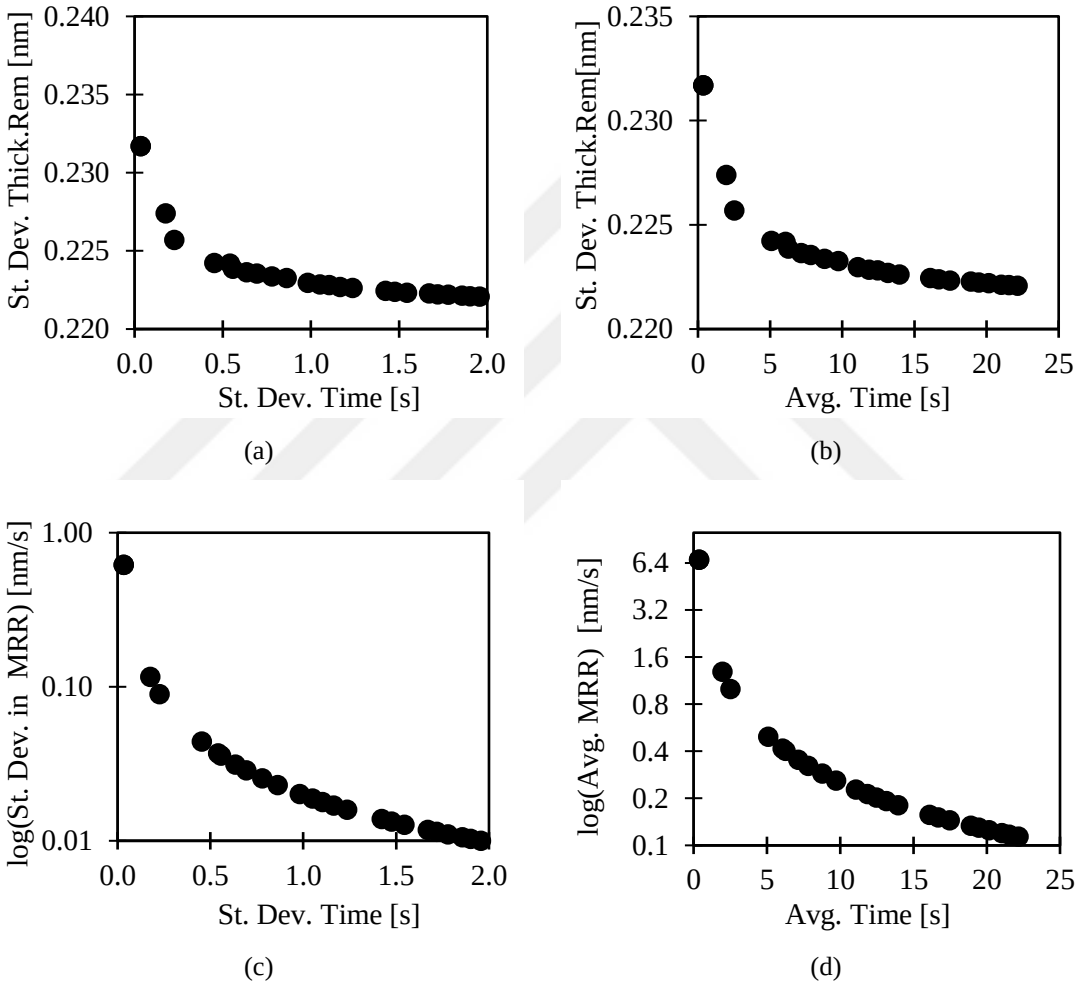

Figure 3.6 Pareto Front from optimization (a) average time required to remove 2.5nm thickness of Cu, Mn and MnN vs standard deviation in time (b) average time required to remove 2.5nm thickness of Cu, Mn and MnN vs standard deviation in MRR. (c) log of standard deviation in MRR vs standard deviation in time (d) log of average MRR vs average time.

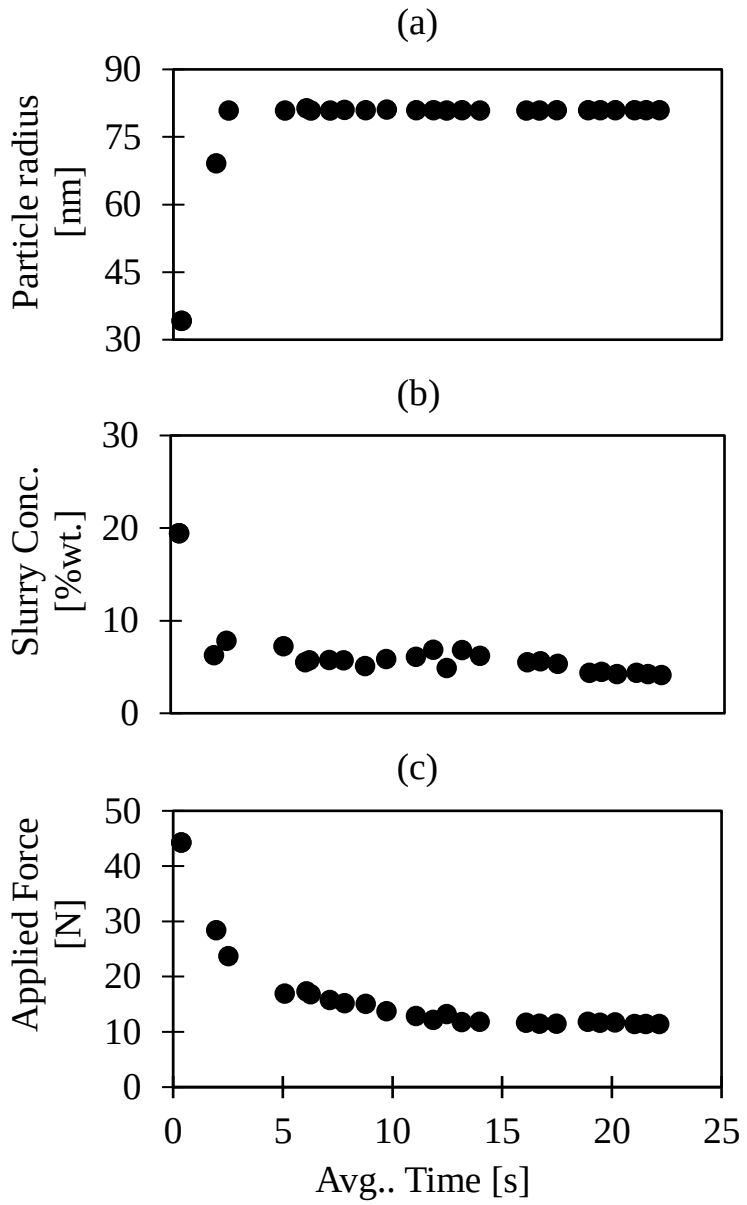

Figure 3.7 Relationship between the average time needed to remove 2.5 nm thickness and (a) abrasive particle radius, (b) slurry solid concentration (c) applied force (on wafer area of 15*15mm^2)

3.6 Conclusion

In this work, we conducted a model-based optimization to obtain the desired material removal selectivity in Cu/barrier CMP by varying only the mechanical parameters of the process. A coupled material removal model developed in our previous

work has been utilized. The process parameters investigated in this work include downforce, slurry solid concentration, and abrasive particle radius.

Optimization was done in two steps. In the First step, we initially optimized the process parameters to maximize average MRR and minimize the difference in MRR when Cu and SiO_2 when they are simultaneously polished. Then conducted the optimization for Cu and barrier layer i.e. Mn and MnN. The objectives of optimization were i) maximize average MRR and ii) minimize the standard deviation in MRR of Cu, Mn, and MnN. It was found that an increase in MRR results in increasing the standard deviation in MRR, which is undesirable when we are trying to achieve similar material removal selectivity. Therefore, decreasing MRR can result in obtaining the desired material removal selectivity.

In the second step, the optimization is conducted for the planarization of Cu, Mn, and MnN system i.e. removing equal thickness. The objectives of optimization were i) minimize the standard deviation in average time required to remove 2.5 nm thickness of each material and ii) minimize the standard deviation in the thickness removed in average time. It was found that obtaining the same thickness removal for different materials the CMP process needs to be conducted for a longer time i.e. MRR needs to be minimized. Lower MRR results in lower standard deviation in the thickness removed and a relatively smoother surface can be obtained. To obtain a smoother surface of a patterned wafer we propose the application of lower downforce, decreased the concentration of solid abrasive particles in the slurry, and using higher radii abrasive particles.

CHAPTER IV

A METHODOLOGY FOR CMP PROCESS OPTIMIZATION TO ACHIEVE DESIRED MATERIAL REMVOVAL SELECTIVITY OF COPPER AND BARRIER MATERIALS

4.1 Introduction

Advanced integrated circuits (IC) utilize copper (Cu) as interconnect material due to its high melting point and lower electrical resistivity as compared to aluminum (Al) [63]. Cu wires are separated by barrier materials. The purpose of barrier material is to prevent the diffusion of Cu into the neighboring region [64]. Different transition metals have been used as barrier layers such as tantalum (Ta), tungsten (W), titanium (Ti) and their composites with nitrogen (N), carbon (C), or Si, such as Ta/TaN, W2N, TiN, TiC, TaSiN, Si3N4 [65–73].

These barrier materials pose different challenges during CMP in chip manufacturing. For example, they have less material removal rates as compared to Cu,[74] and the inert nature of these material may cause erosion, dishing or even galvanic corrosion of Cu [75]. To achieve a desired material removal selectivity, CMP consumables such as slurry needs to play a key role. CMP of Cu/barrier is expected to obtain certain level of material removal selectivity. The chemical role of slurry in obtaining global planarity in case of patterned wafer has been reported by several researchers.

Researchers at IMEC Belgium, used EKC9011/9003 slurry and reported material removal rates of 90, 46-54, 55 and 4 nm/min for Ta/TaN, TiN, Cu, and SiO_2 respectively, at 2 psi [93]. Lily Yao [94] developed silica based slurry having hydroxylamine, for

barrier CMP. The slurry demonstrated a 1:3-10:~1 material removal selectivity for Cu:TaN:ILD system. An abrasive free slurry (HS-T815-X) developed by Hitachi, showed 1:1:1 material removal selectivity on Cu:TaN:SiOC system [95]. Gottfried et al. [96] used silica slurry with H_2O_2 as an oxidizer and pH ranging from 2.7 to 3 for TaN barrier layer. They obtained removal rates of 100-150, 40-50 and 7-8 nm/min for TaN, Cu and SiO_2, respectivel. They developed an alkaline colloidal silica based slurry with solid loading < 10 wt%, and H_2O_2 as an oxidizer [97]. The slurry also uses proprietary additives for controlling material removal selectivity of barrier, Cu and Low-k materials, and minimizing dishing and oxide layer loss. HEBUT China [98] have developed colloidal silica based slurries with alkaline additives having multiple functional groups. Upon reaction with Cu these functional groups (tertiary amine, acetic acid and ethanol) form complex ions. In Cu CMP slurry, BTA (benzotriazole) is a common passivating agent. With the creation of a monolayer adsorbed on the Cu surface and a multilayer created on top of the monolayer, it is a very effective corrosion inhibitor. Baoguo Zhang [79] developed BTA free slurries for Cu and barrier CMP. The slurries exhibited satisfactory performance in terms minimizing dishing and oxide corrosion. Maryama et al. compared the CMP performance of Ru and Ta and formulated a slurry resulting in dishing of copper less than 30nm when Ru is used as barrier liner [75]. The dishing of Cu reported is less with Ru as compared to dishing of Cu when Ta is used as a barrier liner. Cao studied the MRR of TiN, NDC, and Cu and found an optimized slurry formulation that can meet the requirements of the new integration scheme. The slurry results in high MRR of TiN, very low MRR of NDC, and a tunable MRR of Cu [78].

As discussed above different slurry chemistries have been developed for CMP of Cu and different barrier materials. CMP of Cu/barrier still face some challenges. First, the CMP is a two-step process, (first the overburden Cu is removed then in next step the

barrier material is removed). Second, CMP of Ru based barrier liner produce toxic RuO_4.[75] Third, when BTA is used as a corrosion inhibitor, it forms Cu-BTA complex which results in BTA residues on the copper surface after post-CMP cleaning. In addition, BTA is a carcinogenic substance [98]. Finally, in a patterned wafer, the contact between Cu and barrier materials may lead to galvanic corrosion of Cu which may adversely affect the device performance due to increased defectivity across the Cu/barrier interface [83]. Recently, Mn-based materials have been proposed as new barrier liner [74,85].

Therefore, we need to develop a methodology to address the issue of non-uniform material removal in case of Cu/Mn/MnN system. In this study, we use ex-situ electrochemical analyses to investigate the effect of different concentrations of H_2O_2. Then, we relate the MRR obtained during CMP of blanket wafers with slurry having different concentrations of H_2O_2 and 2.5 %wt. of abrasive particle loading. We also investigate of mechanical factors such as applied downforce and different concentrations of slurry solid loading. We propose an environmentally benign slurry with optimized oxidizer concentration and mechanical parameters to address the issue of material removal selectivity on Cu/Mn/MnN system.

4.2 Materials and Methods

4.2.1 Materials

200 mm CVD deposited copper(Cu), manganese(Mn) and manganesenitride (MnN) wafers were obtained from Texas Instruments Inc. USA. The wafers were cut into 15*15mm square shaped coupons for electrochemical analyses and CMP experiments. Before, electrochemical tests, each sample was cleaned by immersing into pH 9 DIW and ultrasonicated for 10mins to remove any native oxides from the wafer surface. 34.5-36.5 %wt. H_2O_2 obtained from Sigma Alrdrich, Germany was used as an oxidizer in ex-situ

electrochemical analyses as well as in CMP experiments. The concentrations of oxidizer used for electrochemical analyses as well as CMP experiments were 0.1 M, 0.2 M, 0.3 M and 0.5 M of H_2O_2. Silica nanoparticles (SiO_2) 30%wt. obtained from NyaCol was diluted to 2.5%wt and then the required amount of H_2O_2 was added for use in CMP experiments. The pad used in CMP of the coupons was IC1000/Suba IV stacked pad. All the tests were conducted at room temperature of 25˚C.

4.2.2 Methods

4.2.2.1. Potentiostatic

Electrochemical analyses were conducted using Gamry Interface 1000 Potentiostat. Each coupon was used working electrode. A platinum wire was used as a counter electrode while a saturated calomel electrode (SCE) was used as reference electrode. Potentiostatic scans (current vs time transients) were obtained, at a very low input potential (100μV vs. E_{ref}), for 1000 seconds. The tests were run at a scan speed of 10 mV/s. 200ml of different concentrations of H_2O_2 were used as electrolyte for the tests. After the tests the samples were rinsed with DI water and dried with nitrogen for post potentiostatic surface characterization.

4.2.2.2. Potentiodynamic:

Potentiodynamic scans were obtained for Cu, Mn and MnN coupons in all four H_2O_2 solutions. Open circuit potentials were measured for 10 seconds, before starting polarization scans. The scans were obtained for input potential from -5 to 5V. Scan rate and step size were set at 50 mV/s and 1 mV, respectively. The output signal (current I_m) was plotted verses the potential. Output parameters for each scan were obtained by using Tafel data. The output parameters include (i) the electrochemical corrosion potential (E_{corr}), (ii) the corrosion current and (iii) the corrosion rate.

4.2.2.3. Surface characterization:

Wettability: Wettability of a surface is related to its surface free energy and is affected by the surface topography as well as surface chemistry. After potentiostatic scans, wettability of the coupons was evaluated by measuring contact angle of DI water. The contact angles were measured using a sessil drop method with KVS AttentionTheta Optical Light Goniometer. Before wettability evaluations, the coupons were rinsed with ethanol, and cleaned by ultrasonication in DI water for 10 minutes. The coupons were then dried with nitrogen.

Surface Roughness: Surface topography of coupons was investigated using atomic force microscopy (AFM). Surface topography images of the coupons were obtained by scanning an of 10*10 µm at a scan speed of 5 µm/s. The images were obtained using AFM, by Nanomagnetics Instruments. in contact mode. To obtain an average value of surface roughness and standard deviation in surface roughness, three images were taken for each coupon. Before surface roughness measurements, the coupons were rinsed with ethanol, and cleaned by ultrasonication in DI water for 10 minutes. The coupons were then dried with nitrogen

4.2.2.4. CMP experiments:

CMP experiments were conducted on Tegramin 30 table-top polisher by Struers. IC1000/Suba IV stacked pad, while silica based commercial CMP slurry having 2.5%wt abrasive particles (average diameter 80nm) at different concentrations of H_2O_2 were used for CMP. Rotation speed was set to 150 RPM for the head as well as the platen. Downforce of 30 N (~133 kPa) was applied on the coupon and the polishing was for performed for 30 seconds. After polishing the coupons were cleaned with acetone and DI water in ultrasonic bath for 10 minutes. The coupons were finally dried with nitrogen.

After cleaning the coupons, contact angles and surface roughness were measured as discussed before. Material removal rate (MRR) of coupon was calculated by pre and post CMP weight. The weights were determines using a high precision digital balance (PrecisaGravimetrics) with accuracy of 10µg.

4.3 Results and Discussion

4.3.1 Potentiodynamic polarization

Figure 4.1 shows the potentiodynamic polarization behavior of Cu, Mn and MnN in different concentrations of H_2O_2. All the polarization curves show similar cathodic behavior in the presence of H_2O_2. As the applied voltage reaches zero the current measured on the film surface decreases and the progresses in the anodic portion of the polarization curve. Table 4.1 lists the Tafel parameters calculated for the used films and H_2O_2 concentrations. Cu shows a gradual increase in corrosion rate upto 0.3M H_2O_2. However, a sharp rise in the corrosion rate of Cu has been observed at 0.5M H_2O_2. Mn shows a decreasing corrosion rates with increasing H_2O_2 concentrations which can be attributed to its ability of forming a protective film. MnN have lowest corrosion rates for any concentration of H_2O_2 as compared to Cu and Mn. The corrosion rate of MnN shows a gradual increase with in H_2O_2 concentration. While an abrupt increase in corrosion rate has been observed at 0.5M H_2O_2. Among the concentrations of H_2O_2, at 0.3M H_2O_2 we see similar corrosion rates of Mn and MnN, and very close to corrosion rate of Cu. For other concentrations we see significant differences in the corrosion rates of Cu, Mn and MnN.

Therefore, lower concentration of H_2O_2 needs to be used since the oxidation process become uncontrollable at higher concentrations of oxidizer.

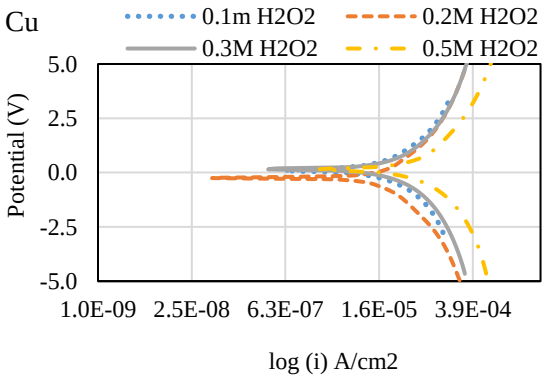

(a)

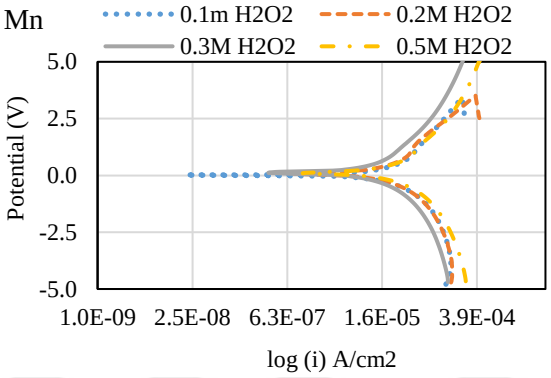

(b)

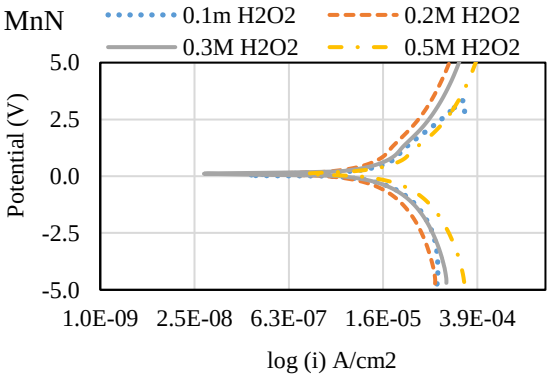

(c)

Figure 4.1 Potentiodynamic polarization curves of (a) copper (b) manganese and (c) manganese nitride in 0.1 M, 0,2 M, 0.3 M and 0.5 M hydrogen peroxide.

Table 4.1 Tafel parameters obtained from potentiodynamic scans

Material	Tafel parameter	H_2O_2 concentration			
		0.1 M	**0.2 M**	**0.3 M**	**0.5 M**
Cu	I_{corr} (µA/cm²)	55.60	44.90	70.80	233.00
	E_{corr} (mV)	110.00	-253.00	164.00	142.00
	Corrosion Rate (mm/yr)	0.65	0.52	0.83	2.72
Mn	I_{corr} (µA/cm²)	659.00	194.00	46.70	106.00
	E_{corr} (mV)	16.90	73.70	129.00	112.00
	Corrosion Rate (mm/yr)	7.70	2.27	0.55	1.23
MnN	I_{corr} (µA/cm²)	31.40	42.10	46.70	92.50
	E_{corr} (mV)	44.70	104.00	110.00	119.00
	Corrosion Rate (mm/yr)	0.37	0.49	0.55	1.08

4.3.2 Potentiostatic

Figure 4.2 show the current vs time transient scans of obtained in different concentrations of H_2O_2 on Cu, Mn and MnN wafers. The figure also provides the AFM images of the wafers obtained after potentiostatic scans at various concentrations of H_2O_2.

For the first ~50 seconds Cu shows an accelerated formation of passive film. It can be seen in Figure 4.2a, by a sharp rise in the current as function of time. After that current gradually increases towards positive. This behavior is observed for Cu in all the concentrations of oxidizer investigated.

Figure 4.2a and b show that after the first ~50 seconds the current the gradually increases for all the concentration of H_2O_2. However, the increase in current in the first

50 seconds increases with increase in the concentration of H_2O_2. This indicates that as the concentration of H_2O_2 increases Mn and MnN quickly form passive surface films.

The AFM images of Copper after potentiostatic scan at 0.2M H_2O_2 shows some pits on the surfaces. These pits can be attributed to the negative corrosion potential (Table 4.1), it is the concentration at which the corrosion rate of copper decreases instead of increasing as seen in corrosion rates at 0.3 and 0.5M H_2O_2.

The formation of modified surface film determines the material removal rate (MRR) and surface quality in CMP. On all the wafers investigated the passivation currents become more negative as the oxidizer concentration increases.

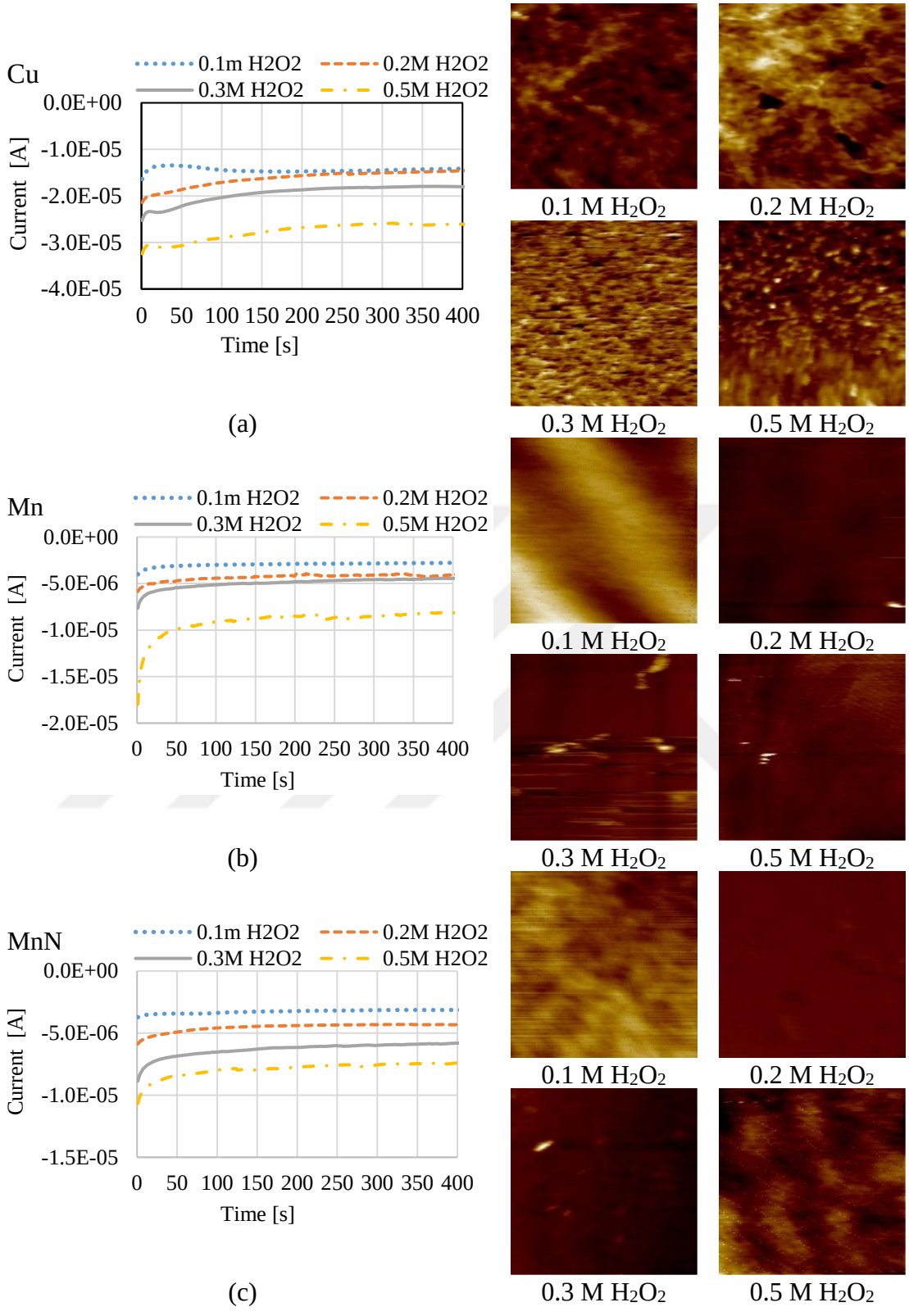

Figure 4.2 Potentiostatic scans (current vs time transients) of (a) copper (b) manganese and (c) manganese nitride in 0.1 M, 0,2 M, 0.3 M and 0.5 M hydrogen peroxide and post-potentiostatic analysis AFM images.

4.3.3 AFM and wettability (Post potentiostatic scans)

The wettability of a surface is a measure of its surface energy and is known to affect MRR in CMP process. The wettability, evaluated as contact angle, of DI water on the wafer surfaces after potentiostatic scans can be seen in Figure 4.3 a. It can be seen the Cu has the highest contact angles for each concentration of H_2O_2. Mn and MnN have comparable contact angle values and behave more hydrophilic as compared to Cu. The contact angle for copper increases with increase in oxidizer concentration which indicates increasing corrosion and increasing surface roughness as can be seen in Figure 4.3b. At 0.3M H_2O_2 the contact angles for Cu, Mn and MnN differ more than at any concentration. This can help in achieving the objective of obtaining uniform MRR for the wafer studied.

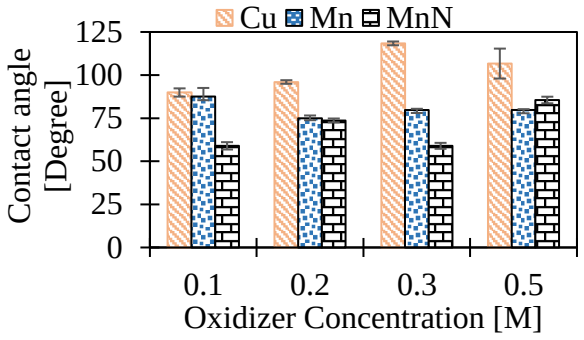

(a)

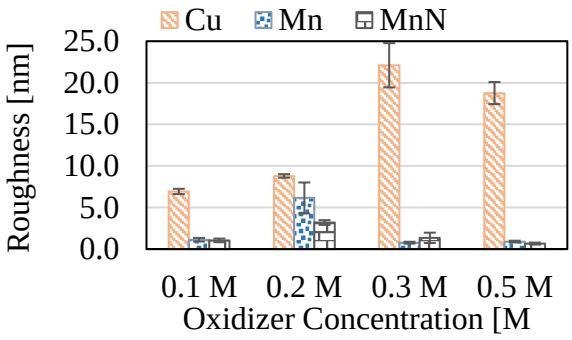

(b)

Figure 4.3 Post-potentiostatic analysis (a) contact angles and (b) surface roughness of copper, manganese and manganese nitride in 0.1 M, 0,2 M, 0.3 M and 0.5 M hydrogen peroxide.

4.3.4 CMP experiments MRR

The effect of different concentrations of H_2O_2 on CMP performance was evaluated in terms of MRR, post CMP surface roughness and contact angle measurements on wafer. Figure 4.4 illustrates the MRR of Cu, Mn and MnN obtained for a slurry solid concentration of 2.5 wt% and different concentrations of oxidizer in the slurry. The material removal rate shows that MRR increases with increasing the concentration of H_2O_2. This can be attributed to decreasing passivation currents as the oxidizer concentration increases as shown Figure 4.2. MRR of Cu shows a linear increase while MRR of Mn and MnN increases gradually as the concentration of H_2O_2 increases.

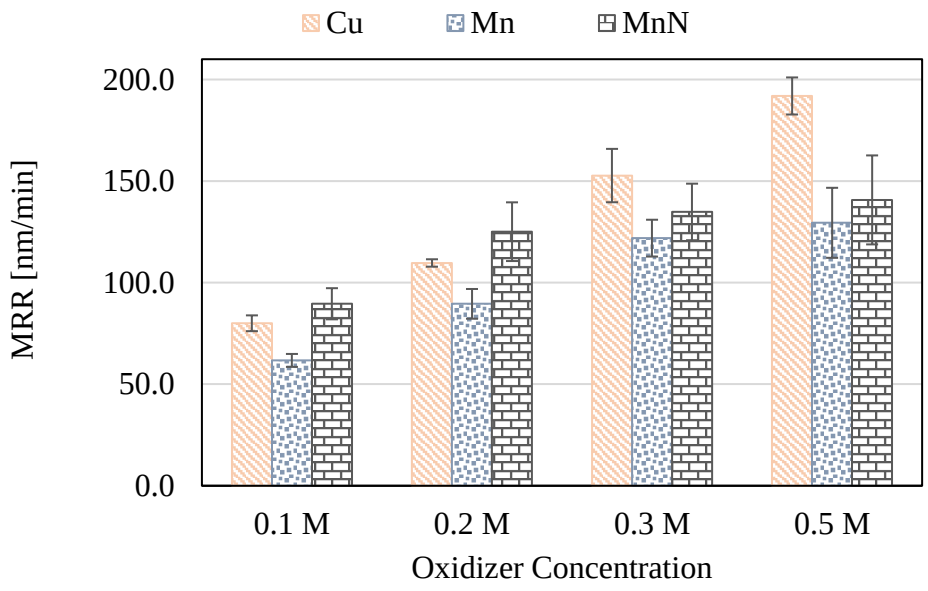

Figure 4.4 Material removal rate copper manganese and manganese nitride with slurry having 0.1 M, 0.2 M, 0.3 M and 0.5 M hydrogen peroxide.

4.3.5 Post CMP surface characterization and selectivity

Figure 4.5 and Table 4.2 provides the material removal rates and normalized MRR of Cu, Mn and MnN obtained after CMP with 2.5 %wt. of abrasive concentration and 0.1

M, 0.2 M, 0.3 M, and 0.5 M of H_2O_2 in the slurry. To understand the MRR selectivity the MRR is normalized with the MRR of Cu for each concentration of oxidizer.

Table 4.2 Average MRR of copper manganese and manganese nitride and material removal selectivity on Cu/Mn/MnN system during CMP with slurry having 0.1 M, 0.2 M, 0.3 M and 0.5 M hydrogen peroxide.

H_2O_2 concentration	**Average MRR**			**Removal Selectivity (Normalized MRR)**			
	Cu	**Mn**	**MnN**	**Cu**	**Mn**	**MnN**	**St. Dev.**
0.1 M	79.99	61.71	89.60	1.00	0.77	1.12	0.18
0.2 M	109.68	89.55	125.08	1.00	0.82	1.14	0.16
0.3 M	152.71	121.90	134.80	1.00	0.80	0.88	0.10
0.5 M	191.91	129.45	140.73	1.00	0.67	0.73	0.17

It has been observed that the MRR of wafer increases with increasing oxidizer concentration. This can be attributed to the rate of passive film formation on the surface, since the measured currents in the current vs time transients decreased with increasing concentration of the oxidizer.

Figure 4.5a and b show the surface roughness and the contact angle values obtained after CMP with different slurry formulations. It can be seen that the contact angles and the surface roughness measured have similar trends except for CMP with 0.1 M H_2O_2 slurry. This can be attributed to the significant differences in the passivation currents and MRR at 0.1 M H_2O_2. Overall the contact angles measured after CMP are less than the contact values after potentiostatic scans. However, the values are more consistent after CMP.

From Table 4.2 and Figure 4.5 it can be seen that the optimized oxidizer concentration of oxidizer is 0.3 M which results in the lowest standard deviation (0.1 nm/min) in the MRR of Cu, Mn and MnN. Among the concentrations used in this study, higher standard deviation in the MRR has be seen when highest or lowest concentrations of the oxidizer are used.

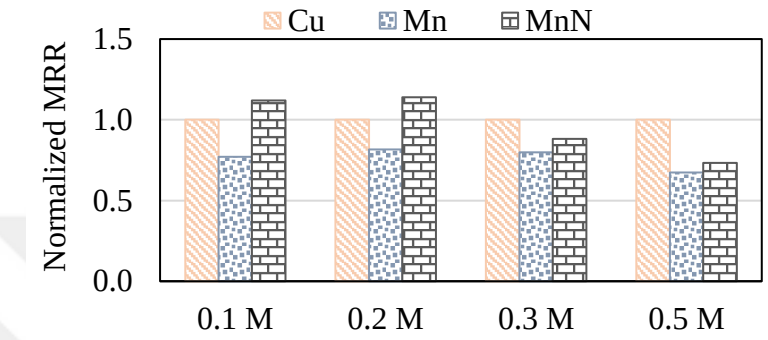

(a)

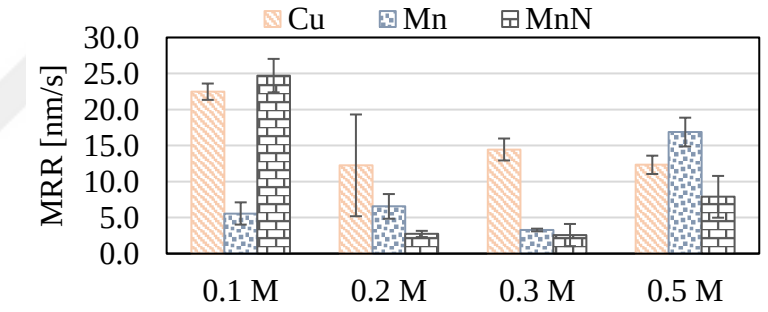

(b)

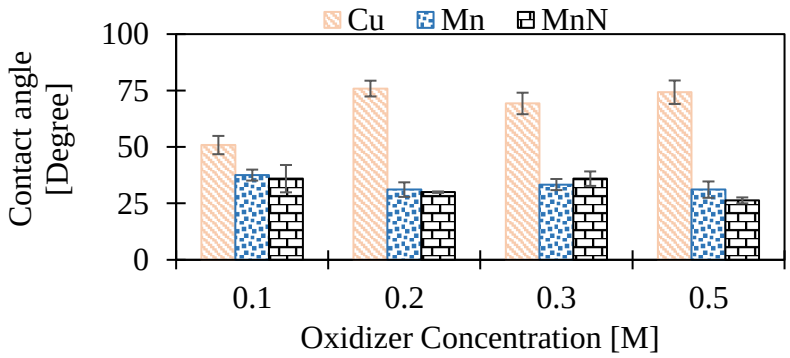

(c)

Figure 4.5 Material removal selectivity and post-CMP surface characterization (a) MRR normalized average MRR of Cu (b) surface roughness (c) contact angles DI water on copper, manganese and manganese nitride after CMP with slurry having 0.1 M, 0,2 M, 0.3 M and 0.5 M hydrogen peroxide.

4.4 Mechanical inputs effects on removal selectivity

Figure 4.6 shows the effect of mechanical parameters of CMP on the removal selectivity of Cu/Mn/MnN system. As we have shown in previous work, it can be seen in Figure 4.6. that with increase in slurry solid concentration and/or applied force the deviation in the material removal increases. This can be attributed to the fact that MRR increases with in either both or one of the slurry solid concentration and applied force. The three different sets of input parameters are defined as follows

Set 1	2.5 %wt. SiO2 + 0.3M H_2O_2 and FORCE =30N
Set 2	10 %wt. SiO2 + 0.3M H_2O_2 and FORCE = 30N
Set 3	2.5 %wt. SiO2 + 0.3M H_2O_2 and FORCE =50N

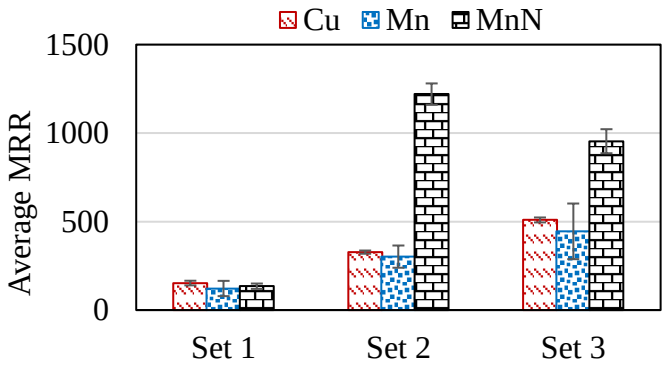

(a)

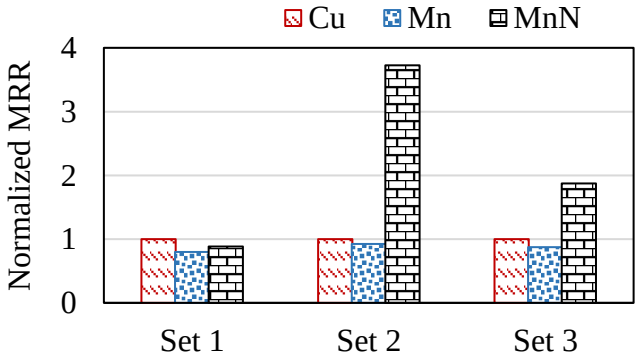

(b)

Figure 4.6 Effect of mechanical parameters of CMP on material removal selectivity of Cu/Mn/MnN system for three different sets of input parameters (a) Average MRR of Cu, Mn and MnN (b) MRR normalized with average MRR of Cu for set of input parameters.

4.5 Conclusion

CMP process is expected to control the material removal selectivity and planarity of barrier layer for the advanced interconnect integration schemes for sub-10 nm nodes. In this work, we investigated the effect of oxidizer concentration, the slurry solid concentration and applied down force on the removal selectivity on Cu/Mn/MnN system. Initially, the effect of different concentrations of oxidizer was evaluated through potentiostatic scans and potentiodynamic polarization. Potentiostatic scan showed decrease in passivation currents with increasing concentration of the oxidizer, indicating the formation chemically modified surface oxide film. Potentiodynamic polarization data was used to obtain Tafel data. It was observed that the corrosion rates of Cu, Mn and MnN increases with increasing oxidizer concentration. At 0.3 M H_2O_2 the comparable corrosion rates for the Cu, Mn and MnN were observed. Post-potentiostatic scnas the contact angles increased with increasing oxidizer concentration which can be attributed to increasing surface roughness.

In the next step, MRR obtained during CMP was compared with the results of electrochemical analyses. It was concluded that slurry formulation having 0.3 M H_2O_2 can minimize the standard deviation in the MRR of Cu, Mn and MnN. Surface characterization after CMP showed similar trends in surface roughness and wettability.

Finally, the mechanical components such as slurry solid concentration and the applied down force were investigated for their role in material removal selectivity. It was found that the as the slurry solid concentration and/or the applied down force increases the standard deviation in the MRR of Cu, Mn and MnN, also increases. Therefore, it is concluded (for the investigated parameters) that 0.3 M H_2O_2 and lower solid concentration in the slurry under lower applied down force, can result in 1: ~1: ~1 material

removal selectivity for Cu/Mn/MnN system. Hence, the experimental approach proposed in this work can be beneficial to the barrier layer CMP for advanced interconnect integration schemes for sub-10 nm.

CHAPTER V

CONCLUSIONS AND FUTURE RECOMMENDATIONS

5.1 General Conclusion

In CMP processes both the chemical and mechanical effects work simultaneously. For a model to correctly predict MRR in CMP processes both effects need to be consistently modelled and coupled. The model presented in the work utilizes elastoplastic contact between the wafer and particle, and particle and the asperity while the chemical effects are modelled as diffusion of water into the wafer. The elastoplastic contact model shows a linear dependence of MRR on the applied pressure but under-predicts MRR. Coupling of chemical effects with contact model provides in depth understanding of material removal mechanism and nonlinear i.e. non-Prestonian behavior of MRR in CMP. It is the formation of thicker modified layer at low pressures that results in increased MRR. Therefore, at low down pressure the MRR is determined by chemical effects while at higher pressure it is dominated by mechanical effects. Moreover, the updated initial condition for diffusion results in near linear decrease in wafer surface hardness which in turn results in increase in MRR as function of time. The model can be further improved by adjusting the diffusion coefficient value to correctly account for chemical agents in the slurry in CMP processes.

In this work, we conducted a model-based optimization to obtain the desired material removal selectivity in Cu/barrier CMP by varying only the mechanical parameters of the process. A coupled material removal model developed in our previous work has been utilized. The process parameters investigated in this work include downforce, slurry solid concentration, and abrasive particle radius.

Optimization was done in two steps. In the First step, we initially optimized the process parameters to maximize average MRR and minimize the difference in MRR when Cu and SiO_2 when they are simultaneously polished. Then conducted the optimization for Cu and barrier layer i.e. Mn and MnN. The objectives of optimization were i) maximize average MRR and ii) minimize the standard deviation in MRR of Cu, Mn, and MnN. It was found that an increase in MRR results in increasing the standard deviation in MRR, which is undesirable when we are trying to achieve similar material removal selectivity. Therefore, decreasing MRR can result in obtaining the desired material removal selectivity.

In the second step, the optimization is conducted for the planarization of Cu, Mn, and MnN system i.e. removing equal thickness. The objectives of optimization were i) minimize the standard deviation in average time required to remove 2.5 nm thickness of each material and ii) minimize the standard deviation in the thickness removed in average time. It was found that obtaining the same thickness removal for different materials the CMP process needs to be conducted for a longer time i.e. MRR needs to be minimized. Lower MRR results in lower standard deviation in the thickness removed and a relatively smoother surface can be obtained. To obtain a smoother surface of a patterned wafer we propose the application of lower downforce, decreased the concentration of solid abrasive particles in the slurry, and using higher radii abrasive particles.

CMP process is expected to control the material removal selectivity and planarity of barrier layer for the advanced interconnect integration schemes for sub-10 nm nodes. In this work, we experimentally investigated the effect of oxidizer concentration, the slurry solid concentration and applied down force on the removal selectivity on Cu/Mn/MnN system. We propose a systematic approach to achieve ~1: ~1: ~1 material removal selectivity for Cu/Mn/MnN system.

Initially, the effect of different concentrations of oxidizer was evaluated through potentiostatic scans and potentiodynamic polarization. Potentiostatic scan showed decrease in passivation currents with increasing concentration of the oxidizer, indicating the formation chemically modified surface oxide film. Potentiodynamic polarization data was used to obtain Tafel data. It was observed that the corrosion rates of Cu, Mn and MnN increases with increasing oxidizer concentration. At 0.3 M H_2O_2 the comparable corrosion rates for the Cu, Mn and MnN were observed. Post-potentiostatic scnas the contact angles increased with increasing oxidizer concentration which can be attributed to increasing surface roughness. In the next step, MRR obtained during CMP was compared with the results of electrochemical analyses. It was concluded that slurry formulation having 0.3 M H_2O_2 can minimized the standard deviation in the MRR of Cu, Mn and MnN. Surface characterization after CMP showed similar trends in surface roughness and wettability. Finally, the mechanical components such as slurry solid concentration and the applied down force were investigated for their role in material removal selectivity. It was found that the as the slurry solid concentration and/or the applied down force increases the standard deviation in the MRR of Cu, Mn and MnN, also increases.

Therefore, it is concluded (in the investigated parameters) 0.3 M H_2O_2, lower down force, lower solid concentration in the slurry can result in ~1: ~1: ~1 material removal selectivity for Cu/Mn/MnN system. The experimental findings are agreement with our model based optimization of CMP process input parameters for Cu/Mn/MnN system. Hence, the experimental approach proposed in this work can be beneficial to the barrier layer CMP for advanced interconnect integration schemes for sub-10 nm.

5.2 Recommendations for Future Work

The model developed and validated model can be improved by incorporating the anisotropic behavior of the wafer.

The model takes only the diffusion of water into the wafer as the sole chemical effect of the slurry. Moreover, it ignores the following two interactions

i. Interaction between slurry Chemicals and the abrasive particles

ii. Interaction between the slurry chemicals and pad

Integrating the above two types of interactions with the develop model can further improve its performance.

In case of metal CMP the MRR is a strong function of slurry chemistry and therefore, there is a room for further improving the model by incorporating the wafer dissolution or the rate of passive film formation. The model in that case will be complete and will provide deep insight into the actual material removal process in CMP.

In terms of optimization of the input parameters for obtaining a desired MRR or material removal selectivity the effects of following parameters can also be investigated.

i. Surface topography of the pad

ii. Mechanical properties of the pad

iii. Mechanical properties of the abrasive particle

iv. Shape of the abrasive particles

v. The chemical effects can also be exploited

The electrochemical analyses provide a basic understanding of the relationship between MRR and the oxidizer concentration, slurry solid loading, and the applied force. The oxide films forming on the surface need to be characterized to better

understand/control the material removal selectivity during simultaneous polishing of different materials.

Another potential application of the model is in the field of liquid honing for surface finish of micro holes. In honing process, a highly viscous fluid is flown through micro holes to remove the protruded parts on the internal surface and results in a smooth interior surface. Abrasive particles can be distributed in the viscous fluid. While the highly viscous fluid can be modelled as the pad with certain hardness and elastic modulus. The internal surface of the hole can be assumed as a flat plate in contact with spherical abrasive particles.

REFERENCES

[1] J. Seo, “A review on chemical and mechanical phenomena at the wafer interface during chemical mechanical planarization,” *Journal of Materials Research*, vol. 36, no. 1. Springer Nature, pp. 235–257, 01-Jan-2021.

[2] M. Krishnan, J. W. Nalaskowski, and L. M. Cook, “Chemical Mechanical Planarization : Slurry Chemistry , Materials , and Mechanisms,” pp. 178–204, 2010.

[3] Robert L. Rhoades, “CMP Historical Perspective and Future Outlook,” in *CSTIC Conference*.

[4] H. Lee and H. Jeong, “A wafer-scale material removal rate profile model for copper chemical mechanical planarization,” *Int. J. Mach. Tools Manuf.*, vol. 51, no. 5, pp. 395–403, 2011.

[5] D. Lee, H. Lee, and H. Jeong, “The effects of a spray slurry nozzle on copper CMP for reduction in slurry consumption The effects of a spray slurry nozzle on copper CMP for reduction in,” no. December, 2015.

[6] M. Jeong *et al.*, “Chemical mechanical planarization of copper bumps on printed circuit board,” *Int. J. Precis. Eng. Manuf.*, vol. 12, no. 1, pp. 149–152, 2011.

[7] L. M. Cook, “Chemical processes in glass polishing,” *J. Non. Cryst. Solids*, vol. 120, no. 1–3, pp. 152–171, 1990.

[8] J. Luo and D. Dornfeld, Integrated Modeling of Chemical Mechanical IC Fabrication. .

[9] F. Preston, “The theory and design of plate glass polishing machines.No Title,” *J. Glas. Technol.*, vol. 11, no. 44, pp. 214–256.

[10] J. F. Archard, “Contact and rubbing of flat surfaces,” *J. Appl. Phys.*, vol. 24, no. 8, pp. 981–988, 1953.

[11] J. Maury, A., Ouma, D., Boning, D., & Chung, “A modification to Preston’s equation and impact on pattern density effect modeling,” in *Program Abstracts, Advanced Metalization and Interconnect Systems for ULSI Applications,* 1997.

[12] Q. Luo, S. Ramarajan, and S. V. Babu, “Modification of the Preston equation for the chemical-mechanical polishing of copper,” *Thin Solid Films,* vol. 335, no. 1–2, pp. 160–167, 1998.

[13] P. Wrschka *et al.*, “Polishing Parameter Dependencies and Surface Oxidation of Chemical Mechanical Polishing of Al Thin Films,” *J. Electrochem. Soc.*, vol. 146, no. 7, pp. 2689–2696, 1999.

[14] W. Tseng and Y. Wang, “Re-examination of Pressure and Speed Dependences of Removal Rate during Chemical-Mechanical Polishing Processes,” *J. Electrochem. Soc.*, vol. 144, no. 2, pp. L15–L17, 1997.

[15] F. G. Shi and B. Zhao, “Modeling of chemical-mechanical polishing with soft pads,” *Appl. Phys. A Mater. Sci. Process.*, vol. 67, no. 2, pp. 249–252, 1998.

[16] L. M. E. Scott R. Runnels, “Tribology Analysis of Chemical-Mechanical Polishing,” vol. 141, no. 6, pp. 1698–1701, 1994.

[17] S. Srikanth, Dipto G. Thakurta, W. S. Donald, P. M. Shyam, and N. G. William, “Two-Dimensional Wafer-Scale Chemical Mechanical Planarization Models Based on Lubrication Theory and Mass Transport,” vol. 146, no. 2, pp. 1969–1970, 1970.

[18] C. H. Cho, S. S. Park, and Y. Ahn, “Three-dimensional wafer scale hydrodynamic modeling for chemical mechanical polishing,” *Thin Solid Films*, vol. 389, no. 1–2, pp. 254–260, 2001.

[19] T. Nishioka, K. Serine, and Y. Tateyama, “Modeling on hydrodynamic effects of pad surface roughness in CMP process,” *Proc. IEEE 1999 Int. Interconnect Technol. Conf. IITC 1999*, pp. 89–91, 1999.

[20] L. Shan, J. Levert, L. Meade, Tichy J, and S. Danyluk, “Interfacial fluid mechanics and pressure prediction in chemical mechanical polishing,” *J. Tribol.*, vol. 122, no. 3, pp. 539–543, 2000.

[21] J. M. Chen and Y. C. Fang, “Hydrodynamic characteristics of the thin fluid film in chemical-mechanical polishing,” *IEEE Trans. Semicond. Manuf.*, vol. 15, no. 1, pp. 39–44, 2002.

[22] C. F. Higgs, S. H. Ng, L. Borucki, I. Yoon, and S. Danyluk, “A Mixed-Lubrication Approach to Predicting CMP Fluid Pressure Modeling and Experiments,” *J. Electrochem. Soc.*, vol. 152, no. 3, p. G193, 2005.

[23] D. G. Thakurta, C. L. Borst, D. W. Schwendeman, R. J. Gutmann, and W. N. Gill, “Three-Dimensional Chemical Mechanical Planarization Slurry Flow Model Based on Lubrication Theory,” *J. Electrochem. Soc.*, vol. 148, no. 4, p. G207, 2001.

[24] J. Tichy, J. A. Levert, L. Shan, and S. Danyluk, “Contact Mechanics and Lubrication Hydrodynamics of Chemical Mechanical Polishing,” *J. Electrochem. Soc.*, vol. 146, no. 4, pp. 1523–1528, 1999.

[25] K. Nagayama, H. Morishita, K. Kimura, and K. Tanaka, “A Computational Study on Slurry Flow between a Wafer and CMP Pad with Grooves,” pp. 5–8.

[26] S. H. Bae, S.-M. Yang, and D. H. Kim, “Effects of chemical reaction on the polishing rate and surface planarity in the copper CMP,” 2002.

[27] Y. B. Tian, S. T. Lai, and Z. W. Zhong, “Slurry flow visualisation of chemical mechanical polishing based on a computational fluid dynamics model,” *Adv. Mater. Res.*, vol. 565, pp. 324–329, 2012.

[28] Y. Jeng and H. Tsai, “Tribological analysis on powder slurry in,” vol. 1585.

[29] S. R. Runnels, “Feature-Scale Fluid-Based Erosion Modeling for Chemical-Mechanical Polishing,” *J. Electrochem. Soc.*, vol. 141, no. 7, pp. 1900–1904, 1994.

[30] J. Larsen-Basse and H. Liang, “Probable role of abrasion in chemo-mechanical polishing of tungsten,” *Wear*, vol. 233–235, pp. 647–654, 1999.

[31] C. Liu, B. Dai, W. Tseng, and C. Yeh, “Modeling of the Wear Mechanism during Chemical-Mechanical Polishing,” *J. Electrochem. Soc.*, vol. 143, no. 2, pp. 716–721, 1996.

[32] F. Zhang, A. A. Busnaina, and G. Ahmadi, “Particle Adhesion and Removal in Chemical Mechanical Polishing and,” vol. 146, no. 7, pp. 2665–2669, 1999.

[33] A. R. Mazaheri and G. Ahmadi, “Modeling the Effect of Bumpy Abrasive Particles on Chemical Mechanical Polishing,” *J. Electrochem. Soc.*, vol. 149, no. 7, p. G370, 2002.

[34] T. Yu, C. C. Yu, and M. Orlowski, “A statistical polishing pad model for chemical-mechanical polishing,” *IEEE Int. Electron Devices Meet.*, pp. 865–868, 1993.

[35] G. Ahmadi and X. Xia, “A Model for Mechanical Wear and Abrasive Particle Adhesion during the Chemical Mechanical Polishing Process,” pp. 99–109, 2001.

[36] J. Luo and D. A. Dornfeld, “Material Removal Regions in Chemical Mechanical Planarization for Submicron Integrated Circuit Fabrication : Coupling Effects of Slurry Chemicals , Abrasive Size Distribution , and Wafer-Pad Contact Area,” *IEEE Trans. Semicond. Manuf.*, vol. 16, no. 1, pp. 45–56, 2003.

[37] J. Luo and D. A. Dornfeld, “Material Removal Mechanism in Chemical Mechanical Polishing : Theory and Modeling,” vol. 14, no. 2, pp. 112–133, 2001.

[38] J. Luo and D. A. Dornfeld, “Effects of Abrasive Size Distribution in Chemical Mechanical Planarization : Modeling and Verification,” vol. 16, no. 3, pp. 469–476, 2003.

[39] Y. Zhao and L. Chang, “A micro-contact and wear model for chemical-mechanical polishing of silicon wafers,” *Wear*, vol. 252, no. 3–4, pp. 220–226, 2002.

[40] Y. Zhao, D. M. Maietta, and L. Chang, “An asperity microcontact model incorporating the transition from elastic deformation to fully plastic flow,” *J. Tribol.*, vol. 122, no. 1, pp. 86–93, 2000.

[41] Yongsik Moon, “Mechanical aspects of the material removal mechanism in chemical mechanical polishing (CMP),” 1999.

[42] Y. Zhao, L. Chang, and S. H. Kim, “A mathematical model for chemical-mechanical polishing based on formation and removal of weakly bonded molecular species,” *Wear*, vol. 254, no. 3–4, pp. 332–339, 2003.

[43] S. Oh and J. Seok, “An integrated material removal model for silicon dioxide layers in chemical mechanical polishing processes,” *Wear*, vol. 266, no. 7–8, pp. 839–849, 2009.

[44] S. R. R. and L. M. Eyman, “Tribology Analysis of Chemical-Mechanical Polishing,” *J. Electrochem. Soc.*, vol. 141, no. 6, pp. 983–990, 1994.

[45] and W. N. G. Srikanth Sundararajan, Dipto G. Thakurta, Donald W. Schwendeman, Shyam P. Murarka, “Two-Dimensional Wafer-Scale Chemical Mechanical Planarization Models Based on Lubrication Theory and Mass Transport,” *J. Electrochem. Soc.*, vol. 146, no. 2, pp. 761–766, 1999.

[46] T. K. Yu, C. C. Yu, and M. Orlowski, “A Statistical polishing pad model for Chemical-Mechnical polishing,” *Int. Electron Devices Meet.*, pp. 865–868, 1993.

[47] T. K. Yu, C. Yu, and M. Orlowski, “Combined asperity contact and fluid flow model for chemical-mechanical polishing,” *1994 Int. Work. Numer. Model. Process. Devices Integr. Circuits, NUPAD 1994*, pp. 29–32, 1994.

[48] Y. Moon, “Mechanical aspects of the material removal mechanism in chemical mechanical polishing (CMP). University of California, Berkeley, 1999.,” 1999.

[49] J. Seok *et al.*, “Inverse analysis of material removal data using a multiscale CMP model,” *Microelectron. Eng.*, vol. 70, no. 2–4, pp. 478–488, 2003.

[50] J. Luo and D. A. Dornfeld, “Material removal mechanism in chemical mechanical polishing: Theory and modeling,” *IEEE Trans. Semicond. Manuf.*, vol. 14, no. 2, pp. 112–133, 2001.

[51] Y. R. Jeng and P. Y. Huang, “A material removal rate model considering interfacial micro-contact wear behavior for chemical mechanical polishing,” *J. Tribol.*, vol. 127, no. 1, pp. 190–197, 2005.

[52] J. A. Greenwood, “Contact of nominally flat surfaces,” *Proc. R. Soc. London. Ser. A. Math. Phys. Sci.*, vol. 295, no. 1442, pp. 300–319, 1966.

[53] M. Tomozawa and K. Hirao, “Diffusion of water into oxides during microhardness indentation,” *J. Mater. Sci. Lett.*, vol. 6, no. 7, pp. 867–868, 1987.

[54] E. Paul, F. Kaufman, V. Brusic, J. Zhang, F. Sun, and R. Vacassy, “A Model of Copper CMP,” *J. Electrochem. Soc.*, vol. 152, no. 4, p. G322, 2005.

[55] P. Shewmon, *Diffusion in Solids*. McGraw-Hill. New York52., 1963.

[56] B. Šarler, “Stefan’s work on solid-liquid phase changes,” *Eng. Anal. Bound. Elem.*, vol. 16, no. 2, pp. 83–92, 1995.

[57] M. Bielmann, U. Mahajan, and R. K. Singh, “Effect of particle size during tungsten chemical mechanical polishing,” *Mater. Res. Soc. Symp. - Proc.*, vol. 566, pp. 103–108, 1999.

[58] G. Fu, A. Chandra, S. Guha, and G. Subhash, “A plasticity-based model of material removal in chemical-mechanical polishing (CMP),” *IEEE Trans. Semicond. Manuf.*, vol. 14, no. 4, pp. 406–417, 2001.

[59] and L. J. C. Shih, S. Y., “Thermal characteristics study of CMP low dielectric constant material,” in *Proc. Third Int. Chemical-Mechanical Planarization for ULSI Multilevel Interconnection Conf.*, 1998.

[60] L. Charns, M. Sugiyama, and A. Philipossian, “Mechanical properties of chemical mechanical polishing pads containing water-soluble particles,” *Thin Solid Films*, vol. 485, no. 1–2, pp. 188–193, 2005.

[61] M. Forsberg, “Effect of process parameters on material removal rate in chemical mechanical polishing of Si(1 0 0),” *Microelectron. Eng.*, vol. 77, no. 3–4, pp. 319–326, 2005.

[62] H. Lee, S. Joo, and H. Jeong, “Mechanical effect of colloidal silica in copper chemical mechanical planarization,” *J. Mater. Process. Technol.*, vol. 209, no. 20, pp. 6134–6139, 2009.

[63] Z. Li, Y. Tian, C. Teng, and H. Cao, “Recent advances in barrier layer of cu interconnects,” *Materials (Basel).*, vol. 13, no. 21, pp. 1–22, 2020.

[64] C. A. Chang, “Outdiffusion of Cu through Au: Comparison of (100) and (111) Cu films epitaxially deposited on Si, and effects of annealing ambients,” *Applied Physics Letters*, vol. 55, no. 26. pp. 2754–2756, 1989.

[65] K. Holloway and P. M. Fryer, “Tantalum as a diffusion barrier between copper and silicon,” *Appl. Phys. Lett.*, vol. 57, no. 17, pp. 1736–1738, 1990.

[66] K.-S. Park and S. Kim, “Seedless Copper Electrodeposition onto Tungsten Diffusion Barrier,” *J. Electrochem. Soc.*, vol. 157, no. 12, p. D609, 2010.

[67] C. Y. Ting and M. Wittmer, “The use of titanium-based contact barrier layers in silicon technology,” *Thin Solid Films*, vol. 96, no. 4, pp. 327–345, 1982.

[68] N. Fréty, F. Bernard, J. Nazon, J. Sarradin, and J. C. Tedenac, “Copper diffusion into silicon substrates through TaN and Ta/TaN multilayer barriers,” *J. Phase Equilibria Diffus.*, vol. 27, no. 6, pp. 590–597, 2006.

[69] T. Uekubo, M., Oku, T., Nii, K., Murakami, M., Takahiro, K., Yamaguchi, S., ... & Ohta, “WNx diffusion barriers between Si and Cu,” *Thin Solid Films*, vol. 286, no. 1–2, pp. 170–175, 1996.

[70] J. Uhm and H. Jeon, “TiN diffusion barrier grown by atomic layer deposition method for Cu metallization,” *Japanese J. Appl. Physics, Part 1 Regul. Pap. Short Notes Rev. Pap.*, vol. 40, no. 7, pp. 4657–4660, 2001.

[71] S. J. Wang, H. Y. Tsai, and S. C. Sun, “Characterization of Sputtered Titanium Carbide Film as Diffusion Barrier for Copper Metallization,” *J. Electrochem. Soc.*, vol. 148, no. 8, p. C563, 2001.

[72] M. S. Angyal, Y. Shacham-Diamand, J. S. Reid, and M. A. Nicolet, “Performance of tantalum-silicon-nitride diffusion barriers between copper and silicon dioxide,” *Appl. Phys. Lett.*, vol. 67, no. 1995, p. 2152, 1995.

[73] J. W. Klaus, A. W. Ott, A. C. Dillon, and S. M. George, “Atomic layer controlled growth of Si3N4 films using sequential surface reactions,” *Surf. Sci.*, vol. 418, no. 1, 1998.

[74] K. V. Sagi, L. G. Teugels, M. H. van der Veen, H. Struyf, and S. V. Babu, “Chemical Mechanical Polishing and Planarization of Mn-Based Barrier/Ru Liner Films in Cu Interconnects for Advanced Metallization Nodes,” *ECS J. Solid State Sci. Technol.*, vol. 6, no. 5, pp. P259–P264, 2017.

[75] K. Maruyama, M. Shiohara, K. Yamada, S. Kondo, and S. Saito, “Galvanic corrosion control in chemical mechanical polishing of Cu interconnects with ruthenium barrier metal film,” *Jpn. J. Appl. Phys.*, vol. 48, no. 4 PART 2, 2009.

[76] and H. H. Hojoong Kim, Kyewon Seo, Jinok Moon, Hyunsoo Kim, “Barrier Metal Slurry for Low Defect Copper Damascene Chemical Mechanical Polishing,” in *ECS Transactions*, 2015, vol. 64, no. 40, pp. 85–90.

[77] J. Yao, Y., Jing, J., Wang, Y., Qiu, T., Cai, X., Chen, B., & Zhang, "Barrier Slurry Innovation for Cu-ULK Process," *ECS Trans.*, vol. 60, no. 1, pp. 587–593, 2014.

[78] C. Cao, K. Song, Y. Yao, J. Jing, and Y. Wang, "Barrier Slurry Innovation for Advanced Node," *ECS Trans.*, vol. 60, no. 1, pp. 573–579, 2014.

[79] B. Zhang, Y. Liu, and C. Wang, "BTA Free Alkaline Slurries Developed for Copper and Barrier CMP," *ECS J. Solid State Sci. Technol.*, vol. 4, no. 11, pp. P5112–P5117, 2015.

[80] J. Jing, Y. Wang, J. Zhang, and X. Cai, "Development of Cu CMP Slurry with High Throughput and Low Dishing Jianfen Jing, Yuchun Wang, Jian Zhang, Xinyuan Cai, Xucheng Wang, Yanting Xu, Fengjun Shi Anji Microelectronics (Shanghai) Co., Ltd., Shanghai, 201203, China," vol. 52, no. 1, pp. 569–574, 2013.

[81] Y. Yang, W., Li, T., Zhou, H., Huang, Z., Fu, C., Chen, L., Li, Mangbo., & Kuang, "Electrochemical and anti-corrosion properties of octadecanethiol and benzotriazole binary self-assembled monolayers on copper," *Electrochim. Acta*, vol. 220, pp. 245–251, 2016.

[82] C. Tanwar, K., Canaperi, D., Lofaro, M., Tseng, W. T., Patlolla, R., Penny, C., & Waskiewicz, "Cu CMP Process Evaluation for Advanced Technology Nodes," *JES F OCUS I SSUE E LECTROCHEMICAL P ROCESSING I NTERCONNECTS BEOL*, vol. 160, no. 12, pp. 3247–3254, 2013.

[83] O. Yu, K., Thomas, N., Venkataraman, S. S., Pillai, K. S., Hurd, T., Boggs, K., & Chyan, "Study of Cu Bimetallic Corrosion in CMP Chemical Environments Using Optical Scanning and Micropattern Corrosion Screening," *ECS Trans.*, vol. 35, no. 8, pp. 173–184, 2019.

[84] Q. Xu, L. Chen, F. Yang, and H. Cao, “Influence of slurry components on copper CMP performance in alkaline slurry,” *Microelectron. Eng.*, vol. 183–184, pp. 1–11, 2017.

[85] N. Jourdan, “CVD/ALD-Mn (Nx) As Copper Diffusion Barrier For Advanced Interconnect Technologies.,” in *In ECS Meeting Abstracts No. 29*, 2013, p. 2081.

[86] W. Akbar and O. Ertunc, “A Coupled Material Removal Model for Chemical Mechanical Polishing Processes,” *ECS J. Solid State Sci. Technol.*, 2021.

[87] K. Deb, Multi-Objective Optimization using Evolutionary Algorithms, 1ed. John Wiley & Sons, 2001.

[88] M. Tabassum, “A Genetic Algorithm Analysis Towards Optimization Solutions,” *Int. J. Digit. Inf. Wirel. Commun.*, vol. 4, no. 1, pp. 124–142, 2014.

[89] R. Ihnfeldt and J. B. Talbot, “Effect of CMP Slurry Chemistry on Copper Nanohardness,” *J. Electrochem. Soc.*, vol. 155, no. 6, p. H412, 2008.

[90] “https://www.azom.com/article.aspx?ArticleID=9102.” .

[91] H. Cao, Y. Su, D. Cui, D. Zhang, and Q. Ouyang, “Microstructural characterization, mechanical properties and thermal expansion of antiperovskite manganese nitride Mn3.1Zn0.5Sn0.4N fabricated by combing vacuum sintering and spark-plasma sintering,” *Mater. Charact.*, vol. 160, no. May 2019, p. 110100, 2020.

[92] Y. Li, APPLICATIONS OF CHEMICAL MECHANICAL Edited by. .

[93] I. Vos, “Copper CMP challenges for ULK & advanced barriers,” in *CMPUG*.

[94] L. Yao, B. Small, and K. Z. Kadowaki, “7th Annual International CMP Conference Tuning Hydroxylamine Slurries for Copper Barrier Polishing for (SiLK TM) Low-k Integration,” *Agenda*, 2002.

[95] J. Amanokura, K. Mabuchi, T. Sakurada, Y. Nomura, M. Habiro, and H. Akahoshi, “Development of planarity improved abrasive-free copper CMP slurry and practical non-selective barrier CMP slurry based on electrochemical study,” *ICPT 2007 - Int. Conf. Planarization/CMP Technol. Proc.*, pp. 337–342, 2007.

[96] K. Gottfried, I. Schubert, S. E. Schulz, and T. Gessner, “Cu/barrier CMP on porous low-k based interconnect schemes,” *Microelectron. Eng.*, vol. 83, no. 11–12, pp. 2218–2224, 2006.

[97] K. Delbridge, G. Moyaerts, G. Sayles, and S. Mohseni, “Advanced Barrier Slurry Development for 65nm and Beyond Presentation Overview :,” no. June, pp. 1–16, 2005.

[98] M. Huilai, W. Shengli, L. Zhenxia, X. Wenzhong, and X. Xia, “Study on optimization of CMP slurry for tantalum in ULSI based on Taguchi method,” *Adv. Mater. Res.*, vol. 129–131, pp. 794–798, 2010.

VITA

Wazir Akbar received his BSc. degree from mechanical engineering department of UET Peshawar, Pakistan and MSc. degree from Ozyegin University, Istanbul. His MSc thesis focused on developing functional particles and systems for applications in textiles. He started working as PhD student under the supervision of Dr. Ozgur Ertunc in 2019 at the department of mechanical engineering at Ozyegin University. He is currently working on the physics based modeling and process parameters optimization of chemical mechanical polishing of semiconductor materials. His research interests include semiconductor materials processing, materials and surface science, and mathematical modeling and optimization.